AD-A166 580 VECTORED THRUST DIGITAL FLIGHT CONTROL FOR CREW ESCAPE 1/3
VOLUME 1(U) SCIENTIFIC SYSTEMS INC CAMBRIDGE MA
J V CARROLL ET AL. DEC 85 AFWAL-TR-85-3116-VOL-1
UNCLASSIFIED F33615-C-82-3402 F/G 1/4 NL

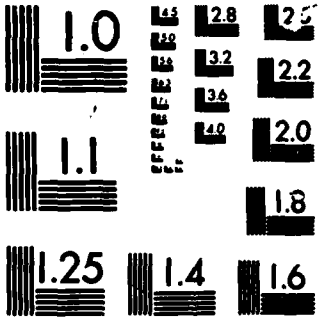

MICROCOPY CHART

(2)

AFWAL-TR-85-3116
Volume I

VECTORED THRUST DIGITAL FLIGHT CONTROL FOR CREW ESCAPE

James V. Carroll
Robert F. Gendron

Scientific Systems Inc.
54 Cambridge Park Extension
Cambridge MA 02140

AD-A166 580

December 1985

Final Report for Period June 1982 - February 1985

Approved for public release; distribution is unlimited

DTIC
ELECTE
APR 14 1986
S D
B

FLIGHT DYNAMICS LABORATORY
AIR FORCE WRIGHT AERONAUTICAL LABORATORIES
AIR FORCE SYSTEMS COMMAND
WRIGHT-PATTERSON AIR FORCE BASE, OHIO 45433

NOTICE

When Government drawings, specifications, or other data are used for any purpose other than in connection with a definitely related Government procurement operation, the United States Government thereby incurs no responsibility nor any obligation whatsoever; and the fact that the government may have formulated, furnished, or in any way supplied the said drawings, specifications, or other data, is not to be regarded by implication or otherwise as in any manner licensing the holder or any other person or corporation, or conveying any rights or permission to manufacture use, or sell any patented invention that may in any way be related thereto.

This report has been reviewed by the Office of Public Affairs (ASD/PA) and is releasable to the National Technical Information Service (NTIS). At NTIS, it will be available to the general public, including foreign nations.

This technical report has been reviewed and is approved for publication.

Lanny A. Jines

LANNY A. JINES, P.E.
Project Engineer

B J White

B. J. WHITE
Group Leader
Aircrew Escape Group

FOR THE COMMANDER

Rudi Berndt

RUDI BERNDT
Acting Chief
Vehicle Equipment Division

"If your address has changed, if you wish to be removed from our mailing list, or if the addressee is no longer employed by your organization please notify AFWAL/FIER *, W-PAFB, OH 45433 to help us maintain a current mailing list".*

Copies of this report should not be returned unless return is required by security considerations, contractual obligations, or notice on a specific document.

UNCLASSIFIED

SECURITY CLASSIFICATION OF THIS PAGE

AD-A166580

REPORT DOCUMENTATION PAGE

1a. REPORT SECURITY CLASSIFICATION UNCLASSIFIED	1b. RESTRICTIVE MARKINGS
2a. SECURITY CLASSIFICATION AUTHORITY	3. DISTRIBUTION/AVAILABILITY OF REPORT Approved for public release; distribution is unlimited.
2b. DECLASSIFICATION/DOWNGRADING SCHEDULE	
4. PERFORMING ORGANIZATION REPORT NUMBER(S)	5. MONITORING ORGANIZATION REPORT NUMBER(S) AFWAL-TR-85-3116, Vol I
6a. NAME OF PERFORMING ORGANIZATION Scientific Systems Inc. 6b. OFFICE SYMBOL (If applicable)	7a. NAME OF MONITORING ORGANIZATION Flight Dynamics Laboratory (FIER) AF Wright Aeronautical Laboratories, AFSC
6c. ADDRESS (City, State and ZIP Code) 54 Cambridge Park Extension Cambridge MA 02140	7b. ADDRESS (City, State and ZIP Code) Wright-Patterson AFB OH 45433-6553
8a. NAME OF FUNDING/SPONSORING ORGANIZATION Flight Dynamics Laboratory 8b. OFFICE SYMBOL (If applicable) AFWAL/FIER	9. PROCUREMENT INSTRUMENT IDENTIFICATION NUMBER F33615-C-82-3402
8c. ADDRESS (City, State and ZIP Code) Wright-Patterson AFB, Ohio 45433	10. SOURCE OF FUNDING NOS. PROGRAM ELEMENT NO. 62201F; PROJECT NO. 2402; TASK NO. 240203; WORK UNIT NO. 24020342
11. TITLE (Include Security Classification) Vectored Thrust Digital Flight Control for Crew Escape Vol I (Uncl)	
12. PERSONAL AUTHOR(S) Carroll, James V. Gendron, Robert F.	
13a. TYPE OF REPORT Final 13b. TIME COVERED FROM 82 Jun 01 TO 85 Feb 28	14. DATE OF REPORT (Yr., Mo., Day) December 1985 15. PAGE COUNT 201
16. SUPPLEMENTARY NOTATION AFWAL-TR-85-3116 consist of Vols I, II, III, and IV (cont fr p B) Vols III & IV are software computer	

17. COSATI CODES		
FIELD	GROUP	SUB. GR.
0607		

18. SUBJECT TERMS (Continue on reverse if necessary and identify by block number)
Modern Control Theory, Acceleration Control, Model Algorithmic Control, Ejection Seat Control.

19. ABSTRACT (Continue on reverse if necessary and identify by block number)

Work of Meyer and Cicolani was adapted for application to open seat escape systems in current Air Force fighter aircraft. The control system design is a fully self-contained system whose major on-seat components are: acceleration, rate, attitude and altitude sensors, real-time control logic imbedded on a microprocessor chip, rocket thrusters with thrust vectoring and throttling capability, and various avionics and support subsystem hardware items (e.g., power supply). The control concept is based on a comparison of measured translational and rotational accelerations with desired values; the propulsion system is then configured to provide adequate energy to follow the desired trajectory and simultaneously eliminate acceleration errors. The concept uses nonlinear models and incorporates state and control constraints. This Volume I contains the detailed documentation of specification development, control logic design, hardware identification, and trade study efforts. Volume II contains a description of the prototype design, real time breadboard simulation, and the results and analysis of the verification task. Volume III (AD A166 596)

20. DISTRIBUTION/AVAILABILITY OF ABSTRACT UNCLASSIFIED/UNLIMITED ☒ SAME AS RPT. ☐ DTIC USERS ☐	21. ABSTRACT SECURITY CLASSIFICATION UNCLASSIFIED
22a. NAME OF RESPONSIBLE INDIVIDUAL Lanny A. Jines	22b. TELEPHONE NUMBER (Include Area Code) (513) 255-3305 22c. OFFICE SYMBOL AFWAL/FIER

DD FORM 1473, 83 APR EDITION OF 1 JAN 73 IS OBSOLETE.

UNCLASSIFIED

SECURITY CLASSIFICATION OF THIS PAGE

contains the supporting appendices for Volumes I and II. Volume IV details the results of the real time hybrid computer simulation effort. Keywords: (Top A)

FOREWORD

The design study described in this report was conducted by Scientific Systems, Inc. (SSI), Cambridge, Mass., under Contract F33615-82-C-3402. The project was administered by Mr. Lanny A. Jines in the Crew and Escape Subsystems Branch of the Vehicle Equipment Division, Flight Dynamics Laboratory, Air Force Wright Aeronautical Laboratories, Wright-Patterson Air Force Base, Ohio. SSI was supported in this project by the following subcontractors: Stencel Aero Engineering Corp., Martin Marietta Orlando Aerospace, Boeing Military Airplane Co., and Unidynamics/Phoenix.

Dr. James V. Carroll of SSI was Program Manager. His co-workers were R. Gendron, D. Martin, and B. Chan. Dr. Raman Mehra, President of SSI, played an active technical role in the early phases of the project. Key subcontractor participants were: Dr. C. Kylstra of Stencel, S. Baumgartner of Boeing, M. K. Klukis, A. J. Ciaponi and W. Hester of Martin Marietta, and J. Roane of Unidynamics.

The timely and efficient support of the SSI Publications Department, led by Alina Bernat, was greatly appreciated.

DTIC
ELECTE
APR 1 4 1986
S D
B

Accession For
NTIS GRA&I
DTIC TAB
Unannounced
Justification
By
Distribution/
Availability Codes
Dist | Avail and/or Special
A-1

QUALITY INSPECTED 3

TABLE OF CONTENTS

VOLUME I

1. INTRODUCTION AND SUMMARY 1

2. PRELIMINARY DISCUSSION 4

2.1 Statement of Problem 4
2.2 Design Approach 4
2.3 Project Organization 5
2.3.1 Task 1: Specification Development 5
2.3.2 Task 2: Control Logic Design 7
2.3.3 Task 3: Hardware Integration; Trade Study . . . 8
2.3.4 Task 4: Prototype Design; Real Time Breadboard Simulation 9

3. TASK 1: SPECIFICATION DEVELOPMENT 10

3.1 Introduction 10
3.2 Basic Theory 11
3.2.1 Description of Seat Dynamics 11
3.2.2 Rocket Nozzle Configurations and Controllability 30
3.3 Detailed Description of Requirements 43
3.3.1 Flight Conditions for TVC Design 43
3.3.2 Minimum, Maximum State and Control Variable Specifications 47
3.3.3 Disturbances 54
3.3.4 Crew Escape Energy Requirements 58

4. TASK 2: CONTROL LOGIC DESIGN 88

4.1 Unique Features, Problems in Ejection Seat Control 89
4.1.1 Development of Control Design Methodology . . . 90
4.2 Review of Candidate Control Synthesis Techniques 91
4.2.1 Linear Quadratic Regulator (LQR) 94
4.2.2 Basic Model Algorithmic Control (MAC) 98
4.2.3 Frequency Domain (Classic) 104
4.2.4 Computation of Optimal Trajectories Using ESOP 106
4.2.5 Other Related Programs (MPES) 110

TABLE OF CONTENTS (cont'd)

VOLUME I

4.3 Acceleration Control 111
4.3.1 Evolution of Design 111
4.3.2 Features of Final Design 112
4.3.3 Linear Analysis; Stability 126

5. TASK 3: HARDWARE IDENTIFICATION; TRADE STUDY 137

5.1 Introduction 137
5.2 Task 3 Objectives 138
5.3 Microprocessor Survey 139
5.4 Microprocessor Design 142
5.5 Control System Components Tradeoff Analysis 162
5.5.1 Sensor Hardware 163
5.5.2 Thrust Actuation Hardware 189
5.5.3 Summary and Recommendations 200

VOLUME II (Under Separate Cover)

6. Task 4: Prototype Design; Real Time Breadboard Simulation 187

6.1 Overview of Hybrid Simulation Model 191
6.2 Model Structure 201
6.2.1 Aerodynamic Model 201
6.2.2 Six DOF Flight Model 203
6.2.3 Sensor Models 204
6.2.4 Actuator Dynamics Model 208
6.2.5 Resultant Evaluation 211
6.2.6 Summary of Analog Simulation Models 212
6.3 Digital Algorithms 213
6.3.1 Control Algorithms 213
6.4 Hardware Design Issues 219
6.4.1 Requirements 219
6.4.2 High Force Gain Valve Configuration (MMOA) 219
6.4.3 Alternative Configurations 221
6.4.4 Modes of Hybrid Simulation Operation 224

7. RESULTS AND ANALYSIS 225
7.1 Overview of Chapter 7 225
7.2 Comparison of Alternative Operational Modes of the Hybrid Simulation 225
7.2.1 Interpretation of the Strip Chart Results 226

TABLE OF CONTENTS (continued)

7. RESULTS AND ANALYSIS

7.3 Low Altitude Escape Conditions 230
7.4 Results with Variations of the Initial Attitude 240
7.5 Basic Conclusions on the Scenarios Investigated 258
7.6 Microprocessor Memory and Throughput 264
7.7 Dynamic Occupant CG Results 267
7.8 Nominal Pilot Results 274
7.9 Robustness; Sensitivity Analysis 279

8. CONCLUSIONS AND RECOMMENDATIONS 365

REFERENCES 375

VOLUME III (Under Separate Cover)

Appendix A: Seat Equations of Motion A-1

Appendix B: Blueline Drawings B-1

Appendix C: VAX Control Logic Software C-1

Appendix D: State Estimation D-1

Appendix E: Selected Control Systems Specifications E-1

VOLUME IV (Under Separate Cover)

Appendix F: MMOA Report, Hybrid Results ..... F

LIST OF FIGURES

Figure 2.1: Overview Block Diagram of SSI Control Design for Ejection Seats .....

Figure 3.1: E and S Frame Geometry .....

Figure 3.2: S and R Frame Geometry .....

Figure 3.3: Aces II Ejection Seat as Modeled by EASIEST .....

Figure 3.4: Representative Nozzle Geometry .....

Figure 3.5: Three Degree-of-Freedom Controllability Schematic, One Nozzle .....

Figure 3.6: Design Flight Envelope for High Q Ejection Seat .....

Figure 3.7: MIL-S Condition 1 .....

Figure 3.8: MIL-S Case 1; Burn Time = 0.60 sec. .....

Figure 3.9: MIL-S Case 1; Burn Time = 0.90 msec. .....

Figure 3.10: High Q, Wings Level Case; No Thrust Limiting .....

Figure 3.11: Seven-Nozzle Configuration, Based on Martin-Marietta Design .....

Figure 4.1: Systems Linear Matrix, Uncontrolled Run

Figure 4.2: System Linear Matrix, Controlled Run

Figure 4.3: Impulse Response Representation of a Linear System .....

Figure 4.4: IDCOM Components .....

Figure 4.5: Baseline Control System Overview .....

Figure 4.6: Selected Structure in Conventional Design .....

Figure 4.7: Structure of Proposed Perturbation Controller .....

Figure 5.1: Operation Counts for Attitude Controller .....

LIST OF TABLES

Table 3.1: Low Level Escape Performance (from MIL-S-9479B) .....

Table 3.2: Aces II Thrust Sizing Study .....

Table 3.3: State, Control and Dynamic Constraints .....

Table 4.1: High-Q System Matrix (A), T=0.0 .....

Table 4.2: High-Q System Matrix (A), T=0.1 .....

Table 4.3: High-Q System Matrix (A), T=0.2 .....

Table 4.4: High-Q Control Matrix (B) .....

Table 4.5: Stabilizing Gain Matrix (C), T=0.0 .....

Table 4.6: Stabilizing Gain Matrix (C), T=0.1 .....

Table 4.7: Stabilizing Gain Matrix (C), T=0.2 .....

Table 5.1: Microprocessor Architecture Tradeoff Analysis, Specific Configuration .....

Table 5.2: Microprocessor Architecture Tradeoff Analysis, General Architectures .....

Table 5.3: Vax I/O Procedure .....

Table 5.4: MC68000 (controller) IO Procedure .....

Table 5.5: IO Transfer Formats .....

Table 5.6: Examples .....

Table 5.7: Northrop GR-G5 Gyroscope .....

Table 5.8: Attitude/Altitude Decision Matrix .....

Table 5.9: Attitude/Altitude Performance Decision Matrix .....

Table 5.10: Rate Sensor Decision Matrix .....

Table 5.11: Rate Sensor Performance Decision Matrix .....

Table 5.12: Angular Accelerometer Decision Matrix .....

Table 5.13: Angular Accelerometer Performance Decision Matrix .....

LIST OF TABLES (cont'd)

Table 5.14: Accelerometer Decision Matrix .....

Table 5.15: Accelerometer Performance Decision Matrix .....

Table 5.16: Pressure Sensor Decision Matrix .....

Table 5.17: Pressure Sensor Performance Decision Matrix .....

Table 5.18: Air Data Sensor Decision Matrix .....

Table 5.19: Air Data Sensor Performance Decision Matrix .....

Table 5.20: Thrust Vectoring, Modulation Decision Matrix .....

Table 5.21: Thrust Vectoring, Modulation Performance Decision Matrix .....

Table 5.22: Thrust Vectoring, Modulation Capability Decision Matrix .....

GLOSSARY OF SYMBOLS AND TERMS

a	translational acceleration (inertial)
A	system matrix, $\partial\dot{x}/\partial x$
B	control matrix, $\partial\dot{x}/\partial u$
C	aerodynamic coefficient; e.g., C_y = side force coefficient
C_D	drag coefficient
CG	center of gravity, usually of seat/pilot
E	phase plane space for acceptable trajectories $(x,\dot{x})$ within escape envelope, Figure 3.6.
f	force vector; vector function
g,G	gravity constant; load factor acceleration
h	altitude of seat/pilot CG above sea level; (-z)
h^D	hydraulic diameter of seat/pilot
J	cost functional
k,K	various control gains
m	seat/pilot mass
M	Mach number
p	roll rate
q	pitch rate
$\bar{q}$,Q	dynamic pressure
r;R	yaw rate; moment arm (e.g. r^D)
S	seat reference area
T	thrust magnitude; sample interval
u	control vector; x-body component of velocity of seat/pilot
v	translational velocity; y-body component of velocity of seat/pilot
V	speed (velocity magnitude) of seat/pilot

GLOSSARY OF SYMBOLS AND TERMS (cont'd)

w	z-body component of velocity of seat/pilot
x	state variables; roll axis
y	output (observed, measured) variables; pitch axis
z	yaw axis
α	angle of attack
β	sideship angle
δ	small deflection angle, e.g., nozzle deflection
τ	torque on seat/pilot system
ϕ	roll angle
θ	pitch angle
χ	yaw angle
ω	angular velocity of seat/pilot with respect to inertial reference
$\dot{\omega}$	angular acceleration of seat/pilot (inertial)

PLOT VARIABLE DEFINITIONS

FANGX, FANGY, FANGZ	angles locating thrust vector in seat/pilot coordinates (degrees); (see Figure)

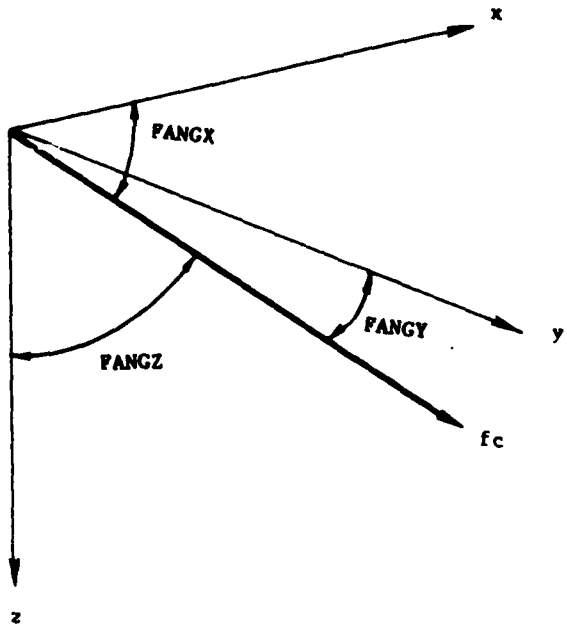

FCMAG	Magnitude of command force (lb.)
KEAS	Knots Equivalent Air Speed
MACH	Ratio of TCMAG to FCMAG (Ft.)
P	roll rate (degrees per second)
PITCH	pitch angle (degrees)
PITNZ1	nozzle 1 pitch deflection, $\delta\theta$ (degrees); see Figure 3.4
Q	pitch rate (degrees per second)
R	yaw rate (degrees per second)
RAD	acceleration radical, Equation 3.34
ROLL	roll (blank) angle (degrees)

CHAPTER 1

INTRODUCTION AND SUMMARY

This report is the final report for the project, "Vectored Thrust Digital Flight Control for Crew Escape", contract number F33615-82-C-3402, sponsored by AFWAL/FIER. It represents a summation of the work performed under contract to the Air Force during the period June 1982 to February 1985. The major project goal was to investigate the feasibility of designing a closed loop control system for ejection seats utilizing vectored thrust propulsion systems. This goal was achieved most affirmatively via the development of a fast, relatively simple and relaible control logic which is particularly suited to the crew escape problem. This central activity was the primary item in Task 2 of the project.

It requires much more than developing an algorithm to determine feasibility, and so the project addressed several related key issues, including: (1) developing requirements and specifications, and synthesis and analysis simulation capability (Task 1); (2) control component hardware survey and trade study (Task 3); and (3) prototype simulation on a real time facility of the control logic on a breadboard controller (Task 4). For many of these activities, SSI received the support of the following subcontractors: Stencel Aero Engineering provided ejection seat design experience and useful insight into meaningful analysis methods; Boeing Military Airplane Company assisted in the hardware survey and provided engineering support in the use of their EASIEST software package; Unidynamics/Phoenix designed and fabricated the wire-wrapped controller; and, Martin Marietta of Orlando provided engineering support in the area of propulsion configurations, as well as supplying personnel and facilities for developing the real time hybrid simulation.

The combination of declining survival statistics during crew escape in recent years and improving control component technology have made this control design study timely and practical. The control technique is based on nonlinear acceleration control, which exploits very well the unique and highly nonlinear characteristics of the pilot/seat system. This report

reviews the design of the controller, including the related actuator configuration and microprocessor architecture issues.

A bread board hybrid simulation utilizing a wire-wrapped electronic digital controller and a unique vectored thrust actuation concept, has been developed for real time analysis of the concept, and is also discussed in this report. Examples presented show that this design represents a reasonable approach for the control of the seat in its harsh, highly constrained environment, over several diverse escape conditions. The results reported here are derived from a project funded by the Air Force, AFWAL/FIER, Wright-Patterson AFB.

We wish to emphasize here that this project is a feasibility study, aimed at providing conclusive answers as to whether the self-contained, vectored thrust crew escape control concept is valid when used with state-of-the-art hardware. The scope of the project is limited primarily to this issue, which is a very critical and important one. As a consequence, however, there are other important issues which will not be fully addressed by this project, or in this report. These include a full design to incorporate fault tolerance, redundancy management, hardware reliability, and many hardware component design and implementation aspects.

This report consists of four Volumes. Volume I, containing Chapters 1 through 5, reports primarily on the first three project tasks. Chapter 2 introduces the basic design problem, and Chapter 3 presents the results of the Task 1 activity, control system requirements and specifications analysis. Chapter 4 presents details of the control law design, as developed under project Task 2, and Chapter 5 concludes Volume I with a discussion of the control system hardware identification and trade study, the primary Task 3 activity.

Volume II, containing Chapters 6 through 8, is devoted to the last project task, the development of the real time hybrid simulation system (Chapter 6), simulation results (Chapter 7), and to a summary of the project results (chapter 8). Volume III contains Appendices A through E, which support text in Volumes I and II. Appendix A presents the seat

equations of motion used in this design effort. Appendix B shows the blueline drawings of conceptual vectored thrust concepts based on the ACES II prototype seat. Appendix C contains a listing of VAX-developed software, and Appendix D discusses aspects of state estimation. Appendix E describes components specifications for selected control hardware elements which have potential ejection seat application. Finally, Volume IV consists of Appendix F, the Martin Marietta hybrid simulation design report.

The authors wish to acknowledge the invaluable support received during the course of this project by many fine people and organizations. In particular, Steve Baumgartner of Boeing, Chet Kylstra of Stencel, Larry LaClair and Jerry Roane of Unidynamics, and Keith Klukis, Al Ciaponi, Bill Hester and Les Canney of Martin Marietta; at SSI, Dan Martin (who authored Sections 5.3 and 5.4), Raman Mehra, Kitkoon Chan and Alina Bernat.

CHAPTER 2

PRELIMINARY DISCUSSION

2.1 Statement of Problem.

When the latest generation of attack and fighter aircraft became operational, the increases in performance, maneuverability, and combat effectiveness brought with them a disturbing drop in both combat and non-combat ejection survival rates. The Air Force has in the past few years become acutely aware of this trend, and is initiating a high-priority, multifaceted effort aimed at developing a new generation escape system whose survival envelope is capable of matching the performance envelopes of the host aircraft to a much greater degree.

The object of the current project reviewed in this report is to provide detailed specifications and a preliminary engineering design for a vectored thrust capable "on-seat" closed loop flight control system; further, to conduct feasibility and hardware trade studies, and real time breadboard simulations. As such, this project is recognized by SSI as playing a crucial role in the Air Force's overall effort to upgrade crew escape technology and, more importantly, save the lives of more flight personnel.

2.2 Overall Approach to Control Design.

Our overall approach to the TVC design involves a hierarchical structure consisting of: (a) Open loop acceleration profiles and ejection seat trajectories obtained using cross-product steering or a trajectory optimization algorithm such as ESOP (Section 4.2.4) for a range of ejection conditions, and implemented on line in a closed loop mode using a MAC-based acceleration control approach; (b) real-time monitoring of the ejection seat dynamics around the open loop trajectories obtained in Step (a), and (c) design of closed loop feedback control laws using the acceleration control approach for maintaining stability around the reference trajectories and minimizing the effect of disturbances on overall escape system performance.

A block diagram of the control design consisting of three hierarchical levels is shown in Figure 2.1.

The reason for using the above approach is that the Ejection Seat Dynamics is highly nonlinear, whereas both the LQR and the MAC approaches require linear models. The design of an optimal nonlinear feedback law requires solution to a dynamic programming problem, which cannot be solved except for systems with one or two state variables. The above approach is similar in spirit to that of Bryson and Ho (1969) for control of nonlinear dynamic systems, except that we use a nonlinear programming approach for trajectory optimization. The reason for this choice is that it is extremely difficult to handle state inequality constraints such as the pilot acceleration limits by trajectory optimization techniques based on the Calculus of Variations or Maximum Principle. The nonlinear programming approach, especially ESOP described in section 4.2.4, is very well suited for handling large numbers of constraints on both the state and the control variables.

2.3 Project Organization.

To meet the major objectives of the design effort - which are to design, simulate and test a closed loop control law for ejection seats, and to assess the design's feasibility on state-of-the-art hardware - four tasks have been defined. These tasks will be outlined in this section, and they include: control law specification development, Task 1 (Section 2.3.1); control logic design, Task 2 (Section 2.3.2); control hardware integration and trade study, Task 3 (section 2.3.3); and, prototype design and real time breadboard simulation, Task 4 (Section 2.3.4).

The project team assembled to accomplish these tasks was headed by SSI as Prime Contractor. Subcontractors were Stencel Aero Engineering and Boeing Military Airplane Co. for Tasks 1 through 3, and Martin Marietta and Unidynamics/Phoenix for Task 4.

2.3.1 Task 1: Specification Development. The primary goal of Task 1 was to develop specifications to be used in the control system design phase. This goal translates into one of finding the amount of control

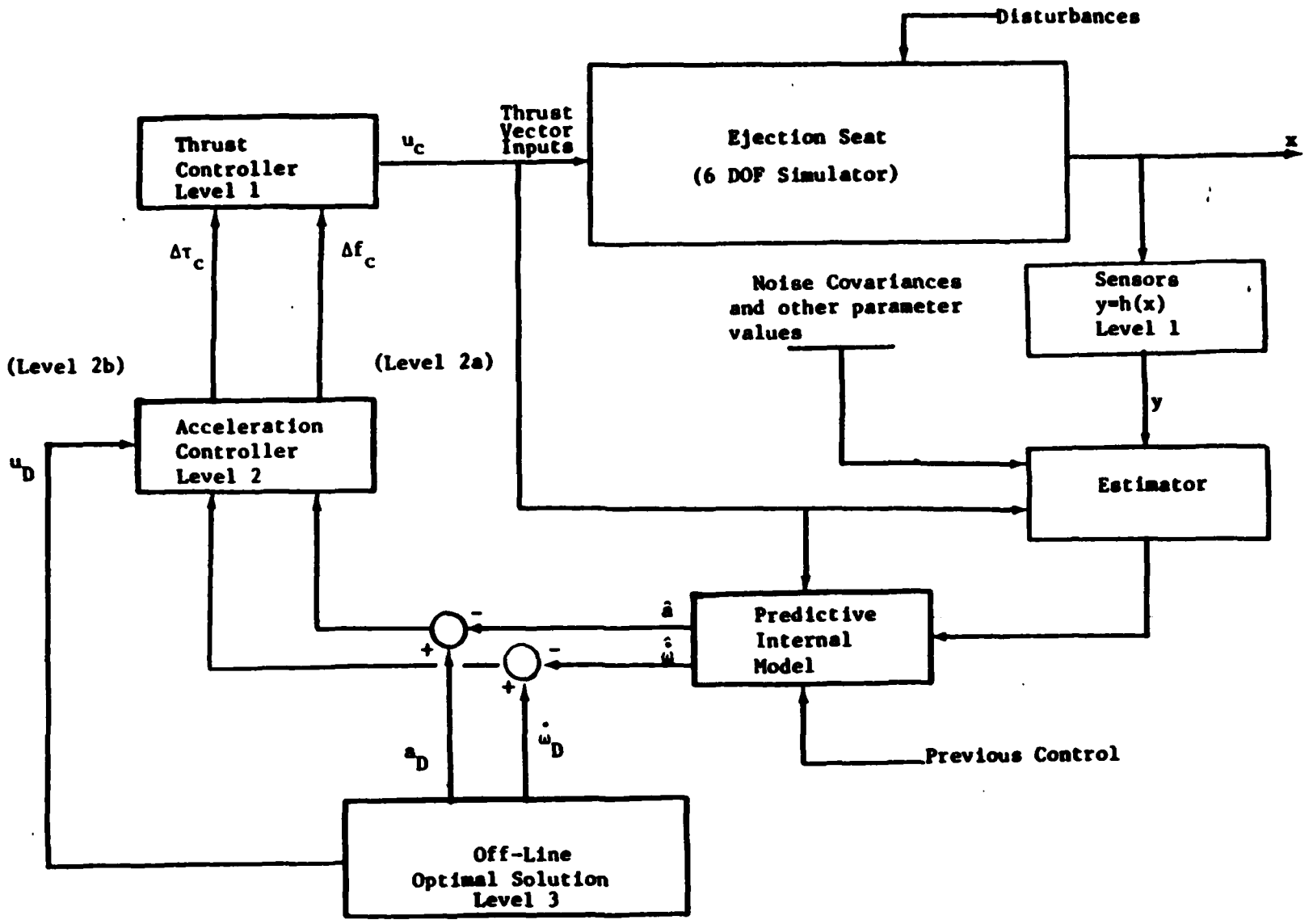

Figure 2.1. Overview Block Diagram of SSI Control Design for Ejection Seats.

authority required of the on-seat energy sources to effect safe crew escape. Within the scope of this project, safe crew escape is achieved when:

(1) The escape is initiated within the flight envelope specified by MIL-S-9479B (briefly, from 0/0 conditions to altitudes of 50,000 feet and airspeeds of 687 KEAS - knots equivalent air speed), and within aircraft translational acceleration limits specified in MIL-S-9479B.

(2) The acceleration environment on the pilot is modified or maintained so as to keep the acceleration radical from exceeding the value 1.0, as defined in paragraph 3.4.11.2 of MIL-S-9479B.

(3) The attitude of the seat/pilot combination is maintained within the range of orientations and rates necessary to support item (2) above.

(4) Attitude and steering control is such that the escaping seat/pilot avoids any aircraft sections, e.g., tail or wing, and altitude is maximized for complete and safe deployment of the main chute.

In addition to the primary Task 1 goal, other critical Task 1 activity involves conducting a preliminary sensor, energy source, and microprocessor hardware survey (Chapter 5).

Our analysis of the control problem, conducted during Task 1, has led to a basic control design approach. This approach and the overall control design methodology are presented in Chapter 4. The control design specifications required for this approach are also detailed in Chapter 3.

2.3.2 Task 2: Control Logic Design. As stated in the Task 2 requirements, the goal of this task is to "prepare the final optimal design for the ejection seat vectored thrust digital control system". Subsequent sections of this report will document that the control approach described here has been implemented and demonstrated successfully in the harsh

ejection environment. The cases presented in this report indicate that this implementation represents a feasible and useful design.

The design accommodates very well the realities of its operating environment. Although initially tasked by the Air Force to perform an LQR design, it became apparent early during the project that such a design by itself would be very cumbersome and inefficient, and most likely inadequate. The design approach which evolved is based on sound theory and engineering practice and is unique to the ejection seat environment. It relies on techniques of nonlinear trajectory optimization and uses principles of Model Algorithmic Control and nonlinear decoupling. The final control approach is structurally similar to an acceleration control concept developed by Meyer and Cicolani (1975).

Chapter 4 will present the details of the control design. Briefly stated, the design is hierarchical (see Figure 2.1). It includes real-time access to reference acceleration trajectories. The latter may themselves be computed suboptimally in real time, or the controller may access prestored, optimal nonlinear reference trajectories. This is the outermost level, Level 3. The reference trajectories are supplied to two parallel inner loops which perform angular and linear acceleration control by comparing predicted accelerations against the prestored desired accelerations and processing these through a linear filter (Level 2). A cluster and sensor system dynamics are incorporated in Level 1, the innermost loop.

This control design has displayed robustness and flexibility when tested at extreme design point conditions such as low altitude-high dynamic pressure and inverted attitude. The overall control law is nonlinear, but includes an integral term to eliminate steady state errors. It generates commands for the thrust controller which is assumed to provide the desired thrust.

2.3.3 Task 3: Hardware Integration; Trade Study. The purpose of this task, which is reported on in detail in Volume I, Chapter 5, was to determine if the control concept proposed is compatible with

"off-the-shelf" control hardware components. This was done by surveying current hardware, obtaining key performance and other relevant specifications (for example cost and weight), and by developing a quantifiable measure for each relevant property, with a view towards thrust vectored ejection seat applications, which allows a trade-off comparison to be made among equivalent candidates.

2.3.4 Task 4: Prototype Design; Real Time Breadboard Simulation. Although the control design effort (Section 2.3.2) is central to the entire entire project, Task 4 represents the culmination of that design, in that its performance under more realistic conditions was examined. Inputs from Task 3 allowed for a refinement of the Task 2 design, and the final design sequence for the breadboard simulator, performed in Task 4, exploited the refinements.

The initial scope of this task was more limited. A Tektronix microprocessor development lab hosting a Motorola MC68000 chip was obtained to analyze architecture and implementation issues for the real time version of the control logic (See Volume II, Chapter 6). However, the magnitude of this effort, plus limitations in equipment and microprocessor development software led eventually to an expansion of the scope of this task. This was because the Tektronix system, when coupled with the VAX mainframe processor, was not able to operate in real time on control logic of reasonable logical complexity, when coded in a higher order language.

The amended activity called for the design and fabrication of a wire-wrapped controller, using the same chip and higher order language (Pascal), to be interfaced with a hybrid simulation environment. The VAX-Tektronix system was then to perform an intermediary role in developing and debugging the controller logic, which was then "burned" onto the controller chip. As is described in Chapter 6, several simulation systems were maintained, each with varying degrees of real time capability and changeability, resulting in a flexible breadboard analysis capability. The overall performance results, as described in Volume II, Chapter 7, were most gratifying, and a final confirmation of the practicality of the control design.

CHAPTER 3

TASK I: SPECIFICATION DEVELOPMENT

3.1 Introduction

This chapter discusses performance specifications and quantifies the plant and environment models for the ejection seat vectored thrust control design effort. Task 1 is a requirements development phase, requiring the development of quantified specifications on which the ejection seat control system is to be designed.

The requirement for survivable ejection conditions at all points in the "escape envelope" specified by MIL-S-9479B (USAF) imposes stringent performance specifications on the control system. The control requirements are unique for the seat/pilot vehicle in that crewperson survivability is the primary element of the control system performance index.

The ground rules under which the control system specifications presented here apply include the following. Open seats as typified by the ACES II model built for the Air Force by Douglas Aircraft Corp., in single-seat aircraft, are the focus of the project control design effort. The control system design is to be fully self-contained on the seat, and able to function succesfully without dependence on the aircraft system avionics or other external data sources. The hardware utilized in the final control system design must, as completely as possible, be at or near state-of-the-art. The dynamic environment under which the control system is developed is specified by the digital software contained in the SAFEST and EASIEST 6 degreesof freedom (DOF) computer programs made available to SSI by the Air Force, at operating conditions established in MIL-S-9479B. It is expected that the final design will be sufficiently robust so as to be successfully implemented on prototype hardware.

It is a major purpose of Task 1 to identify the problem, identify key state variables, control variables, fixed and dynamic constraints, and appropriate design point escape conditions. Another critical requirement of Task 1, in the context of the design methodology presented above and

detailed further below, is to quantify the thrust capability required for various worst case scenarios. Results of our analysis in this area are presented. This activity as well as the activity in step (2) above represent major Task 1 results needed for actual control system design.

The robustness of the control design is to be assured by use of a hierarchical structure.

The control approach detailed in Chapter 4 places importance on proper reflection of flight conditions to be used in the design, and also on having a reasonable quantitative understanding of the ranges of values state and control variables may assume. Both of these key issues are dealt with in this chapter.

Section 3.2 will discuss basic theory; that is, equations of motion and related assumptions, escape conditions, etc. which dictate the operating environment for the control system.

Within Section 3.3, section 3.3.1 will discuss flight conditions, and list those which at this time are considered to be the critical design points, as well as cite time domain requirements for these flight conditions. Section 3.3.2 will list all of the constraints, i.e., range of acceptable values, for the state and control variables identified for each trajectory phase. Section 3.3.3 specifies disturbance modeling and disturbance rejection requirements, and Section 3.3.4 places some control design issues in the context of the crew escape problem.

3.2 Basic Theory

This section sets the background for specification development and eventual control law design. This consists primarily of establishing the operating environment for the seat, and specifying its mathematical description.

3.2.1 Description of seat dynamics. In this section, we detail some of the considerations leading to development of the seat/pilot tions dynamical system which is to be used in the derivation of the closed loop

vectored thrust control law. Also, the main sets of dynamic equations are presented and explained. It is important to note that these equations will not approach the detail or complexity of those coded in SAFEST and EASIEST (see Sections 2.4.1 and 2.4.2). The equations represent a compromise between a high level of accuracy and the desire for both a tractable level of complexity and a feasible duty cycle time.

Section 3.2.1.1 will present nonlinear formulations of the "free" (that is, fully detached from the rails, plus any other lines or tethers connecting the seat to the aircraft) seat/pilot system, acted upon by gravity, aerodynamic, and (when appropriate) drogue and rocket forces. Section 3.2.1.2 shows how the propulsive forces and torques are modeled, and Section 3.2.1.3 presents the linearized free body seat/pilot system, as well as the second order spinal compression dynamics. Finally, Section 3.2.1.4 describes aspects of the seat dynamics while the seat is moving up the rails.

3.2.1.1 Nonlinear free body seat/pilot equations. We now present and explain the nonlinear set of dynamic equations to be used in the free body ejection seat TVC control law design. The nonlinear and linear sets each have a use in the overall design approach (Sections 3.2 and 3.3). The appropriate set will be used as part of the constraint equations in the optimal control formulation. The nonlinear set will be used for the off-line optimizations, and the linear set will be used in real time applications. Wherever possible, for continuity, we have retained either explicit SAFEST/EASIEST, or conventional aerodynamic naming conventions. In a like manner, coordinatizations will follow the conventions set by EASIEST. To assist in this area, we make the following definition: v_E^S represents a vector quantity associated with S (seat, or seat/pilot together), which is coordinatized in the E (Earth-fixed) frame. The E frame is considered to be inertial for all of the analysis done here.

The second major axis system is that attached to the seat, whose origin is at the Seat Reference Point (SRP). This is the S frame. A related frame is parallel to the S frame, but its origin is located at the combined seat/pilot center of gravity (CG). Other frames will be defined

as they are introduced. All frames follow the usual right-handed geometry. See Figure 3.1 for a schematic of the E and S frame relationship.

For the purpose of development of appropriate dynamic relationships for control synthesis, we are assuming that the seat/pilot mass, moments of inertia, and CG location are fixed in the S frame, once a given escape trajectory is initiated. Any time-dependent changes in these quantities over the course of a trajectory will be considered as disturbances to the control system. Fixed disturbances which lead to changes in the values of these quantities, but do not change over the course of a trajectory, can be modeled directly by these equations. A consequence of this assumption is the representation of the combined seat/pilot system as a rigid body, during a given trajectory. That is, seat/pilot mass and moment of inertia are constant during a trajectory.

The dynamic equations for free body seat/pilot motion are basically an expansion of the accelerating frame representation of Newton's Law:

$$m\dot{v}^S = -m\omega^{S/E} \times v^S + ma^{ext} \tag{3.1}$$

$$I^S\dot{\omega}^{S/E} = -\omega^{S/E} \times (I^S\omega^{S/E}) + \tau^{ext} \tag{3.2}$$

Here, v^S is the (inertial) velocity of the seat, $\omega^{S/E}$ the (inertial) angular velocity of the seat/pilot, m the combined seat/pilot mass, I^S the composite seat/pilot moment of inertia with respect to the center of gravity, and a^{ext} and τ^{ext} the applied acceleration and torque, respectively.

The applied force environment includes aerodynamic, gravity, all rocket and catapult, and drogue forces. For the time being, the development presented in this section will neglect disturbance effects modeled as noise, in addition to aero forces and torques generated by stabilization devices such as fins. Included in the dynamic model, but not distinguished symbolically here, is the mass-inertia change resulting from drogue deployment. For this model, the drogue will be assumed to deploy instantaneously, and the mass-inertia update will be effected at drogue

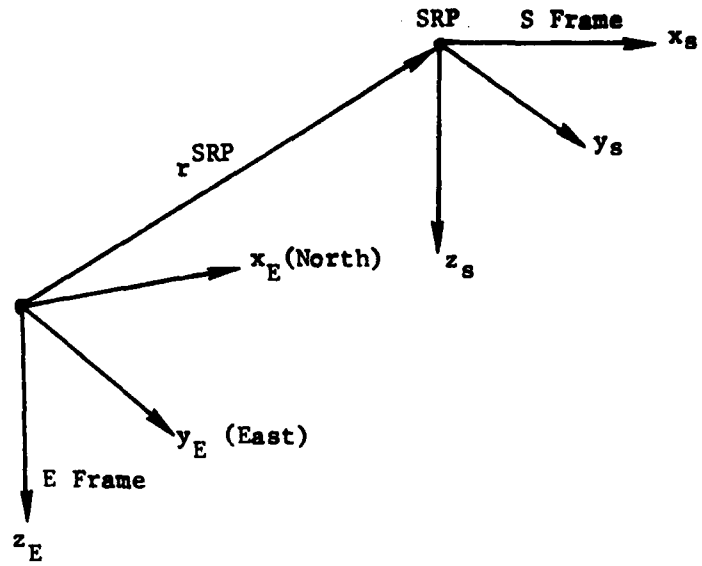

FIGURE 3.1. E and S Frame Geometry. The Euler sequence to the S frame from the E frame is yaw, pitch, roll.

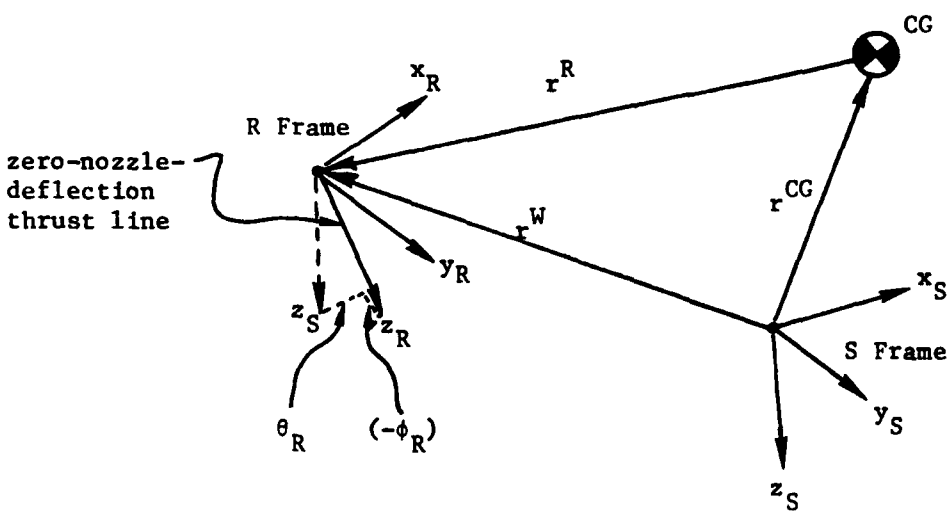

FIGURE 3.2. S and R Frame Geometry. Each rocket has an R frame.

deployment time. Most of the dynamic analysis, however, occurs during the sustainer-on phase, with no drogue chute deployment.

The use of a rotating system for defining the basic dynamics in Equations (3.1) and (3.2) is necessary in order to eliminate severe algebraic difficulties associated with a time varying inertia tensor. In addition, it is most convenient to represent many of the forces in the S frame. Equation (3.1) must be applied twice in order to isolate position variables such as altitude. An alternative method for computing position, which we follow here, is to transform the velocities to the E frame, and then directly integrate the E components. The Euler angles as presented below are already expressed kinematically in a directly integrable form. These angles are assumed to be in the yaw (ψ), pitch (θ), roll (ϕ) sequence, from E to S.

As is done in the EASIEST/SAFEST code, all force and torque components are expressed in the SRP-referenced S frame. They then are combined into a resultant force and torque before being converted to the CG frame. The catapult is assumed not to act on the free seat/pilot vehicle. Aero forces and torques are given as follows:

$$f^A = \bar{q}S \begin{bmatrix} C_x(\alpha,\beta,M) \\ C_y(\alpha,\beta,M) \\ C_z(\alpha,\beta,M) \end{bmatrix} \tag{3.3}$$

$$\tau^A = \bar{q}Sh^D \begin{bmatrix} C_\ell + pC_{\ell_p} \left(\frac{h^D}{2V}\right) \\ C_m + qC_{m_q} \left(\frac{h^D}{2V}\right) \\ C_n + rC_{n_r} \left(\frac{h^D}{2V}\right) \end{bmatrix} \tag{3.4}$$

In these equations, S is the seat/pilot reference area, $\bar{q}$ the dynamic pressure, h^D the hydraulic diameter of the seat/pilot, p, q, r the roll, pitch and yaw rates of the seat/pilot in S coordinates, V the speed in the wind, C_{ℓ_p}, C_{m_q}, and C_{n_r} are (constant) input aero damping coefficients, and the C are the SRP-referenced aerodynamic coefficients, which are modeled in EASIEST/SAFEST as tabular functions of angle of attack (α), angle of sideslip (β), and Mach number (M). We use bicubic spline representations to model the C_i as functions of α and β, based on results from Beale (1975) and White (1974). This model neglects direct Mach-dependent effects. An analytic representation of the aero coefficients in the control system model would greatly ease the computational burden of the control synthesis effort, but we have found it appropriate to evolve indirect schemes for inferring aerodynamic forces and torques. See Chapter 4.

As stated above, the drogue is assumed to deploy instantaneously to a steady state, line stretch condition. If we further assume that, in this condition, the line remains taut and along the wind axis direction, and further assume that the drogue's C_D is constant, then the force and torque on the seat/pilot due to the deployed drogue are:

$$f^D = -F^D\bar{q}\,[C_DS]^D\,v^W \tag{3.5}$$

$$\tau^D = r^D \times f^D \tag{3.6}$$

In these equations, $\hat{v}^W$ is the unit vector of the seat/pilot with respect to the wind, $[C_DS]^D$ is a constant drag parameter of the drogue, and r^D is the

bridle attach point moment arm. Typical values for $[C_D S]^D$ are about 5.0 ft^2.

The remaining forces are due to gravity and the propulsive devices. Gravity forces are expressed in the usual manner in the S frame by means of the Euler angles; the expressions for the propulsive forces and torques are derived in Section 3.2.1.2. We neglect any catapult-related interactions on the free seat/pilot body. Combining all of the above forces and moments (and converting the latter to a CG reference), and expanding the expressions in Equations (3.1) and (3.2) results in the complete nonlinear set of equations. (See Appendix A).

3.2.1.2 Rocket Force, Torque Equations. The arguments of f^R and τ^R in Equation (A.1) represent the major control variables for the seat/pilot system. These are thrust (T), nozzle pitch angles (θ), and nozzle roll angles (ϕ). These are depicted as vector quantities, with indices corresponding to a given nozzle. Note that this convention departs somewhat from that used in SAFEST/EASIEST. The YAW and PIT quantities in EASIEST are used in direction cosines, and do not seem to be as physically meaningful for use as nozzle gimbal angles as the ones we have defined. If each rocket's orientation in the S frame is specified by means of its own R frame (see Figure 3.2), then the zero nozzle deflection thrust is given by:

$$f^R = -T\hat{z}^R \tag{3.7}$$

where T is the rocket thrust magnitude, and $\hat{z}_R$ is the unit vector pointing in the direction of the exhaust plume, along the nozzle's axis of symmetry. The unit vector $\hat{z}_R$ does not necessarily point along the fuel cylinder axis of symmetry. For example, the ACES II sustainer rocket fits in the seat back, pitched back from $(-\hat{z}^S)$, yet the nozzle axis points forward at about 45 degrees in the $(-\hat{z}^S)$-$(\hat{x}^S)$ quadrant, to go through the 50%-ile pilot CG. See Figure 3.3.

The unit vector $\hat{z}^R$ is oriented in the S frame by the angles θ_R and ϕ_R, as shown in Figure 3.2. The nozzle's zero-deflection orientation, as

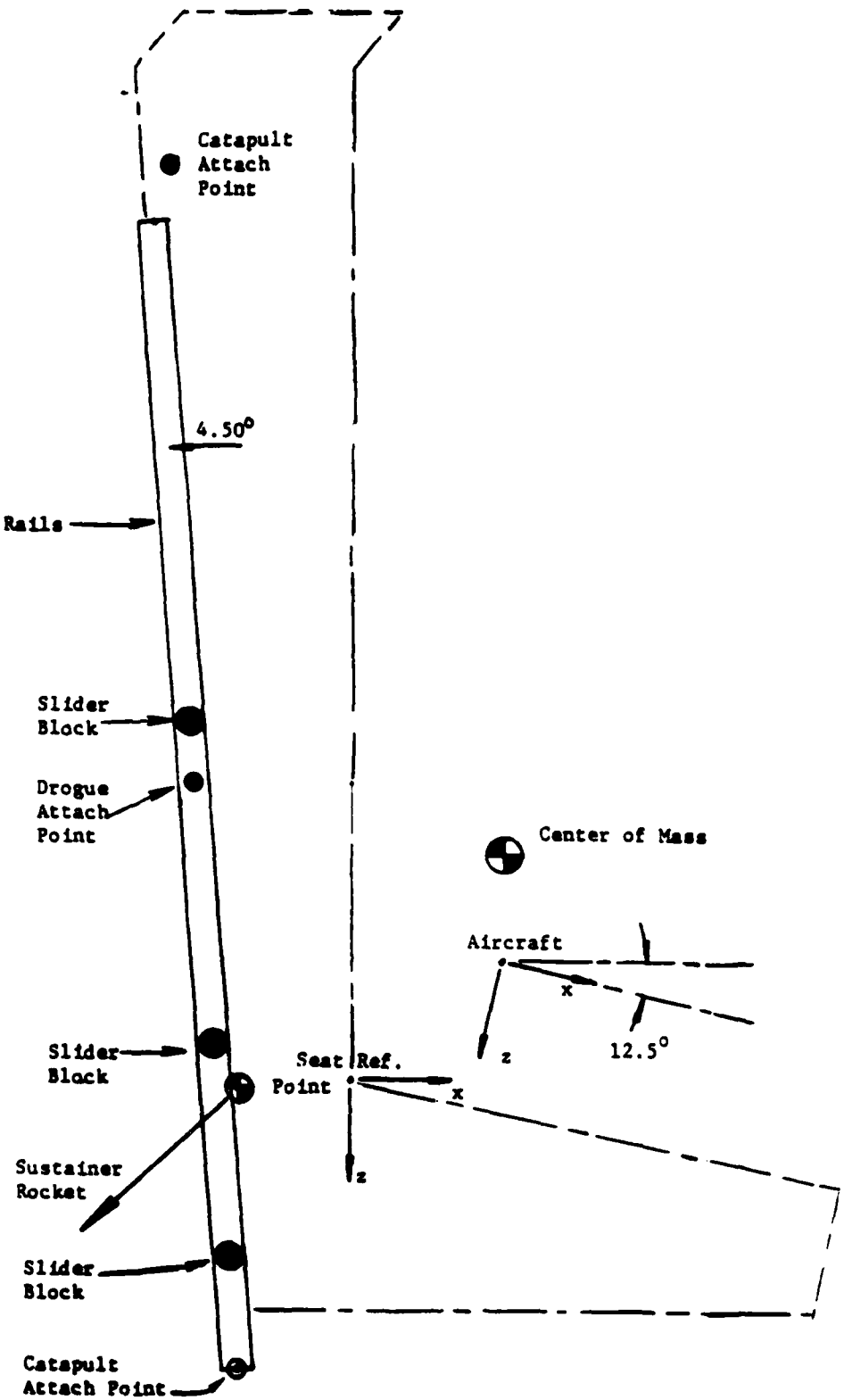

Figure 3.3 Aces II Ejection Seat as Modelled by EASIEST

well as the resultant nozzle deflections, are best defined using pitch (θ_R) and roll (ϕ_R) angles.

The torque on the seat/pilot due to each rocket is given by

$$\tau^R = (r^{RN/S} + (-r^{CG}))xf^R \tag{3.8}$$

In this equation, $r^{RN/S}$ is the location of a given nozzle with respect to the SRP, and r^{CG} is the CG location in the S frame. To quantify, for ACES II with a 95 percentile pilot, the EASIEST value for the CG location in S (in feet) is

$$r^{CG} = \begin{bmatrix} 0.511 \\ 0.0 \\ -0.790 \end{bmatrix} \tag{3.9}$$

For nonzero nozzle deflections, we define $\hat{z}_R^{RN}$ to be a given nozzle principal axis unit vector. Its general orientation in the appropriate R frame is given by

$$\hat{z}_R^{RN} = \begin{bmatrix} c_\phi s_\theta \\ -s_\phi \\ c_\phi c_\theta \end{bmatrix} \tag{3.10}$$

where, for example, $s_\theta = \sin(\theta)$, etc.

For convenience, sub- and superscripts have been omitted here from the nozzle deflection angles θ and ϕ. The general rocket force and torque expressions in the S frame expand to

$$f_S^R = (-T)\begin{bmatrix} C_\phi s_\theta c_{\theta_R} - s_\phi s_{\phi_R} s_{\theta_R} + c_\phi c_\theta c_{\phi_R} s_{\theta_R} \\ 0 \quad - s_\phi c_{\phi_R} \quad + c_\phi c_\theta s_{\phi_R} \\ -c_\phi s_\theta s_{\theta_R} - s_\phi s_{\phi_R} c_{\theta_R} + c_\phi c_{\theta_R} c_{\phi_R} c_\theta \end{bmatrix} \underset{=}{\Delta} \begin{bmatrix} F_x \\ F_y \\ F_z \end{bmatrix} \tag{3.11}$$

$$\tau_S^R = \begin{bmatrix} y_{RN} F_z \quad - (z_{RN} - z_{CG}) F_y \\ (z_{RN} - z_{CG}) F_x \quad - (x_{RN} - x_{CG}) F_z \\ (x_{RN} - x_{CG}) F_y \quad - y_{RN} F_x \end{bmatrix} \underset{=}{\Delta} \begin{bmatrix} \tau_x \\ \tau_y \\ \tau_z \end{bmatrix} \tag{3.12}$$

Each propulsive device modeled on the seat will have relations of the above forms. Note that, based on (3.9), y_{CG} is set equal to 0.0.

The linearized versions of (3.11) and (3.12) are now developed. At this time, it is felt that the linear versions will be appropriate for all control synthesis applications. This is related in part to the fact that the effective nozzle cone angle will probably not exceed 20 degrees. The cosine projection of 20 or 30 degrees generates about a 4 % error in the linear model, and the sine error is about half of that.

Define the linear nozzle deflection angles as δ_θ (pitch) and δ_ϕ (roll). Because these are "sufficiently" small, they may be treated as components of vector quantities, whereas the pure Euler angles can not. However, we retain the sign conventions of the Euler set, so that positive pitch deflection is along $+x_S$, and positive roll deflection is along $-y_S$, as seen in the linearized version of Equation (3.10)

$$\hat{z}^{RN} \simeq \begin{bmatrix} \delta_\theta \\ -\delta_\phi \\ 1 \end{bmatrix} \tag{3.13}$$

Equation (3.13) orients the nozzle, to first order, with respect to its zero deflection axis, $\hat{z}^R$.

SSI Configuration. At this point, it is convenient to represent specific configurations of nozzle locations for seat/pilot TVC. Many of the following assumptions are not necessary. The configuration presented below is best taken as a "generic" one, for it possesses resultant features of many likely hardware configurations. The goal of a given configuration is to provide full, decoupled control of the seat attitude and displacement motion. The configuration presented in Figure 3.4 can achieve this goal at least mathematically, when control of thrust magnitudes is introduced along with thrust vectoring. Controllability studies are an important aid in finalizing the configuration (Section 3.2.2).

The configuration presented here has been of great use in demonstrating feasibility of the control concept, as well as in studying the effect of actuation dynamics on overall system performance. However, this configuration is not practical because certain commanded nozzle deflections and rates lead to thrust impingement on parts of the seat and/or pilot. An alternate, more practical configuration is discussed in Section 3.2.2.4. This configuration uses many more nozzles, and spreads them out over the seat for more responsive, efficient energy management.

Figure 3.4 is a representation of three gimballed nozzles directing the (variable) thrusts of three separately controlled propulsive devices. Number 2 may be thought of as being similar to the current ACES II sustainer rocket in location and thrust capacity, except that here, we allow nozzle deflections. Numbers 1 and 3 can be thought of as vernier rockets, with perhaps less thrust each than Number 2. The thrust modulation and vectored thrust features of Number 2 are primarily for

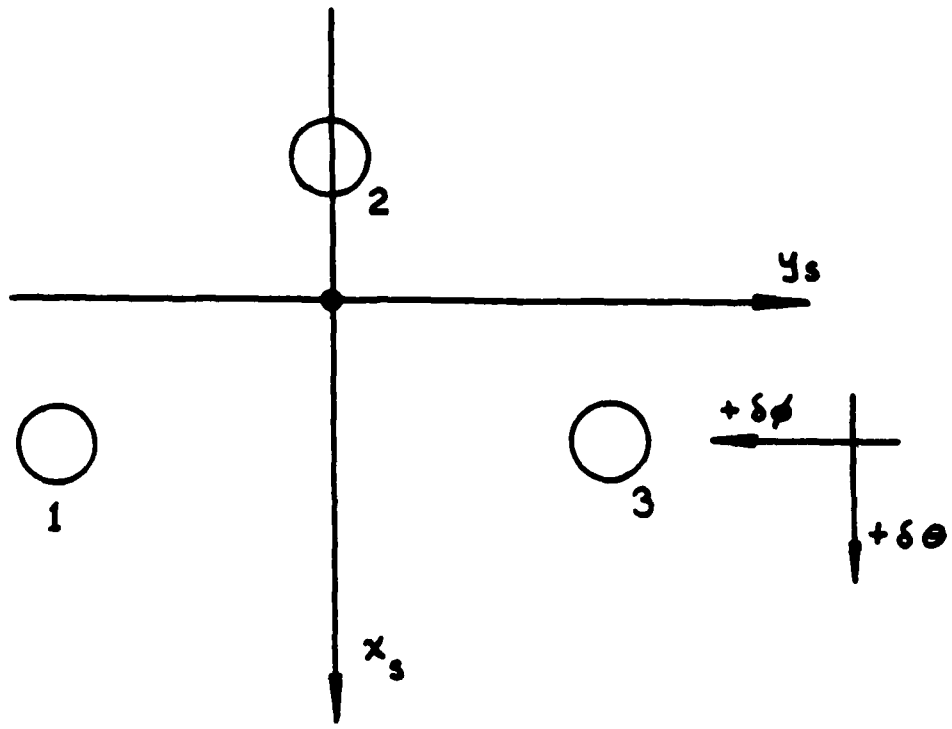

Figure 3.4. Representative Nozzle Geometry; Looking from Below. See also Section 3.2.2.

steering control; however, they would also provide a certain amount of redundancy in attitude control, which is the primary activity of Numbers 1 and 3. It is not important at this time to specify the type of hardware used to vector the nozzles.

The key to Figure 3.4 is the symmetry of nozzle placement with respect to the seat x-z plane:

$$
\begin{aligned}
x_1 = x_3 &\overset{\Delta}{=} x \quad ; \quad y_3 = -y_1 \overset{\Delta}{=} y \quad ; \quad z_1 = z_3 \overset{\Delta}{=} z \\
y_2 &= 0 \quad ; \quad \theta_{R_2} \overset{\Delta}{=} \theta_2 \\
\theta_{R_1} = \theta_{R_3} &\overset{\Delta}{=} \theta_R \quad ; \quad \phi_{R_1} = \phi_{R_2} = \phi_{R_3} = 0 \\
T_1 = T_3 &\overset{\Delta}{=} T
\end{aligned}
\tag{3.14}
$$

Equations (3.14) were used under the following considerations. Nozzle No. 2 should point nominally through the 50%-ile pilot's seat/pilot CG. The geometry for this is seen in Figure 3.2. If r^{CG} is taken to be the 50% CG, then, the nominal zero deflection thrust line is given by

$$r^R = r^N - r^{CG} \tag{3.15}$$

where r^N is the nozzle location with respect to the SRP. The unit normal of $r^N = \hat{z}^R$. Equation (3.10) can define $\hat{z}^R_S$ if we replace θ and ϕ with θ_R and ϕ_R, respectively. If we then equate this version of $\hat{z}^R$ with the normalized components of Equation (3.15), there results

$$\phi_R = -\sin^{-1}\left(\frac{y^N}{d_R}\right) \tag{3.16}$$

where $$\theta_R = \sin\left[\frac{(x^N - x^{CG})}{\sqrt{(x^N - x^{CG})^2 + (z^N - z^{CG})^2}}\right] \tag{3.17}$$

$$d_R = \left[\sqrt{(x^N - x^{CG})^2 + (y^N)^2 + (z^N - z^{CG})^2}\right] \tag{3.18}$$

If Number 1 and 3 nozzles have primarily an altitude control role, it may not be necessary to require them to have a zero deflection thrust line through the 50%-ile CG. This is because these nozzles would thrust only to cancel disturbance torques, and there is no "nominal" direction associated with this activity. This is why all of the ϕ_{R_i} in (3.14) were set to 0.0. This condition could be removed of course, should evolving operational requirements demand it, i.e., for reliability considerations. These rockets may be thought of as RCS clusters of nozzles, with each nozzle fixed. An average thrust direction over time could be generated by proper modulation of thrust pulse widths in the appropriate nozzles.

Under the above assumptions, the linearized force and torque equations for the entire configuration of Figure 3.4 become

$$f_S^R = f_S^{R_0} + \begin{bmatrix} -Tc\theta_R & 0 & -T_2c\theta_R & 0 & 0 \\ 0 & T & 0 & T_2 & 0 \\ Ts\theta_R & 0 & T_2s\theta_2 & 0 & 0 \end{bmatrix} \vec{u} \tag{3.19}$$

$$
\tau_S^R = \begin{bmatrix} 0 & T(z-z_{CG}) & 0 & -T_2(z_2-z_{CG}) & Ts_{\theta_R}y \\ -T[(x-x_{CG})s_{\theta_R} + (z-z_{CG})c\theta_R] & 0 & -T_2[(z_2-z_{CG})c_{\theta_2} + (x_2-x_{CG})s\theta_2] & 0 & 0 \\ 0 & T(x-x_{CG}) & 0 & T_2(x_2-x_{CG}) & Tc_{\theta_R}y \end{bmatrix} \vec{u} \tag{3.20}
$$

where

$$
f^R{}_0 = (-T) \begin{bmatrix} 2s_{\theta_R} \\ 0 \\ 2c_{\theta_R} \end{bmatrix} + (-T_2) \begin{bmatrix} s_{\theta_2} \\ 0 \\ c_{\theta_2} \end{bmatrix} \tag{3.21}
$$

In Equation (3.20), Number 2 has been located in the x-z axis plane of the seat. The control vector $\vec{u}$ arises from the linearity assumption and the particular configuration:

$$
\vec{u} = \begin{bmatrix} \delta\theta_1 + \delta\theta_3 \\ \delta\phi_1 + \delta\phi_3 \\ \delta\theta_2 \\ \delta\phi_2 \\ \delta\theta_3 - \delta\theta_1 \end{bmatrix} \tag{3.22}
$$

3.2.1.3 Linear free body seat/pilot equations. Linearization of Equations (A.1) is an exercise which must be done with care, especially in the case of seat dynamics, because the seat/pilot system and its operating environment is highly coupled and nonlinear. In addition, the nonlinearities are not only in the nature of the usual complicated aerodynamics, inertia coupling, variable mass, and propulsive effects, although these certainly are present here. Additional nonlinearities also arise in seat/pilot dynamics because of discontinuities arising from such events as catapult effects, discontinuous mass/inertia changes due to chute deployments, line stretch effects, and the rockets turning on and off. It is quite obvious, then, that the various assumptions made to linearize be clearly noted, and the limitations which arise from them be observed as closely as possible.

Linearization is assumed to occur about a given nonlinear operating point. It is consistent within the expected accuracies of the seat/pilot linearization process to assume, for the ACES II prototype, that

$$I_{xy} = I_{yz} = 0.0 \tag{3.23}$$

This assumption is not strictly necessary for producing a linear system, but it greatly reduces algebra and eventually, duty cycle requirements; also, it strengthens more standard linear assumptions which allow decoupling of variables which appear as products in the nonlinear equations. In the ACES II 95 %-ile case, the determinant of the full inertia tensor for the seat/pilot system in S coordinates is 2396.2 slug-ft^2, and its value under the assumption (3.23) is 2398.6 slug-ft^2.

The operating point is defined as generally as possible. This is a reflection of the typical highly coupled attitude motions a seat is subjected to under most escape conditions. Thus, all state variables are redefined as follows:

$$x \rightarrow \bar{x} + x \tag{3.24}$$

The left-side variable x is computed from the nonlinear set (A.1); $\bar{x}$ represents the value of this variable at the operating point of interest, and the right-side variable x becomes the linear state variable. Before presenting the equations, we note the following: (i) Linearization is equivalent to generating the system Jacobian matrix. This is done numerically by EASIEST; the analytic Jacobian derived here was verified numerically against a particular EASIEST computation, with good results. (ii) Some nonlinear variables decouple from the main system in the sense that they are not needed to define the dynamics of the major variables. The variables which decouple are x, y, z, and ψ. Of these, x and y are eliminated from the system totally. Altitude ($-z$) and heading (ψ) are retained because of more relevant interest. Altitude, or its estimated value, is an important variable in the steering loop. (iii) Angles of attack and sideslip are defined by the approximations

$$\alpha \simeq w/V \qquad \beta \simeq v/V \tag{3.25}$$

where the CG speed V is related to state variables via

$$V^2 = u^2 + v^2 + w^2 \tag{3.26}$$

(iv) Finally, dynamic pressure was assumed to be constant in the linear set derived here. The realities of high Q ejection could require reassessing this assumption to include first order dynamic effects while keeping air density fixed. The linear seat/pilot system is also shown in Appendix A.

We now present the equations for spinal compression of the crewperson during ejection. These are extracted directly from MIL-S-9479B, and the EASIEST software:

$$\ddot{\delta} + 2\omega_n\zeta\dot{\delta} + \omega_n^2\delta = g_z \tag{3.27}$$

where g_z is the z-axis load factor, δ is the spinal compression in inches, and the natural frequency and damping of this system have the values

$$\omega_n = 52.9 \text{ radians/sec}$$
$$\zeta = 0.224 \tag{3.28}$$

The dynamic response index, DRI, is related to δ by

$$DRI = \frac{\omega_n^2 \delta_{max}}{g} = 86.9\ \delta_{max} \tag{3.29}$$

Equation (3.29) is driven by the z-axis load factor. The seat/pilot load factors, in g's, are defined with respect to the combined CG by the following:

$$\begin{bmatrix} g_x \\ g_y \\ g_z \end{bmatrix} = -\left(\frac{1}{g}\right)[f^{ext} - \dot{\omega}^{S/E} \times r^{CG} - \omega^{S/E} \times (\omega^{S/E} \times r^{CG})]_S \tag{3.30}$$

In this equation f^{ext} represents all external forces applied to the seat/pilot. There is some question as to the adequacy of referencing the load factors to the combined CG, rather than to a more vital location, such as the pilot's head or a particularly sensitive internal organ. However, for this activity, we shall remain within the scope of the level of accuracy of human tolerance modeling as presented currently in EASIEST/SAFEST.

Another consideration entirely appropriate for the system (A.2) is the modeling of the actual nozzle dynamics. At this point, a first order lag model seems acceptable. The consequence of introducing even first order dynamics is to add each nozzle deflection angle to the list of state variables:

If δ_c is the commanded nozzle deflection, then

$$\dot{\delta} = -a\delta + K\delta_c \tag{3.31}$$

where δ is the actual nozzle deflection (state variable), and a is the system break frequency, or inverse time constant. The parameter a is largely set by the physical slew rate of candidate nozzles, and is a key design factor. More complicated models are not really very critical to the control design problem, because of the hierarchical nature of the design method favored here. This hierarchy implies that actuator or valve dynamics occur fast enough to be dynamically nearly "invisible" to lower levels in the hierarchy; and, in any case, first order models are adequate to study dynamic interaction.

3.2.1.4 Seat-on-rails Dynamics. This section covers dynamics of a phase of the escape sequence for which explicit control design was not done. The discussion is included for completeness. A modification of the control approach can be applied during this phase, which also is concerned with initialization, self-test, determining condition, and start-up activities for the main controller function.

The dynamics of the seat/pilot system on the guide rails is naturally determined almost completely by the behavior of the "host" aircraft. For the requirements of the control synthesis effort, the rails will be assumed to be attached rigidly to the aircraft, and to impart to the seat only a friction force as it slides up them, in addition to the contact forces which constrain much of the seat's motion to follow that of the aircraft. The degrees of freedom of the seat on the rails are thus restricted to the translational degree along the rails, until all but one set of attach blocks is free of the rails. At this point, there is also a degree of freedom in pitch.

There are, then, at most two state variables which can be modulated by the seat control system while it is on the rails: rail position and pitch angle with respect to the aircraft reference. The only meaningful control during this phase is supplied by the catapult system. The magnitude of catapult thrust could be controlled between minimum and maximum values as a means of controlling acclerations on the crewperson over the range of escape conditions. A minimum catapult thrust, a value which would vary with escape condition, is needed to ensure clearing the vertical stabilizer

of the aircraft. The maximum value is closely related both to the DRI (dynamic response index) limit the pilot can tolerate, and to the aircraft z-axis acceleration at ejection. Depending on these factors, then, the maximum attainable catapult thrust will likely be modulated.

For the system considered, the seat is assumed to have two degrees of freedom, translation along the rails and a pitch angle about the two slider blocks. The left and right slider blocks are assumed to translate along the rails equal amounts. The possibility that the blocks may bind in the rails due to lateral forces on the seat is ignored in the model.

Explicit consideration of the forces of constraint, i.e., the forces on the slider blocks that keep them in the rails, is avoided by using generalized coordinates and the Lagrangian formulation of mechanics. The equations of motion that result are second order in two variables, or equivalently, first order in four variables. The simplicity is useful in any attempt to obtain purely analytical results concerning the behavior of the seat while it is still on the rails. See equation development details in Appendix A.

3.2.2 Rocket Nozzle Configurations and Controllability.

The use of vectored thrust flight control logic on an ejection seat requires significant upscaling in the propulsion system. Current rocket actuation devices provide a fixed thrust level (at a given temperature) at a fixed attitude. Requirements for closed loop control for the next generation seat lead to propulsion systems which are to be considerably more flexible and responsive than current systems. A key factor in designing properly the configurations of such a system is in determining whether the system is controllable. We now digress a bit to relate this concept to the current design effort.

Loosely speaking, a system is controllable if it can be brought from some given state at t_0, say x_0, to another state, x_1, within a finite time (t_1-t_0). More exact definitions involve other concepts such as "reachability" - i.e., the state x_1 must be reachable using an admissable set of controls.

In the ejection seat problem, attitude and trajectory control are important. If this control is to be obtained strictly via vectored thrust control, ignoring for the time being such devices as the drogue chute, aerodynamic surfaces, momentum wheels (e.g., STAPAC), etc., then it is very important to establish a minimally complex nozzle configuration which will provide the required control of the seat. To scope this problem we are seeking a vectored thrust system which can be packaged on an escape seat - a requirement which results in several performance limitations - and which can provide three-axis attitude and three-axis translational control of the combined seat/pilot system, which is viewed for now as one rigid body. This is the basic 6 DOF control requirement and the major design issue is to develop such a system with current hardware and software technology, which will provide adequate control of attitude and trajectory.

This section addresses vectored thrust control for longitudinal, then the complete longitudinal/lateral (6 DOF) cases. In order to mechanize a minimally capable 6 DOF configuration, we have initially developed a design which has a minimum number of independent nozzles, three for full 6 DOF control. Each nozzle is assumed to be able to supply any thrust orientation and magnitude (within physical limits) independently of any other nozzle/thruster system, although some hardware components could conceivably be shared. Also, the thrust vectoring mechanism is not an issue here.

Ideally, the controller will be "decoupled", that is, one control input affects one output variable only. This goal would be very difficult to accomplish for 6 DOF ejection seat control; furthermore, some coupling is very natural and not a hindrance to control design. For example, the seat can be commanded to an attitude which is not only "safe" (in terms of biodynamic factors) but also orients the net thrust vector appropriately for the specific trajectory requirement. Thus, attitude control is always important, and usually dictates or couples into, trajectory, or steering, control. In short, we are trying to achieve independent attitude and trajectory control, while recognizing that some coupling between them is allowable from the standpoint of controller objectives, and most likely necessary from a mechanization standpoint.

More realistic designs tend to have many more nozzles, and each nozzle is dedicated to the control of one or at most two degrees of freedom. Typically, pairs of nozzles are used for attitude control about each axis, and translational control is provided by other thrusters of larger capacity. By greatly increasing the number of nozzles, each nozzle becomes mechanically simpler, and greater control redundancy, hence reliability results. Many of the nozzles can thereby be fixed in attitude, which further enhances reliability as well as simplicity. We have examined such a configuration also, and it is described in Section 3.2.2.4.

3.2.2.1 3 DOF controllability. For pure longitudinal control, as for more complicated systems, we start with the simplest system, and only reluctantly add more complexity. A single nozzle is thus analyzed first (Figure 3.5). The usual nozzle deflection angle limits (slew rate limits are also very important, but this is not directly a controllability issue) and selectable thrust capability provide less than full controllability at best; however, a configuration will be considered if it can supply sufficient forces and torques for the allowable escape conditions (speed, attitude, altitude).

One nozzle, shown in Figure 3.5, is not sufficient for 3 DOF (longitudinal) control, even when thrust magnitude (T) and deflection angle (δ) can vary independently. By proper design, this nozzle can be located so that its cone angle will produce ranges of the force vector coincident with the majority of desired accelerations. However, the simultaneous satisfaction of an altitude requirement cannot, in general, be met.

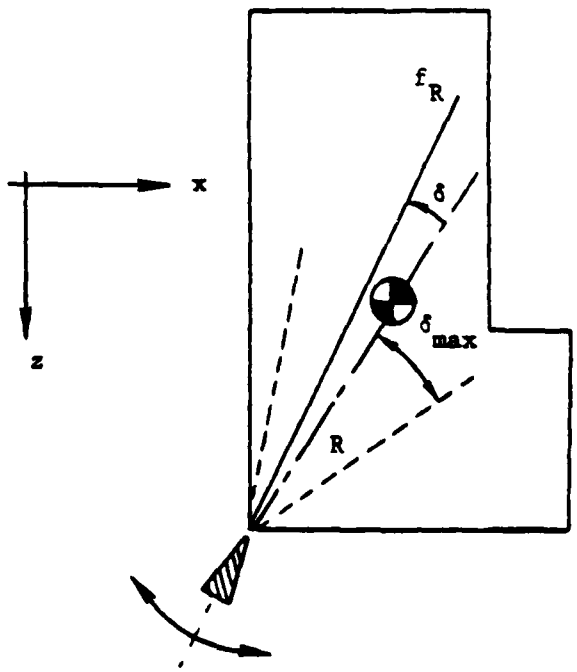

θ	:	defines nominal thrust line
δ	:	(pitch) nozzle deflection angle
δ_{max}	:	nozzle cone angle
R	:	nozzle/CG distance

Figure 3.5 Three Degree-of-Freedom Controllability Schematic, One Nozzle.

There are three basic quantities to be controlled,

$\dot{\omega}_y = \dot{q}$ = pitch acceleration

$a_x = \dot{u}$ = forward acceleration

$$a_z = \dot{w} = \text{vertical acceleration}$$

It is very evident that, with (T,δ) as the only independent controls, only two of the above quantities can be controlled explicitly.

$$M_y = -T\,R\sin\delta$$

$$a_x = T\cos(\theta+\delta)/\text{mass} \qquad (3.32)$$

$$a_z = -T\sin(\theta+\delta)/\text{mass}$$

Given desired values of these quantities, M_{y_D}, a_{x_D}, a_{z_D}, Equation (3.32) shows that, say, $u = (T,\delta)$ can be selected to control $a = (a_x, a_z)$. (θ is a fixed parameter). If this is done, M would be fixed also, and would not, in general, be appropriate for pitch control. Control of at least one of the dynamic variables must be sacrificed with this configuration. (This could be acceptable if, say, θ, T_{min}, R, and δ_{max} were selected so that there were an $|a_z|_{min}$ adequate for high Q tail clearance. However, this value may be inadequate for a 0/0 or other low altitude adverse attitude escape, where more z-axis capability is needed, but would perhaps conflict with the M and a requirements. Control logic could weight which two variables are to be controlled depending on conditions. This type of approach was taken for the configuration discussed in Section 3.2.2.4). Addition of a second, similar nozzle would provide adequate, independent 3 DOF control in the appropriate location (e.g. point B of Figure 3.5). The above analysis suggests that, for this case, a minimum requirement (necessary condition) is that the number of control variables at least equal the number of variables to be controlled. We do not offer a formal proof of this contention, but note that this contention is not true of dynamic systems in general. In the discussion of 6 DOF control which follows, however, we will show by means of an example that this is not also a sufficient condition.

3.2.2.2 <u>6 DOF Controllability</u>. In the last subsection, it was shown that 3 DOF attitude and steering control was not possible with one independent nozzle. One nozzle is thus clearly inadequate for 6 DOF control, even when it can move in a full, 3-D cone and vary thrust

magnitude. One nozzle in 6 DOF applications consists of three basic controls:

$$u = (\delta\theta, \delta\phi, T)$$

Based on the above discussions, it follows that a nozzle with this control capability can control translation, within the usual thrust magnitude and cone angle limits. If devoted to this activity, it will, in general, also generate a non-zero torque. This torque may or may not oppose attitude control objectives, but it cannot be changed without compromising the steering control function.

If we do isolate the translational (CG position) control function, however, one nozzle suffices: nozzle force, $f = -T\,\hat{z}^{RN}$, as defined in Equation (3.10). From this equation, it is evident that any "reasonable" f can be achieved by at least one feasible set $u = (\delta\theta, \delta\phi, T)$. Figure 3.2 defines the basic nozzle geometry. Nominal or zero-deflection thrust is along the $(-\hat{z})$ axis. For ejection seats, this axis will be located to pass through, or close to, the seat/pilot CG.

The above is a case in which m = 3 control variables "fully" control n = 3 output variables[1] (a_x, a_y, a_z). It should not be necessary to use equations here to argue convincingly that, at any given orientation, the 2 orthogonal axes lying in the plane perpendicular to the thrust axis can be controlled via thrust vectoring, but not the thrust axis itself. Thus, if the thrust axis is called the roll axis, then only pitch and yaw attitude control is possible with any one nozzle.

It is therefore only one simple step further to conclude that two nozzles, each with 3 independent controls (6 total) cannot fully control the seat/pilot six degrees of freedom. Any five of these quantities can be controlled using a two nozzle configuration (due to dynamic coupling). Partial control is possible, but may come at the expense of unacceptable operational compromises. We have confirmed this result numerically. A

---

[1]Output variables are often a subset of the state variables, but more generally, they are functions of the state variables.

control matrix $B \triangleq \partial(\dot{x})/\partial u$ for the two nozzle configuration has been set up, using $n = m = 6$. B was shown to have rank 5.

Analytically, it is easier to look at submatrices of B to justify the above conclusions. Consider

$$\begin{bmatrix} \Delta f \\ \Delta M \end{bmatrix} = \begin{bmatrix} B_{11} & B_{12} \\ B_{21} & B_{22} \end{bmatrix} \begin{bmatrix} u_1 \\ u_2 \end{bmatrix} \tag{3.33}$$

where $u_1 = (\delta\theta, \delta\phi, T)$ for nozzle 1, etc., and each of the 4 submatrices of B are 3x3 in size. Equation (3.33) represents the linearization of the force torque equations about some nominal dynamic condition; in this case, u_1 and u_2 represent changes from the (nominal) control settings U_1 and U_2.

B_{11} and B_{12} are very similar in form; one merely refers to nozzle 1 and the other to nozzle 2. The only difference lies in the parameter values which locate the nozzles. Thus, if B_{11} is rank-deficient, so would be B_{12}. The same reasoning applies to the bottom half of B, $[B_{21} B_{22}]$. B_{1j} (where $j = 1,2$) has the form:

$$B_{1j} = \left[\begin{array}{cc|ccc|cc} -T_j & c_{\theta_j} & T_j & s_{\theta_j} & s_{\phi_j} & -c_{\phi_j} & s_{\theta_j} \\ 0 & & T_j & c_{\phi_j} & & s_{\phi_j} & \\ T_j & s_{\theta_j} & T_j & c_{\theta_j} & s_{\phi_j} & -c_{\phi_j} & c_{\theta_j} \end{array}\right]$$

where θ_j and ϕ_j are the angles which orient the nominal thrust line for nozzle j in the seat/pilot body axes, and $c_{\theta_j} = \cos(\theta_j)$, etc.

Controllability implies here invertibility of B_{ij}. If B_{11} is non-singular, than a unique control set u_1 can be found for a given vector Δf. This can be considered a sufficiency condition, but not a necessary condition. Thus if $\det(B_{1j}) \neq 0$, our assertion that one nozzle fully controls 3 axis translation is valid. The determinant computes easier if T_j is set = 1.0, which can be done without loss of generality. Then

$$\det(B_{1j}) = c_{\phi_j}\,[c^2_{\theta_j}\;c_{\phi_j} + c_{\phi_j}\;s^2_{\theta_j}\;] - s_{\phi_j}\,[-c^2_{\theta_j}s_{\phi_j}\;-s^2_{\theta_j}\;s_{\phi_j}]$$
$$= 1.0$$

For a situation in which the 2 nozzles are located symmetrically with respect to the seat/pilot x-z plane,

$$B_{2j} = \begin{bmatrix} -ys_{\theta_j}T_j & -(yc_{\theta_j}s_{\phi_j} + zc_{\phi_j})T_j & (yc_{\phi_j}c_{\theta_j} - zs_{\phi_j}) \\ -(zc_{\theta_j} + xs_{\theta_j})T_j & (zs_{\theta_j}s_{\phi_j} - xc_{\theta_j}s_{\phi_j})T_j & -(zc_{\phi_j}s_{\theta_j} - xc_{\phi_j}c_{\theta_j}) \\ -yc_{\theta_j}\;T_j & (xc_{\phi_j} + ys_{\theta_j}\;s_{\phi_j})T_j & (xs_{\phi_j} - yc_{\phi_j}s_{\theta_j}) \end{bmatrix}$$

where x and z are fixed moment arms to the seat/pilot CG from the nozzle and y is ± depending on whether nozzle 1 or 2 is used (j = 1 or 2). A little more algebra shows that

$$\det(B_{2j}) = 0.0 \quad , \quad j=1,2$$

Thus, for a representative configuration, the general conclusions concerning 6 DOF controllability using 2 nozzles have been quantitatively demonstrated. This means that, even though there are m = 6 free controls, they can control fully only 5 of the 6 output dynamic variables. More control capability, i.e., at least one more nozzle, is required, although the levels of attitude and steering achievable with the pure two-nozzle system may be considered to be marginally adequate. We feel, however, that the complexity of adding extra nozzles is more than offset by the much greater controllability which is achieved. Furthermore, proper design and placement of a three or four nozzle system will most certainly not double the size or weight of a two nozzle system, since, for example, the total system energy requirements are basically fixed. That is, four 2 thousand pound nozzle systems can provide as much energy as one 8 thousand pound rocket, but in a much more usable form for control.

3.2.2.3 A Possible 3-Nozzle Configuration. The following configuration is proposed from a control designer's point of view. See Figure 3.4. This configuration was also discussed in Section 3.2.1.2 in connection with development of the rocket force/torque equations. In terms of packaging, hardware implementation, etc., there may be a need for modification. Our subsequent analyses show that, for the variety of escape conditions and the demands these conditions place on the propulsion system, the minimum three-nozzle configuration produces impractical thrust directions in many cases. That is, very large gimbal angle changes (leading to possibly unrealizable slew rates) and/or exhaust impingement on the pilot or seat often develops. A more realistic configuration is discussed in the next section. One can assume that either RCS values or gimballed nozzles are used. The key concern here is the functional performance of this configuration. A configuration is needed which is able to convert the force and torque commands into specific nozzle deflections andthrust magnitudes. The functionally easiest way to do this is to locate two nozzle clusters at a maximal moment arm location (e.g., off the pilot's shoulders), and dedicate these exclusively to attitude control. These nozzles would be symmetric with respect to the seat/pilot x-z plane. A third nozzle with full gimbal and selectable thrust capability, located about where the ACES II sustainer rocket is, would then provide trajectory/steering control.

We present here a slight modification of the above configuration. Again, it is necessary to emphasize that this is a functional and not a hardware configuration. The modification reflects the fact that some coupling should exist at high Q. To use the trajectory thruster only for acceleration control would effectively "waste" its ability to aid in offsetting the large aero pitch torques at high Q. This would unnecessarily add more to the torque thrusters' energy requirements.

In the new scheme, the 2 symmetric thrusters would provide the only lateral control function, and would assist the central, larger, thruster with its functions, if they had any reserve capacity. The central thruster (No. 2 in Figure 3.4) would have only longitudinal control capability. That is, $u_2 = (\theta_2 , T_2)$. Nozzle 2 can be positioned so that it cancels

most of the high Q aero torque as well as thrusts in the standard, desired direction for escape (up and forward).

For the ACES II prototype, nozzles 1 and 3 in the configuration under consideration need a combined 2000 pound capability and nozzle 2 should be sized for about 9000 pounds. This configuration is invertible: that is, we can solve for u_1, u_2 and u_3's elements by using the force-moment equations given the commanded rocket forces and torques (f_c, M_c). The equations are:

$$\begin{bmatrix} f_x \\ f_y \\ f_z \end{bmatrix}_c = \begin{bmatrix} (X_1 + X_2 + X_3) \\ (Y_1 + Y_3) \\ (Z_1 + Z_2 + Z_3) \end{bmatrix}$$

$$\begin{bmatrix} M_x \\ M_y \\ M_z \end{bmatrix} = \begin{bmatrix} -z(Y_1 + Y_3) + y(Z_3 - Z_1) \\ z(X_1 + X_3) - x(Z_1 + Z_3) + z_2 X_2 - x_2 Z_2 \\ y(X_1 - X_3) + x(Y_1 + Y_3) \end{bmatrix}$$

and, for nozzle j,

$$f^{(j)} = (X_j, Y_j, Z_j)$$

in seat/pilot body coordinators, and the moment arms (e.g., x, z_2) are defined in Equation (3.14). The cartesian elements of $f^{(j)}$ are solved for first, and then readily converted to the "polar" elements (θ_j, ϕ_j, T_j).

The above problem is overdetermined. Thus, we define

$$k = f_{x_c}/f_{z_c}$$

and set

$$X_3 = k Z_1$$

This reduces the inversion problem to an (analytic) 3-by-3 matrix inverse, whose singularity is related only to nozzle location geometry.

3.2.2.4 A Practical Configuration.

The three-nozzle configuration discussed in previous sections is adequate for the preliminary analyses of the earlier project tasks, but a more practical design is needed for an operational seat. From the standpoint of rapid response for attitude control - which can be exceptionally critical in the case of yaw control at high Q, for example - and also simplicity, it is better to have more fixed thrusters than fewer gimballed thrusters. Eventually, weight and complexity considerations limit the number even of the simpler, fixed thrusters.

A careful design which can exploit redundancy, packaging and weight requirements in an efficient manner is beyond the scope of this project. Much of these design issues have been addressed by a parallel Research and Development program, Design of Selectable Thrust Propulsion Systems for Crew Escape.

In addition to this program, our own analyses led to the conclusion that dispersed pairs of thrusters, one pair for each of the three rotational axes, and one main thruster for translational control, represent a much more realistic design than that discussed in Section 3.2.2.3. Such a configuration, depicted "generically" in Figure 3.11 (next page) consists minimally of seven fixed nozzles, although one could be added for redundancy. A specific design, developed by Martin Marietta Orlando Aerospace for this project, was mechanized and tested successfully. Table 3.0 shows the definitions. The formulations for fr (rocket force) and tr (rocket torque) shown in the Table are invertible when optimization criteria are applied to resolve the overdetermined nature of the problem of solving the (fr,tr) system, which has six equations for uc, which has seven variables. The numerical simulations, which were run on the same problems utilizing the three-nozzle configuration of Section 3.2.2.3, show that the values for the uc components are very realistic, and within specifications. The thrust levels for the attitude thrusters, f1 to f6, are in the 0-2500

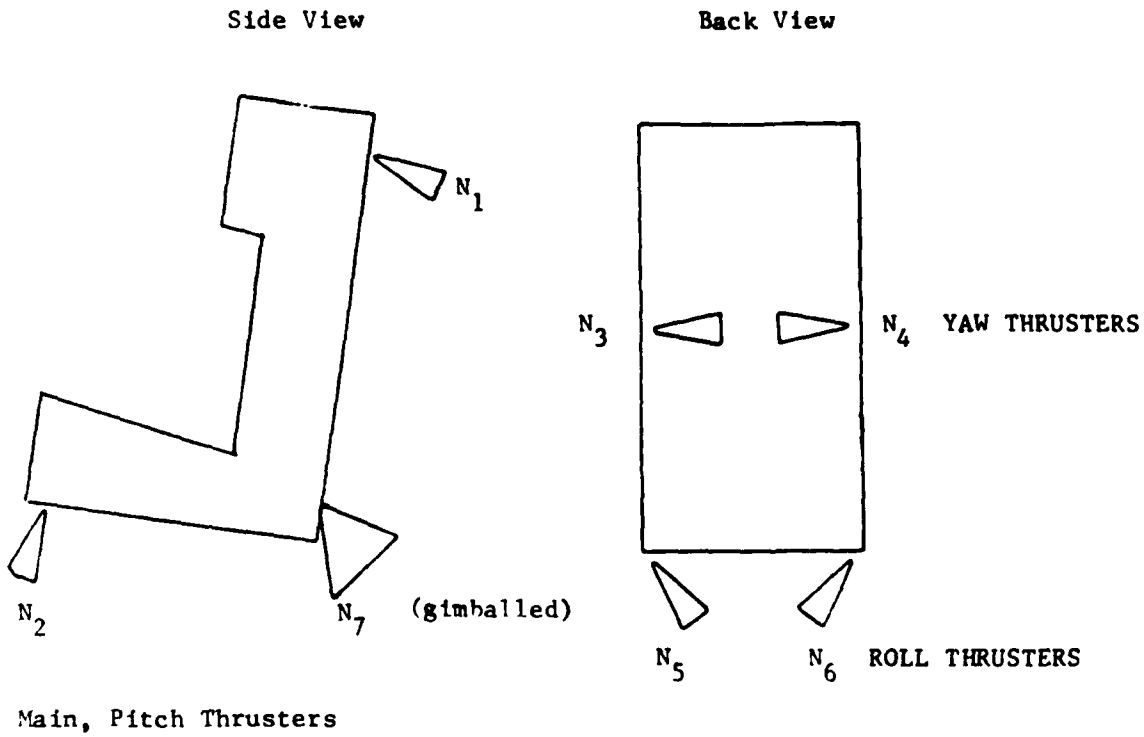

Figure 3.11 Seven-Nozzle Configuration, Based on Martin-Marietta Design. All thrusters are proportional control using MMOA High Force Gain Value Concept.

TABLE 3.0

SEVEN-NOZZLE ROCKET CONFIGURATION

FORCE-TORQUE EQUATIONS

$$\begin{bmatrix} fr \\ tr \end{bmatrix} = f(uc)$$

$$uc = (f_1, f_2, f_3, f_4, f_5, f_6, \theta_7, f_7)$$

where

f_1, f_2	-	pitch pair
f_3, f_4	-	yaw pair
f_5, f_6	-	roll pair
θ_7, f_7	-	main thruster

$$\begin{bmatrix} fr \end{bmatrix} = \begin{bmatrix} c_1 f_1 + c_2 f_2 + s_3 f_3 + s_4 f_4 + s_7 f_7 \\ - c_3 f_3 - c_4 f_4 - c_5 f_5 - c_6 f_6 \\ - s_1 f_1 - s_2 f_2 - s_5 f_5 - s_6 f_6 - c_7 f_7 \end{bmatrix}$$

$$\begin{bmatrix} tr \end{bmatrix} = \begin{bmatrix} l_1 f_5 - l_2 f_6 \\ m_1 f_1 + m_2 f_2 + m_7 f_7 \\ n_1 f_3 - n_2 f_4 \end{bmatrix}$$

pounds force range, for all escape cases studied. The main thruster level, f7, ranged between 3000 and 8500 pounds force, and the main thruster pitch gimbal angle remains within a 25 degree cone.

It is quite evident that the type of configuration described in this subsection is representative of a very efficient design, from a control point of view. See also Appendix B.

3.3 Detailed Description of Requirements.

In this section, we will discuss the control system design requirements. Subsection 3.3.1 defines flight conditions to be used as a baseline, and Section 3.2.2 presents specifications which bound allowable variations in the state and control variables. Section 3.3.3 describes requirements related to disturbances in the dynamic environment, and Section 3.3.4 discusses energy requirements for crew escape.

3.3.1 Flight Conditions for TVC Design. In this subsection, we identify what shall be called the design point flight conditions. These are defined as those conditions within the scope of the requirement of MIL-S-9479B with the followng features:

(1) A minimum set of flight conditions which will lead to a corresponding set of parameters for generating the reference accelerations. Each condition is to have a set of gains which can be used in the neighborhood of that condition. The robust design of the controller permits this type of use. A relatively small subset of pre-stored parameters would then be valid over the entire escape envelope (Figure 3.6).

(2) Each flight condition itself is within the escape envelope.

(3) Aircraft altitude, attitude, airspeed and acceleration are the major quantities specifying flight condition. Lesser parameters such as ambient temperature, nature of terrain, weather (i.e., as it affects visibility), etc. are not considered.

(4) Each flight condition selected will also consist of added aircraft acceleration subconditions: $G_x = -4$ and $2g$, $G_y = -2$ and $+ 2g$, $G_z = -3$ and

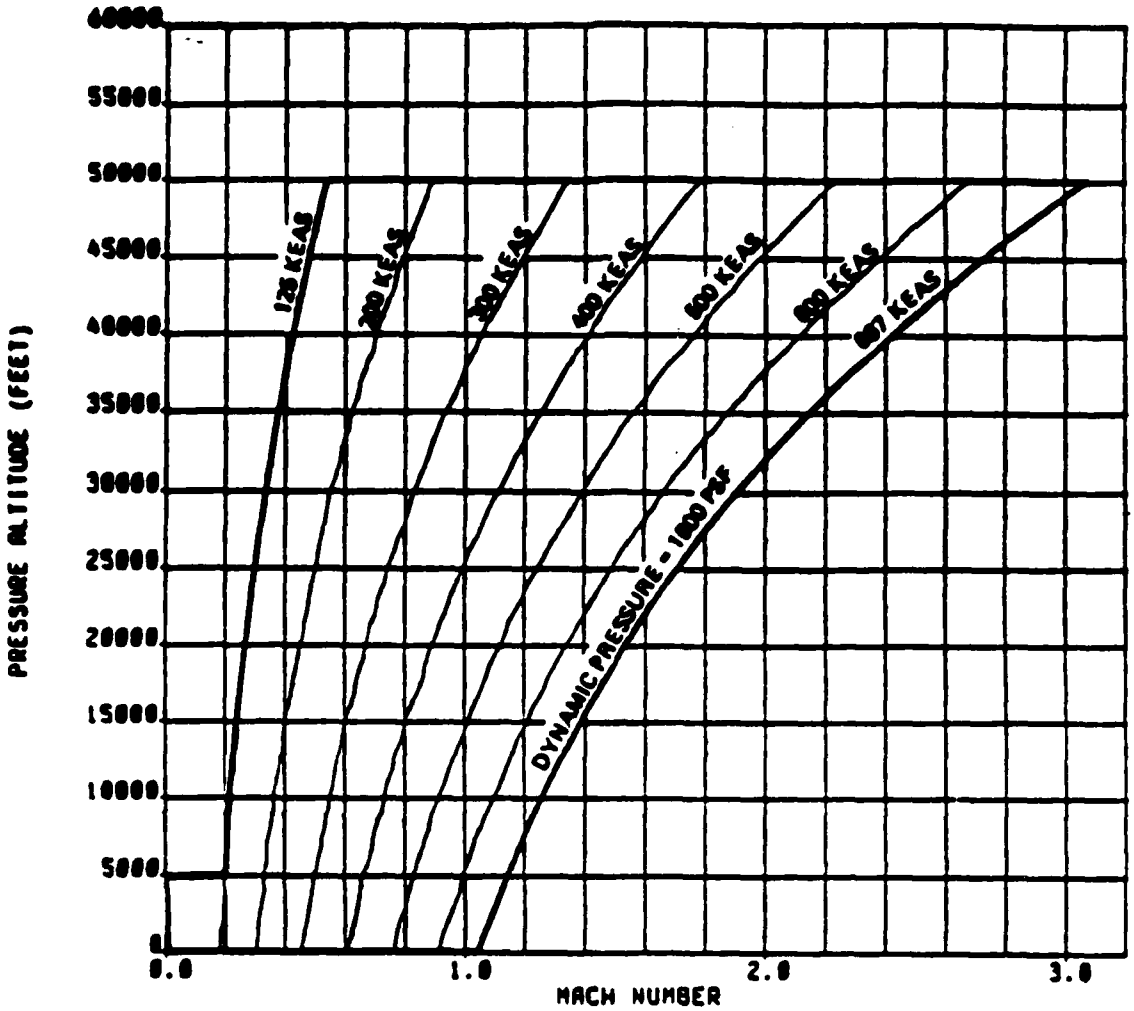

Figure 3-6 Design Flight Envelope for High Q Ejection Seat
(from Bull and Yurczyk, AFWAL-TR-81-3131, 1981)

+ 10g, and zero. These values represent extremes derived from project requirements.

Selection of flight conditions is dictated primarily by the nature of the aerodynamics and rocket or catapult accelerations on the seat. There is no doubt from the literature, and our EASIEST experience confirms this, that the dynamic pressure (Q) environment imposes severe restrictions on seat attitude, within the escape envelope of Figure 3.6. Energy sources must be sized, first, to deal with this problem; yet, they cannot be so excessive in terms of their own acceleration capability, needed for high Q conditions, that the radical value is violated at lower Q conditions. These considerations are quantified below.

The reason that aero and thrust accelerations are so critical is that they directly influence the physiological tolerance limits as quantified in the acceleration radical. Flight conditions are chosen because of their "worst case" on the radical, which is the major consideration over the entire escape envelope. Escape altitude is the second major consideration. There are some situations for which optimizing altitude is the most urgent requirement.

Achieving optimum altitude while meeting radical-imposed acceleration limits is primarily a steering problem. The various adverse altitude conditions specified in MIL-S-9479B (cf. paragraph 3.4.12) are each technically an escape condition; however, a steering law valid at -30 degrees pitch angle will also work at -60 degrees in pitch, as long as the sensors are working, and able to distinguish attitude.

These considerations have led us to select three major crew escape design point flight conditions for the initial control design phase:

(1) Low altitude, 687 KEAS. This condition emphasizes in the extreme both the dynamic pressure and altitude constraints. Our numerical studies (see Section 3.3) done to date show that greater thrust capability than is currently available on ACES II would be needed by a similarly configured seat. Most of this capacity is required to improve the radical by means of offsetting the aerodynamic decelerations, but capcity beyond this is a

necessity, because steering control for maximum altitude is so critical at this condition. Sufficient capacity to clear aircraft extremities at these conditions is required also. It is felt that current systems have this minimal capability. Three-axis attitude control is a very important control design criterion, since accelerations must be maintained along the seat roll axis. This condition is seen as the major challenge for concept feasibility. In Section 3.3 some quantitative requirements are presented.

(2) Low altitude, low speed (0/0). As stated above, the capacity of the energy sources which is needed for condition (1) becomes a potential liability at this condition, because the capacity tends to be excessive when not counteracted by aerodynamic forces. Except for the critical need to optimize altitude, this condition is thus a wholly different one from (1), and almost certainly the control motions will be different. Steering rather than attitude control per se is the predominant control design consideration. However, sufficient attitude control to implement the steering commands is required. Excessive capacity in the energy sources, coupled with aircraft accelerations, can lead to DRI excesses here, unless there is a thrust modulation capability. When this consideration is augmented by adverse attitude steering requirements (e.g., roll angle=180 degrees), it is evident that a truly effective design must have thrust magnitude control capability.

(3) High altitude, 687 KEAS. The major steering problem at this condition is avoidance of aircraft extremeties. The attitude control requirements are otherwise as severe as those of condition (1). By definition, the areodynamic forces on the seat are similar as the condition (1) forces. Another difference at this attitude is in chute deployment sequencing.

The remaining seven conditions are extracted directly from MIL-S-9479B (Table 3.1):

TABLE 3.1 Low Level Escape Performance
(from MIL-S-9479B)*

	Attitude		Velocity (knots)	Altitude (feet)
	Fore and aft	Roll angle		
(4)	Level	60	120	0**
(5)	Level	180	150	200
(6)	Level	0	150	300***
(7)	60 down	0	200	500
(8)	30 down	0	450	500
(9)	60 down	60	200	550
(10)	45 down	180	250	600

* Unless otherwise specified, the cited conditions are at the initiation of the escape sequence.
** Impact occurs at instant of seat/aircraft separation.
*** 10,000 feet per minute sink rate.

Our experience with the basic design and robustness attributes of the contoller indicates strongly that parameter selection for the cases above almost certainly will suffice when a "neighboring" set of parameters is applied to a different escape condition. We were able to exploit this robustness feature to great success during Task 4 activities of the project, relating to real time breadboard simulations. For this activity, twenty new cases were provided by the Air Force for demonstration of the controller (Chapter 7).

3.3.2 Minimum and Maximum State and Control Value Specifications. This subsection reports on various numerical studies conducted in support of Task 1 activity. The ACES II seat was used as the baseline seat model, and also for the most part a 95 percentile pilot. Some studies were also done with a 5 percentile pilot, since 5% high Q ejections represent the worst case load factor conditions.

Relatively simple models of ACES II have been used to date in this effort to quantify control requirements. The accuracy of such models is felt to be sufficient for this purpose. These models do not include components such as STAPAC (or DART), and utilize only basic functional descriptions of the catapult, rocket, and drogue dynamics. The real concern at this time is not in transient behavior or higher order effects (although the actual control design process does consider these, given the nonlinear nature of the problem).

The major question dealt with here is: How much thrust control authority is required to stabilize the seat and at the same time maintain the radical constraint? The approach has been to consider the free 95% ACES II seat/pilot in an airstream at various attitudes. The seat is subjected to aero and/or drogue forces, generated by EASIEST. An offline analysis program was developed to compute the rocket forces and moments required at each initial condition, to satisfy the radical and offset the aero and drogue torques.

<u>Aircraft acceleration field/maximum catapult acceleration</u>. The catapult forces act primarily to effect the dynamic response index (DRI) of the acceleation radical, given by

$$\text{Radical} = \sqrt{\left(\frac{DRI}{DRI_L}\right)^2 + \left(\frac{G_x}{G_{xL}}\right)^2 + \left(\frac{G_y}{G_{yI}}\right)^2} < 1.0 \qquad (3.34)$$

DRI is the dynamic response index, a measure of spinal compression (MIL-S-8479B). The limit on the DRI, DRI_L, is never more than 18g, and is more commonly 16g. In Equation (3.34) G_x and G_y are load factor components. Catapult acceleration can reach the vicinity of 12g, but this value must also consider the aircraft maximum allowable Z acceleration, as shown below

$$-4 < G_x < 2 \quad g's$$

$$-2 < G_y < 2 \quad g's \qquad (3.35)$$

$$-3 < G_z < 10 \quad g's$$

Assuming that the Radical does equal 1.0, and that G_{x_L}=30, G_{y_L}=15, and that DRI =16 (since the acceleration vector will be more than 5 degrees off of the seat/pilot Z axis), then DRI_{max}=15.71. If the aircraft has G =10g's, then the controller must limit the additional load onto the man from the catapult to approximately 5.61 g's. Obviously, the best approach is to have the controller computing the Radical as the ejection is occurring, and if it appears that the future estimated DRI value will exceed the limit, the controller must vent the catapult or otherwise control the maximum acceleration imposed on the pilot. On the other hand, the time to catapult separation increases. Thus, the effect of aircraft acceleration in the X and Y directions is to reduce the maximum catapult acceleration, mainly because the DRI_L changes from 18 to 16 as the acceleration vector shifts more than 5 degrees from the man's Z axis. The further reduction in DRI from 16 to 15.71 as the aircraft X and Y accelerations go from zero to their limits of -4 and ±2 g's, is less than the standard deviation of measurement of DRI (±1).

Once the seat/pilot is free of the aircraft, only the forces on the seat/pilot itself are important. The aero forces on the seat/pilot are estimated here by using the tables of aero coefficients contained in White (1974). The coefficients for a 15 degree pitch, and a Mach No. of 1.2, are used for the maximum Q cases, immediately after catapult separation. For the maximum drogue deployment speed case, the coefficients are for 0 degree pitch and 0.9 Mach No., seat/pilot area (S) of 7 ft. , and a total weight (W) of 415 lbs., are used as constants. This gives the value of "qS/W"=27 g's, which is close to the G_x limit of 30 g's.

A simple curve fit was performed on the force coefficients, resulting in the following relationship for force coefficients as a function of yaw (Y):

$$C_x = -1.0418 - 0.006355Y + 0.000263Y$$

$$C_y = +0.0140 - 0.0346121Y + 0.000160Y \qquad (3.36)$$

$$C_z = -0.1480 + 0.001770Y - 0.000026Y$$

With these relations, plus the values G_{x_L}=30, G_{y_L}=15, and G_{z_L}= 16, replacing DRI_L as a steady state approximation, we can investigate maximum allowable yaw angle at a 1600 Q ejection, first without rockets or drogue. (This result is expanded on later in this section.) The Radical value for zero yaw is a large 0.97. The yaw angle which produces a Radical value of 1.0 is 3.33 degrees. Thus, very little sideslip can be tolerated before the rocket(s) are ignited.

For the maximum sideslip at emergence, the rocket on and no drogue case, the nominal rocket(s) assumed here have a -Z thrust of 3536 lbs., or 8.52 g's, and a +X thrust of 3,000 lbs., or 7.23 g's. This corresponds closely to the current ACES II and the Stencel SIIIS ejection seats. Thrust magnitude is about 4640 lb.

With the forward thrust counteracting the frontal aero force, and the upward thrust counteracting the normally negative "lift" of the seat/pilot, the value of the Radical for zero yaw drops from 0.97 to 0.75. The yaw angle which causes the Radical to equal 1.0 above increases from 3.33 to 10.7 degrees.

Consider now the problem of finding the maximum size drogue at emergence, with rockets, still at 1600 Q. If the drogue is immediately deployed, we are interested in the maximum size drogue that causes the Radical to equal 1.0, with zero yaw and, say, 17 degree pitch.

Solving the Radical leads to an additional negative G_x of 6.45 g's and an additional upward G_z of 1.97 g's that can be tolerated. A drogue area times drag coefficient (C_DS) of 1.75 ft. would add these accelerations to the seat. Thus, only a very small drogue can be used as an immediate drogue at maximum Q, which is not practical. Consider now the speed limit for deployment of fixed C_DS drogue = 5 ft. , with rockets. Assuming that the controller pitches the seat/pilot forward to zero pitch (in order to

minimize the Radical) and obtains a zero yaw angle, and that the seat/pilot slows to approximately 0.9 Mach No. (to use the 0.9 aero coefficients), the maximum speed at which a 5 ft. "CDS" drogue can be deployed is 600 KEAS while the rocket(s) are still thrusting.

This small study highlights the critical requirement for the TVC controller to maintain attitude of the seat/pilot very close to the x-axis at 1600 Q. In addition, the role of the catapult and sustainer thrusters is reducing overall load factor (hence, the radical), by offsetting the aero and drogue effects, is very evident.

This study was expanded upon with the aid of EASIEST runs using the ACES II free seat/pilot combination at 1600 Q, without drogue or rockets. In this case, only the aero forces are computed. This was done for one altitude, at several incremental values of yaw and pitch angles (to the wind). This set up allows for simple readjustment of forces on the seat for either different altitude and/or different airspeed. For the former, the aero forces scale by air density ratios, (ρ_2/ρ_1), if airspeed is fixed, and changing the velocity at fixed altitude scales the aero forces and torques by (V_2/V_1) .

For the sake of sizing the thrust requirements, a relatively simple "static" approach was used. Where the load factor, given by

$$LF = -[f^A + f^D + f^T] \;/\; wt + [(\dot{\omega} x r^{CG}) + (\omega x(\omega x r^{CG})) - g]/GRAV \qquad (3.37)$$

(from EASIEST code), exceeds 1.0 for $f^T = 0$, the vector is given a value which scales LF down enough for the radical to equal 1.0. It turns out that this option results in the old LF, the new LF , and f^T lying in the same direction. This is actually overly restrictive because the radical condition (3.34) plots as an ellipsoid in load-factor space, and LF can be at any point on or within this ellipsoid, not necessarily at the penetration point of LF, to satisfy the radical. When this consideration is combined with the desire to utilize f^T to generate corrective torques to the aero torques, the restrictiveness of the algorithm used is evident. However, a constrained optimization solution, albeit static, is required to

properly position and size f^T. Nevertheless, some very useful information can be obtained with the simpler approach.

In addition to creating a "safe" acceleration environment, it is possible to locate an appropriate moment arm for this f^T, which will offset the aerodynamic and drogue torques as well as generate a torque to correct the seat/pilot attitude, as follows:

The desired torque will reorient the seat/pilot x-axis along the wind. The x-axis is not a point of neutral stability, but does have the advantage of being the minimum radical orientation for a very large acceleration environment. For a given time to recovery, DT (we have chosen 0.05 and 0.10 sec), along with the correction rotation angle, the initial angular acceleration can be computed, which leads to a "desired" restoring torque, TC. For the motion with respect to the CG, this is found from

$$I\dot{\omega} + \omega x(\omega x I) = T^{ext} = TA + TD + TT + TC - r^{CG} \times (f^A + f^D) \qquad (3.38)$$

where

TA = current aero torque on seat/pilot, about SRP
TD = drogue torque on seat/pilot, about SRP
TT = thrust torque generated by rockets, about CG
TC = commanded (desired) recovery torque, about CG
f^A = aerodynamic force on seat/pilot
f^D = drogue force on seat/pilot
I = seat/pilot inertia moment, about CG

In Equation (3.38) the aero and drogue torques are converted to a CG reference from the input SRP-referenced values. This is not an inconsequential correction. The SRP-referenced pitching moment coefficient at 1600 Q, zero angles of attack and sideslip, is 0.104. It becomes -0.150 with respect to the CG. Thus a pitch torque of 3415 foot-lb. about the SRP becomes -4947 foot-lb. about the CG. This has been verified by EASIEST simulations.

Table 3.2 summarizes the results of these runs. The captions are for the most part self explanatory. A "Y" under the Drogue heading means that a steady state drogue force is acting on the seat/pilot, along the wind

Table 3.2

ACES II THRUST SIZING STUDY (95 PERCENTILE PILOT)

θ(α) (degrees)	ψ(-β) (deg)	V_{KEAS}	alt. (feet)	Drogue On	Aircraft acceleration (g's)			Uncorrected (No Thrust) Load Factor (g's)			Radical	Required Thrust; Mag. (pounds)	DT (sec)	CG Moment arm (feet)
0.	0.	687.	2000.	N	0.	0.	0.	41.45	-0.09	-9.15	1.50	(5240. -12.1 -1157.); 5366.	0.1	1.3
0.	0.	687.	2000.	Y	0.	0.	0.	62.4	-0.096	-9.14	2.16	(12780. 0. -1874.); 12920.	0.1	0.23
0.	0.	687.	2000.	N	4.	2.	10.	*	*	*	1.74	(6056. -339. -3097.); 6810.	0.1	0.73
0.	0.	687.	2000.	N	-4.	2.	10.	*	*	*	1.94	(8387. -387. -3534.); 9109.	0.1	0.54
0.	0.	687.	2000.	N	-4.	2.	-3.	*	*	*	1.57	(6293. -290. - 851.); 6357.	0.1	0.78
10.	0.	687.	2000.	N	0.	0.	0.	38.32	-0.09	-5.0	1.31	(3502. -8. - 454.); 3531.	0.1	1.22
10.	0.	687.	2000.	N	0.	0.	0.	38.32	-0.09	-5.0	1.31	(3502. -8. - 454.); 3531.	0.05	1.12
10.	0.	687.	2000.	Y	0.	0.	0.	58.96	-0.09	-1.3	1.97	(11070. -16. - 250.);11070.	0.1	0.35
25.	0.	687.	2000.	N	0.	0.	0.	32.3	-0.02	-14.1	1.39	(3470. - 2.5 -1516.); 3787.	0.1	0.52
25.	0.	687.	2000.	N	-4.	2.	10.	36.3	-2.02	-24.1	1.93	(6704. -376. -4653.); 8057.	0.1	0.25
25.	0.	687.	2000.	Y	0.	0.	0.	51.3	-0.02	-23.0	2.23	(10810. - 5.0 -4840.);11840.	0.1	0.29
0.	5.	687.	2000.	N	0.	0.	0.	41.4	-4.17	- 9.3	1.52	(5424. -546. -1216.); 5585.	0.1	0.88
0.	5.	687.	2000.	N	-4.	2.	10.	*	*	*	1.98	(8569. -1165. -3640.); 9302.	0.1	0.52
0.	5.	687.	2000.	Y	0.	0.	0.	62.3	-6.0	- 9.3	2.19	(12930. -1245. -1928.);13130.	0.1	0.23
0.	10.	687.	2000.	N	0.	0.	0.	38.75	-10.63	- 8.7	1.57	(5372. -1474. -1204.); 5699.	0.1	0.82
0.	10.	687.	2000.	N	-4.	2.	10.	42.75	-12.63	-18.7	2.02	(8264. -2442. -3611.); 9343.	0.1	0.50
0.	10.	687.	2000.	Y	0.	0.	0.	59.39	-14.27	- 8.7	2.26	(12650. -3040. -1849.);13140.	0.1	0.23
0.	0.	600.	2000.	N	0.	0.	0.	*	*	*	1.14	(1540. - 3.5 - 351.); 1579.	0.1	2.40
0.	0.	600.	2000.	N	-4.	2.	10.	*	*	*	1.61	(5142. - 299. -2485.); 5719.	0.1	0.66
0.	0.	600.	2000.	Y	0.	0.	0.	*	*	*	1.65	(7154. - 11. -1085.); 7236.	0.1	0.31

NOTE: * indicates result not recorded

axis line. R indicates the minimum moment arm length needed with the thrust FT, to balance the aerodynamic and drogue torques, and to generate TC.

We have used a "CDS" factor of 5.0 for the drogue, so that its force magnitude at 687 KEAS is 8000 pounds. The value in the table for the Radical is the "no thrust" value. When the rocket generates a thrust of the type indicated, the Radical value becomes 1.0, for all cases. Clearly there are several cases where FT could be oriented better, but we are only using the Radical = 1.0 criterion here. In one case, velocity = 600 KEAS, with no drogue force or aircraft accelerations, FT need only be 1579 pounds to satisfy the Radical, yet this level of thrust needs a moment arm of 2.39 feet to correct the disturbance torques. Another point is that, when one considers only satisfying Radical = 1.0, other problems arise. In the case under discussion, the rocket is generating only 350 pounds along the z-axis, and this is inadequate for tail clearance at 600 KEAS.

These ACES II runs, mostly at 687 KEAS, support the observation made earlier that drogue deployment must be delayed until about 600 KEAS, and that yaw angle effects at high Q are very critical. Also, thrust capability of the order of 9000 pounds is needed just to satisfy the Radical at 687 KEAS, when the aircraft is at all of its acceleration limits. Although this value will be revised downward by using optimum design, there is little question that greater thrust capability will be needed at high Q for safe crew escape. This analysis indicates that a net thrust capability of up to 12,000 pounds for the ACES II is likely.

Finally, Table 3.3 presents the state and control constraint formulations to be used in the optimal control synthesis process.

3.3.3 Disturbances. In this subsection, potential disturbances to the seat/pilot system are identified and discussed.

In brief, disturbances are those phenomena which cannot be modeled well in the expressions for the control design system dynamics, or which behave on the system in a random manner. A proper control design must nevertheless be able to accommodate most of the disturbances likely to be

TABLE 3.3

STATE, CONTROL AND DYNAMIC CONSTRAINTS

States:	u, v, w	(see V_{KEAS} constraint)	
	x	unconstrained	
	y	"	
	z	$-50{,}000$ ft. $< z < 0.$ ($h = -z$)	
	p	$\lvert p \rvert < p_{lim}$	, $p_{lim} = 800$ deg/sec
	q	$q_{min} < q < q_{max}$	, $q_{min} = q_{max} = 800$ deg/sec
	r	$\lvert r \rvert < r_{lim}$	, $r_{lim} = 1000$ deg/sec
	ϕ	$\lvert \phi \rvert < \phi_{lim}$ ($\phi_{lim} = 180°$)	, $\phi_{lim} = 180$ degrees
	θ	$\theta_{min} < \theta < \theta_{max}$	, θ_{min}, θ_{max} are missing speed dependent
	ψ	$\lvert \psi \rvert < \psi_{lim}$	, ψ_{lim} is missing speed dependent
(drogue variables)	q_D	$\lvert q_D \rvert < q_{D_{lim}}$	
	r_D	$\lvert r_D \rvert < r_{D_{lim}}$	
	θ_D	$\theta_{D_{min}} < \theta_D < \theta_{D_{max}}$	
	ψ_D	$\lvert \psi_D \rvert < \psi_{D_{lim}}$	

Dynamic Constraints

$V_{KEAS} < 687.$

Radical < 1.0

(avoid A/C wing tips, tail, etc.)

Controls:*	$T^{(i)}$	$T^{(i)}_{min} < T^{(i)} < T^{(i)}_{max}$
(catapult)	T_c	$T_{c_{min}} < T_c < T_{c_{max}}$
(nozzle angles)	ψ_i	$\lvert \psi_i \rvert < \psi_{i_{max}}$; $\lvert \psi_i \rvert < \psi_{i_{max}}$
	θ_i	$\lvert \theta_i \rvert < \theta_{i_{max}}$; $\lvert \theta_i \rvert < \theta_{i_{max}}$

*Specific values depend on actual control configuration (See Section 3.2.2).

encountered by the system. In order to simulate disturbances for control design and verification, they are divided into two classes, static and dynamic. Static disturbances represent (unknown) differences between actual and modeled parameter values which remain essentially fixed during an escape trajectory. They can also be modeled with drift rates. The bias value and drift rate, if any, can be modeled as random values with given statistics. Dynamic disturbances are random functions in time. It is usually most convenient to model these as pure or filtered white noise of a given power.

Static disturbances. The seat/pilot TVC system must be designed to control disturbances arising from variations in seat/pilot weight, moment of inertia, and center of gravity migration. The required ranges for this variation are expressed in terms of median pilot weight; the control system must work for pilots in the 5 - 95 percentile range. The control system will adjust to such disturbances automatically, due to its closed loop nature. Mass/inertia properties are definitely a design factor; however, they will not appear as specific control parameters in a given implementation. That is, the pilot will not be required to dial his weight, for example, prior to a mission, nor will there be real-time computation or measurement of mass/inertia properties. The extremes of the mass/inertia variations will be used in the design process in order to size control system components, but not as real time inputs. The effect of mass/inertia variations will appear implicitly in the control laws derived.

During preliminary design studies and control synthesis, fixed offset values can be assigned to weight, inertia and CG values. More complete analyses will include dynamic variations in these quantities.

Because the aerodynamic forces and torques are the major concern for the escape control system, aero disturbances must be modeled adequately in the environmental model to ensure robust controller design. In much the same manner as the mass/inertia related variables, quantities such as the seat/pilot aerodynamic frontal area and the center of pressure location (fore and aft, as well as sideways) are to be used in the design, but not explicitly in implementation. Other disturbance quantities relating to the

aerodynamic environment are the main atmospheric variables: pressure, temperature and altitude. Of these, altitude exhibits uncertainties through its measurement. Altitude sensors and their performance are discussed in Section 5.5. For other reasons, e.g., steering control, good knowledge of altitude is important for effective control system operation throughout the flight envelope. Disturbance offsets of low altitude values will be used for robustness and verification studies of the control system.

Temperature and pressure are important influences on the performance of the various pyrotechnic devices. Their direct effect on aerodynamic response, as disturbances, is not as critical, although this will also be studied using simulations with the controller design. Energy performance of the sustainer propulsive system can vary up to 50% over the projected operational temperature range of about -60 F to 140 F. This information, if known to the controller, can greatly reduce undesired uncertainty.

Finally, there are important static disturbances which affect rocket performance. These include thrust asymmetries and variations in burn time and thrust profile. The control design must accommodate this type of disturbance, without explicitly using them in the control law.

Dynamic disturbances. Most of the quantities defined above exhibit both static and dynamic disturbance properties. The CG may be offset statically for a number of reasons, but in all cases, it will migrate with respect to the seat frame throughout the escape trajectory. We have conducted a somewhat limited study of a dynamic single mass model of the pilot moving with respect to the seat. See Section 6.5. While the control system must include energy sources of sufficient size to control the CG migration, it will be design-limited to the basic 5 - 95 % values, plus sideways offsets up two inches. Side forces due to asymmetric thrusting, as well as angular rates, cause even a well-harnessed pilot to move arms, legs and/or torso, in response to nominal and off-nominal accelerations. Such disturbances were only implicitly modeled for the current control design effort.

Asymmetries arising from the position of legs, arms, etc., are relatively minor in terms of effect on CG location; however, they have a

very large effect on the aerodynamic forces. Thus, these disturbances must be a factor in the control design. Another point to make is that CG shifts have a noticeable effect on moment and product of inertia values, especially the latter. Aerodynamic disturbances affect motion in all three dimensions. They are due to asymmetric positioning of hand/arm, knee/leg, or even seat asymmetries. In addition, a heavy pilot tends to contribute upper torso asymmetries, and the whole body of a light pilot is subject to asymmetric disturbances. Other major aerodynamic disturbances arise from vortex shedding and turbulance about the seat. Vortex shedding occurs mostly off the rear of the seat, but also from all protusions. Turbulance arises from many causes, not the least of which are those related to airflow about the open cockpit area of an aircraft at a disabled attitude.

It is necessary to conduct a complete design which will work in the presence of all disturbances cited above. The static disturbances are generally easy to model in the 6 DOF simulator, but this is not always the case for the dynamic disturbances. Many of the realtive seat/pilot motions are simulated in EASIEST; it will be necessary to construct appropriate EASIEST turbulence and wind gust components.

The remaining source of uncertainty in the control design process is in the area of measurement sensor disturbances. Their attributes are discussed in Section 5.1. We mention here that the attributes of interest to ejection seat TVC design include accelerometer noise due to sensor start-up, vibrational noise from the rocket, and modal interaction with the seat structure. The rate gyros have a major source of error due to precession in an acceleration field.

Appendix E presents the outline for an algorithmic means of dealing with process disturbances.

3.3.4 Crew Escape Energy Requirements. In this subsection, thrust energy requirements needed for safe ejection at all conditions are discussed. For this project, the control system must ensure pilot survival from sea level to 50,000 feet altitude, and from zero ground speed (at low altitudes) to velocities equivalent to 1600 Q ("pounds per square foot")

dynamic pressure, or 687 KEAS (Figure 3.6). The control logic presented later in this report has been used in the following numerical study.

In order to perform the analysis required, it was necessary to develop a working simulation model of a representative rocket nozzle configuration. Such a module converts the rocket angular and translational commands into specific thrust magnitudes and orientations for each nozzle (motor) assembly. This "inversion" problem is a key aspect of acceleration control design.

High Q escape conditions have a direct bearing on energy requirements, but there are also conditions at lower speeds which must be considered. For this reason, several MIL-S baseline conditions are used in quantifying thrust energy requirements.

3.3.4.1 Energy Requirements and MIL-S Escape Conditions. As stated above, the main driver for determining required thrust energy is the high Q escape region. This manifests itself both in attitude and steering control requirements. At high speeds, aerodynamic deceleration is so severe that several fatal scenarios may develop: the seat can be blown into the vertical stabilizer(s) or some otherpart of the aircraft; the seat attitude or the size of the aero-induced g forces can be such that the acceleration environment is not survivable (loads of approximately 30 g's short duration can be tolerated, but only if pointed normal to the pilot's chest; spinal or lateral load factor tolerance is much less, about one half); and, the aero forces acting on the seat cause unstable attitude behavior, which at best jeopardizes steering control (e.g., altitude gain), and at worst can convert a survivable attitude into a fatal one.

The controller developed by SSI is well suited for meeting control objectives and for performing in this harsh environment. This is because it operates directly on accelerations: force and torque accelerations are its primary commanded outputs. An input quantity, the desired final acceleration, is also a key trajectory shaping parameter.

At high Q, energy requirements are dictated both by immediate issues of survivability, and by the need to decelerate enough over the powered

phase of the ejection so that the main chute is safely deployed. These constraints dictate required propulsive impulse, and hence burn-time limits. Dynamic pressure is a key "decision variable" in high Q escape. That is, it is a key part of the controller logic.

One potential concern in low Q escapes is that the energy needed at high Q can be fatally excessive at low speeds. Thrust modulation is a sound requirement for a design capable of operation over all regimes. The low Q cases can establish a "floor" on energy requirements: enough vertical acceleration is still needed for aircraft aviodance, and to orient the seat properly for chute deployment. Variable catapult thrust is also needed so that smooth acceleration profiles obtain at all times on the ejectee. But there are also high energy requirements at low Q. This will occur in many of the low altitude, adverse attitude cases such as are found in MIL-S-9479B. Our studies, discussed in this chapter, indicate that, while energy comparable to high Q cases may be needed at lower speeds, the upper extreme of energy requirements is still dictated by high Q conditions.

An important factor in the design of acceptable escape trajectories is the burn time of the sustainer rocket. See the Case 6 discussion. The reference run is shown in Figure 3.7, and had a duration of 250 msec.

In all of the simulation results presented in this report time (t)=0 corresponds to the instant of sustainer rocket ignition. This point in time typically occurs after tip off, so that we are in effect also assuming that the motion begins in free stream air. Refer to the Glossary for a definition of symbols.

Figures 3.8 and 3.9 show the same run, except that burn times are 600 and 900 msec, respectively. In both cases, there is adequate attitude and trajectory control for escape, although comparison of the original and these two results tends to favor a burn time close to 600 msec for this condition. There is excess thrust capacity, no problem with the Radical response, and reasonable thrust vectoring response. There is no question in Figure 3.8 that pitch, roll and yaw are well controlled, and the angular rates decay acceptably.

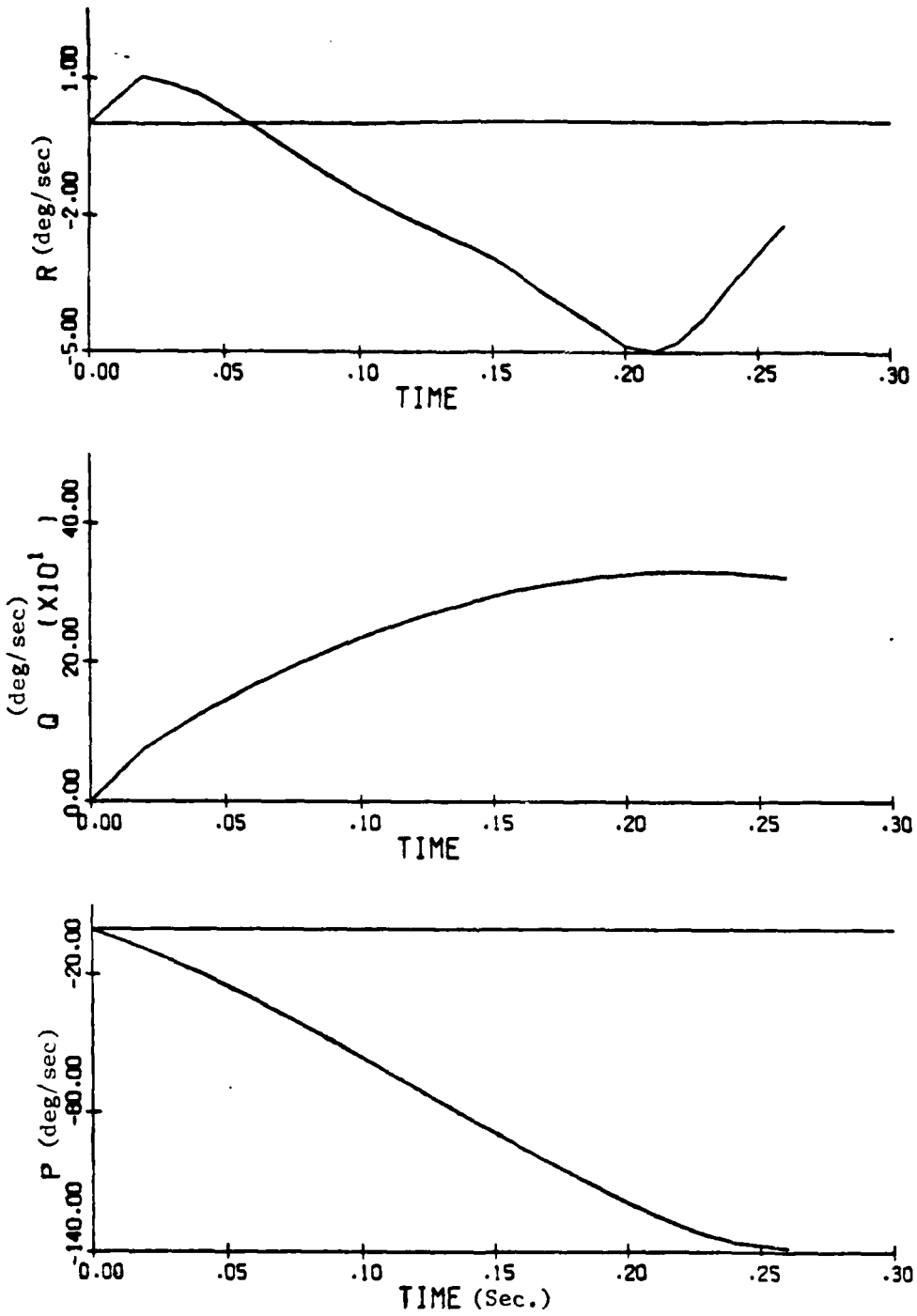

Fig. 3.7(a)
MIL-S Condition 1

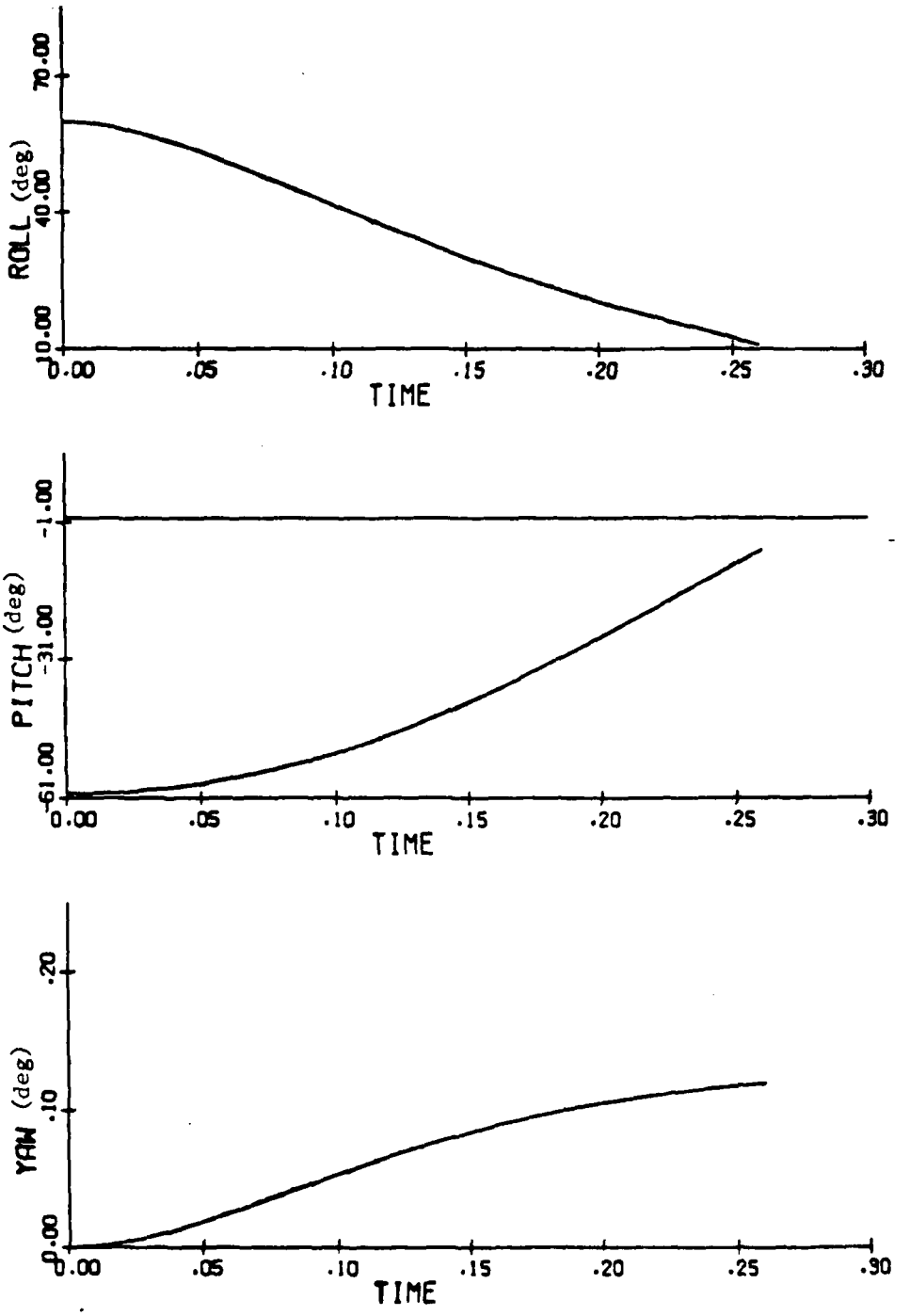
70.00
40.00
10.00
ROLL (deg)
0.00
.05
.10
.15
.20
.25
.30
TIME
-1.00
-31.00
-61.00
PITCH (deg)
0.00
.05
.10
.15
.20
.25
.30
TIME
.20
.10
0.00
YAW (deg)
0.00
.05
.10
.15
.20
.25
.30
TIME

Fig. 3.7(b)

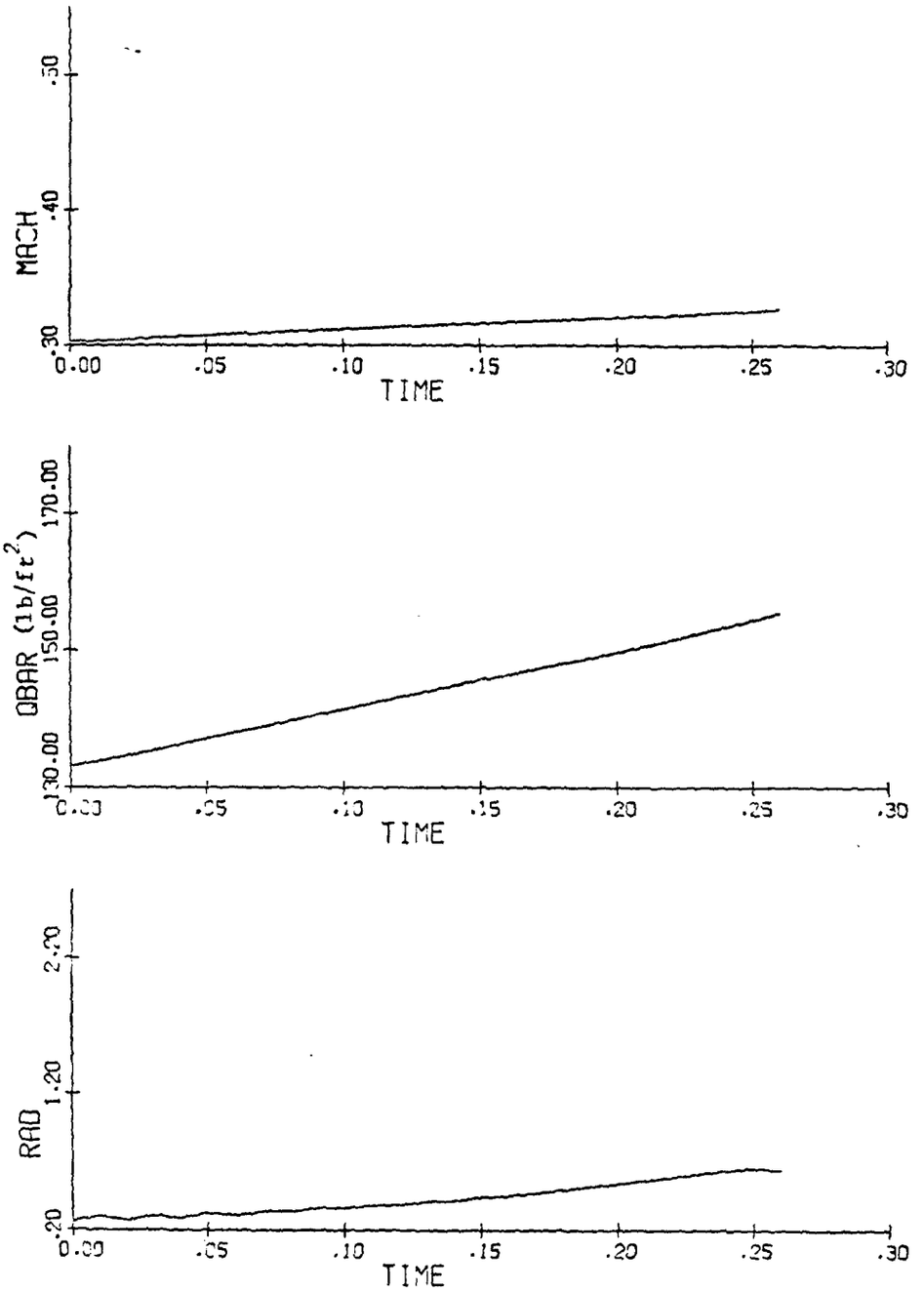
MACH
.30
.40
.50
0.00
.05
.10
.15
.20
.25
.30
TIME
QBAR (lb/ft^2)
130.00
150.00
170.00
0.00
.05
.10
.15
.20
.25
.30
TIME
RAD
.20
1.20
2.20
0.00
.05
.10
.15
.20
.25
.30
TIME

Fig. 3.7 (c)

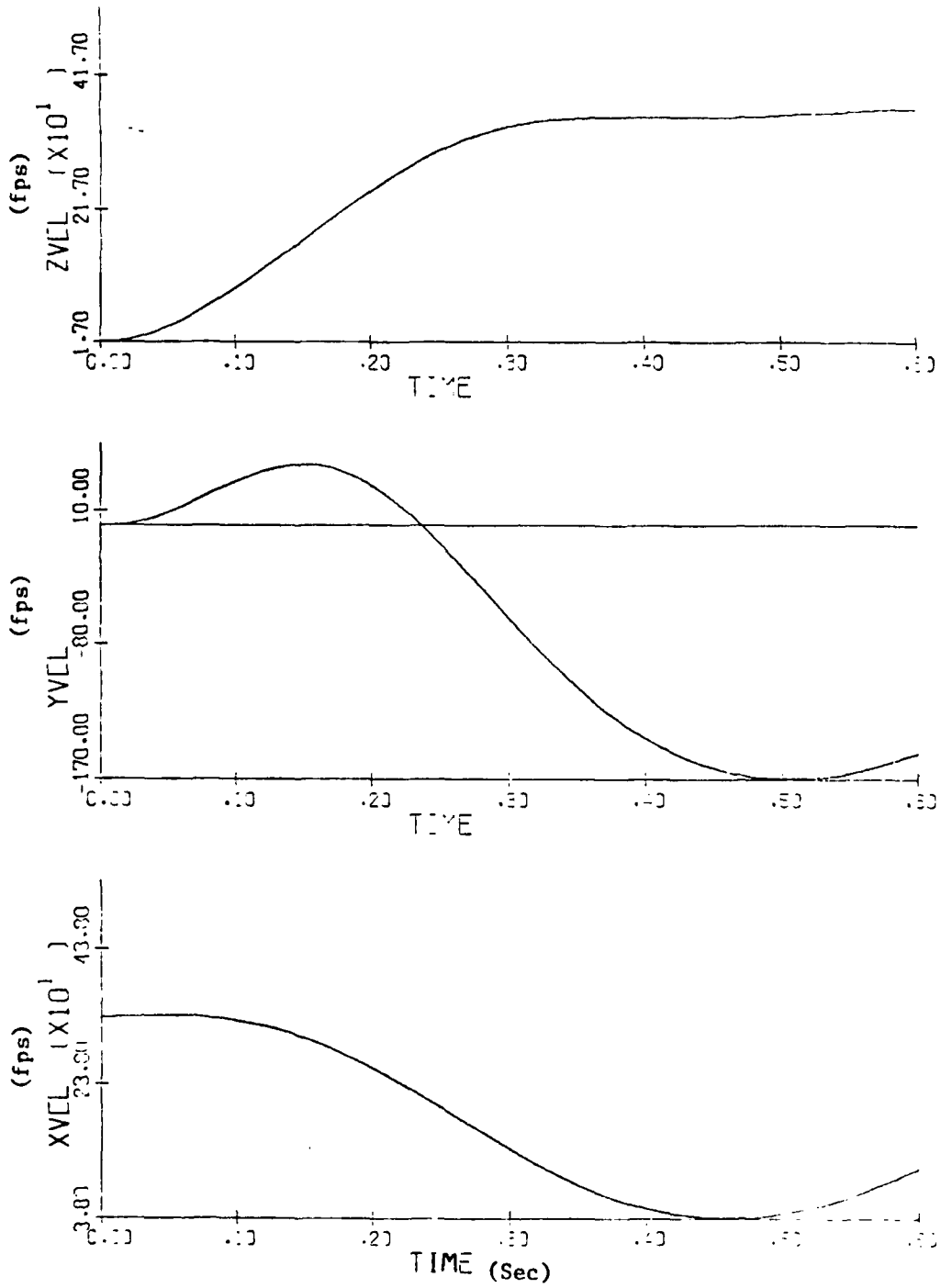

Fig. 3.8 (a)
MIL-S Case 1; Burn Time = 0.60 sec.

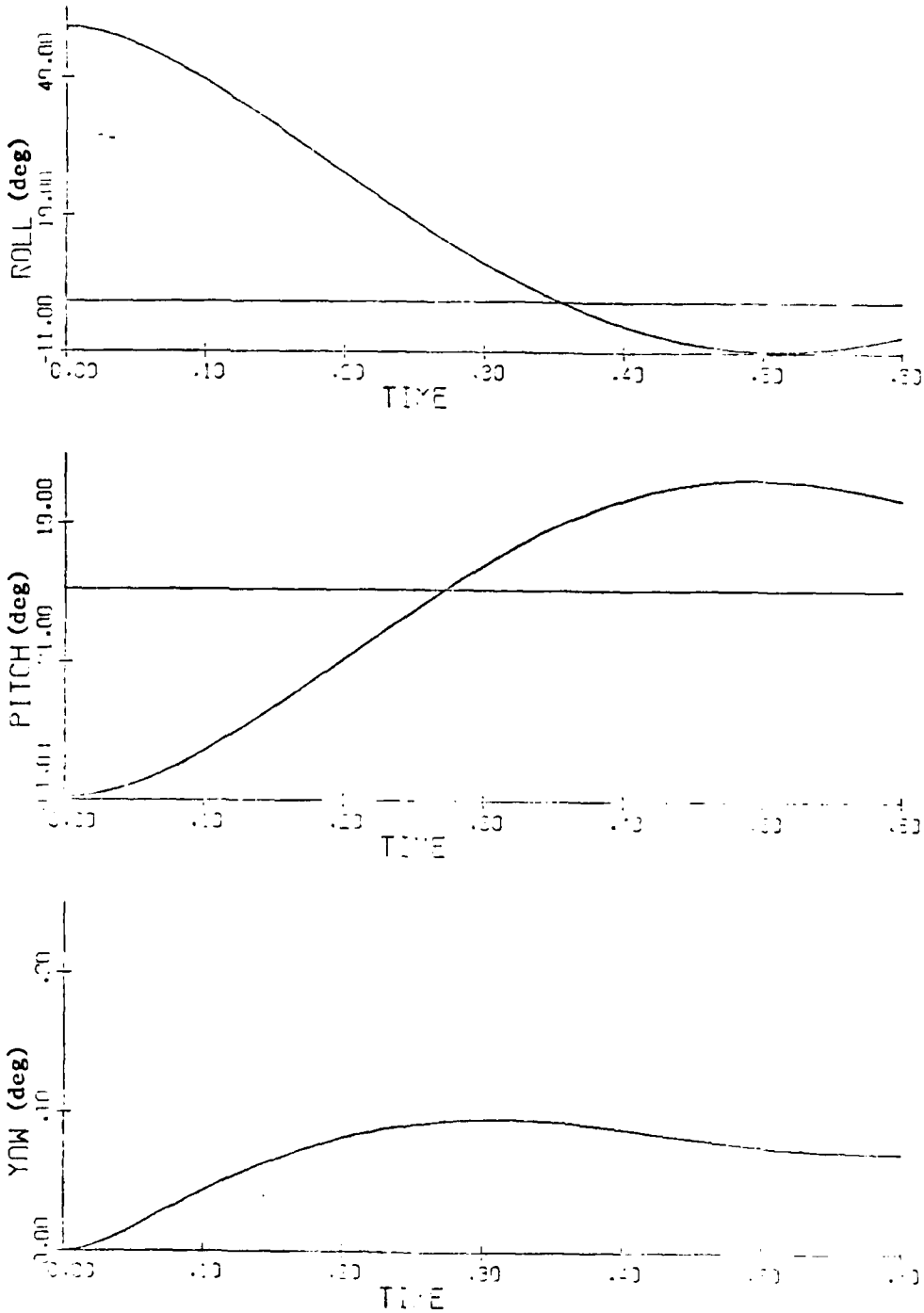
ROLL (deg)
40.00
-11.00
0.00
.10
.20
.30
.40
TIME
PITCH (deg)
10.00
TIME
YAW (deg)
.10
0.00
TIME

Fig. 3.8 (b)

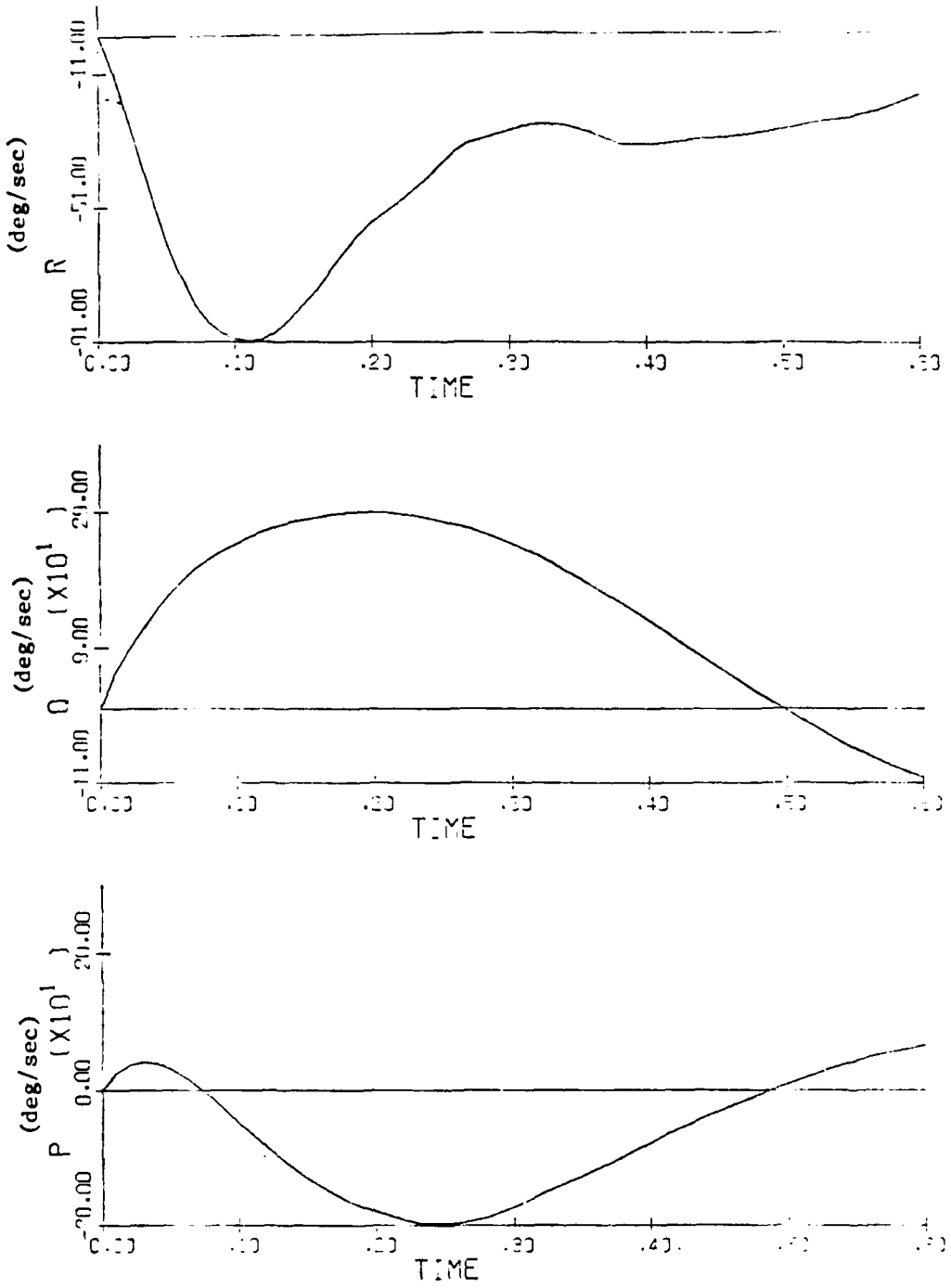
R
(deg/sec)
-11.00
-51.00
-91.00
0.00
.10
.20
.30
.40
.50
.60
TIME
Q
(deg/sec)
(X10^1)
20.00
9.00
-11.00
TIME
P
(deg/sec)
(X10^1)
20.00
0.00
-20.00
TIME

Fig. 3.8 (c)

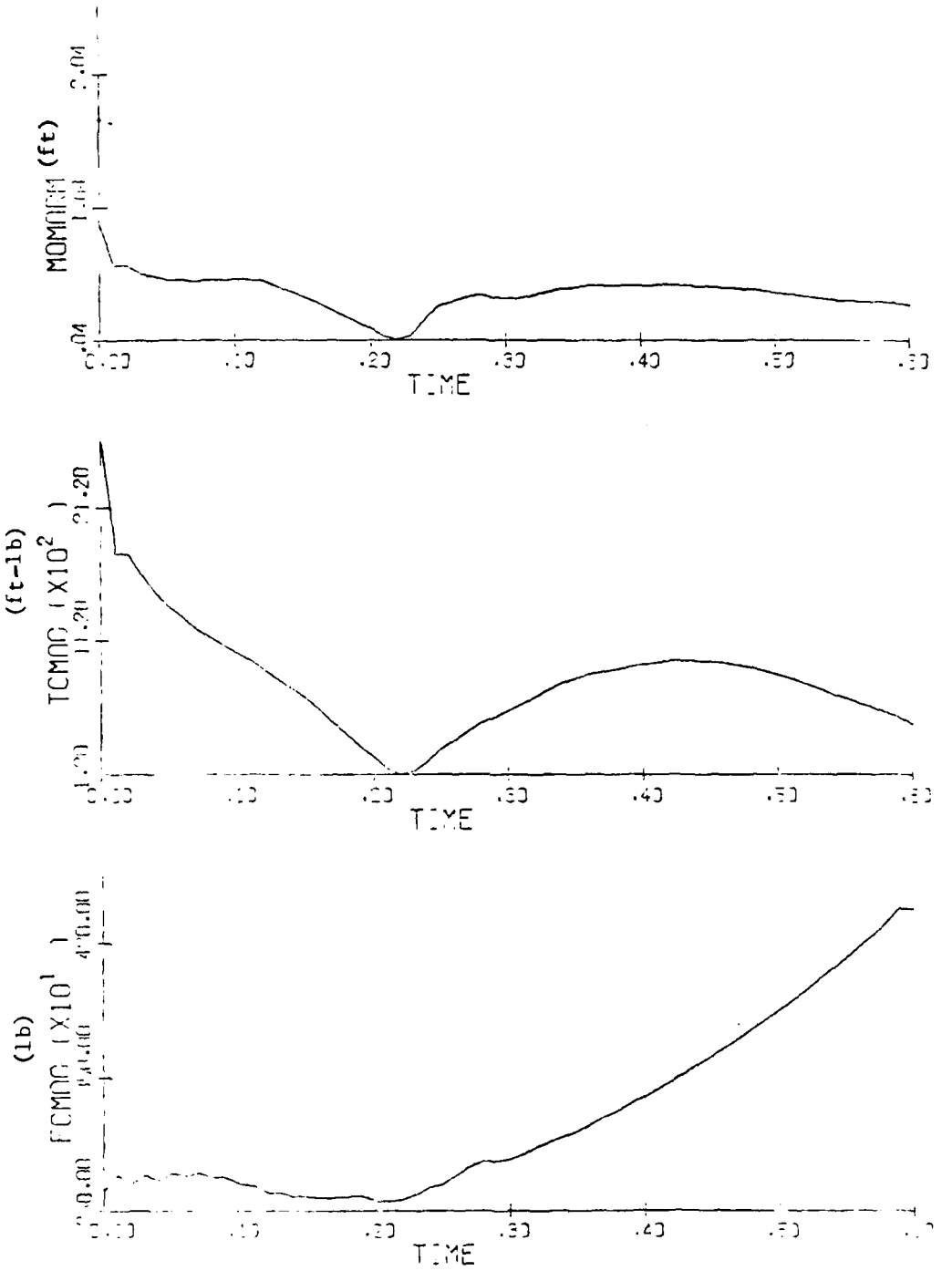

Fig. 3.8 (d)

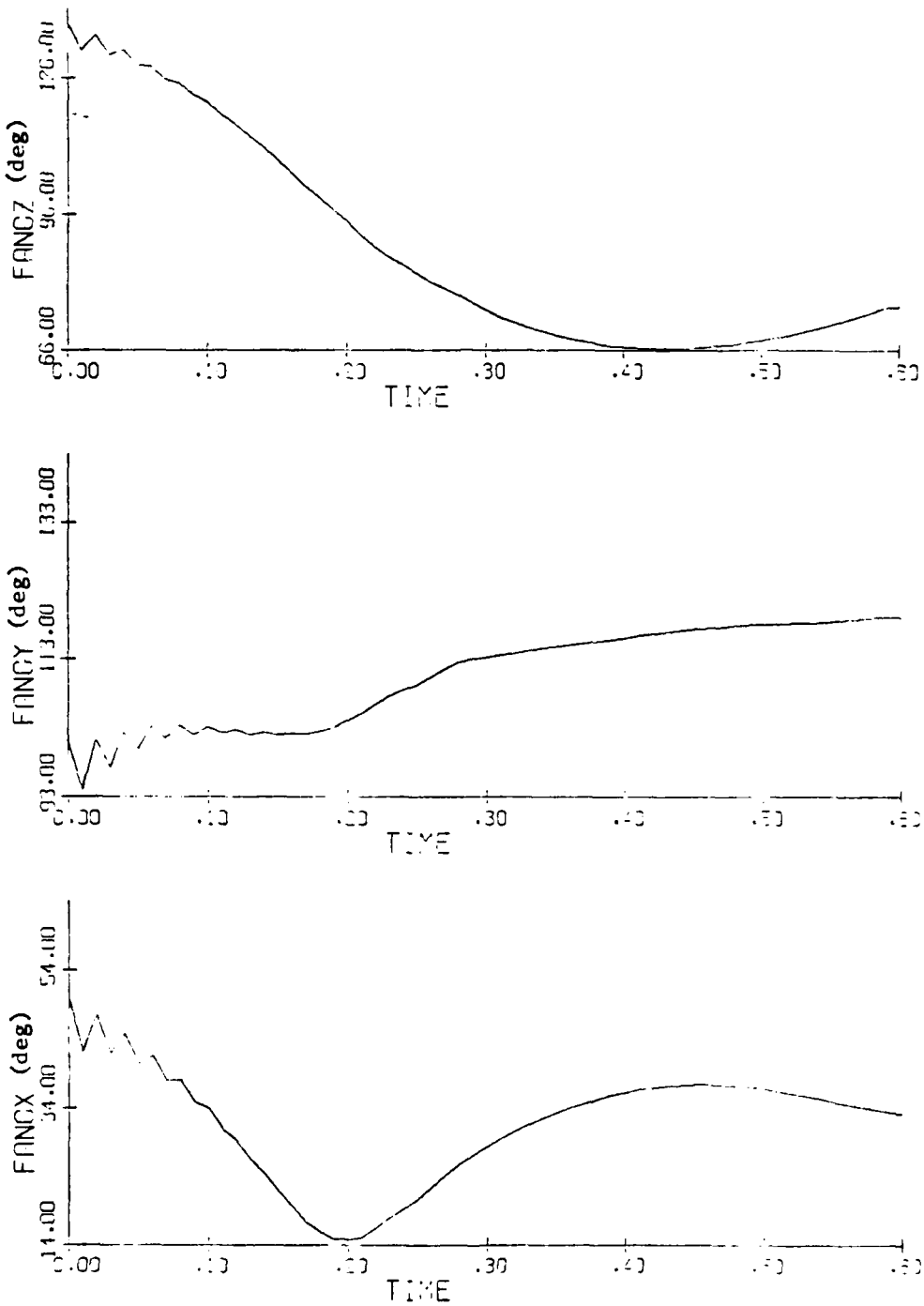
FANCZ (deg)
126.00
96.00
66.00
0.00
.10
.20
.30
.40
.50
.60
TIME
FANCY (deg)
133.00
113.00
93.00
0.00
.10
.20
.30
.40
.50
.60
TIME
FANCX (deg)
54.00
34.00
14.00
0.00
.10
.20
.30
.40
.50
.60
TIME

Fig. 3.8 (e)

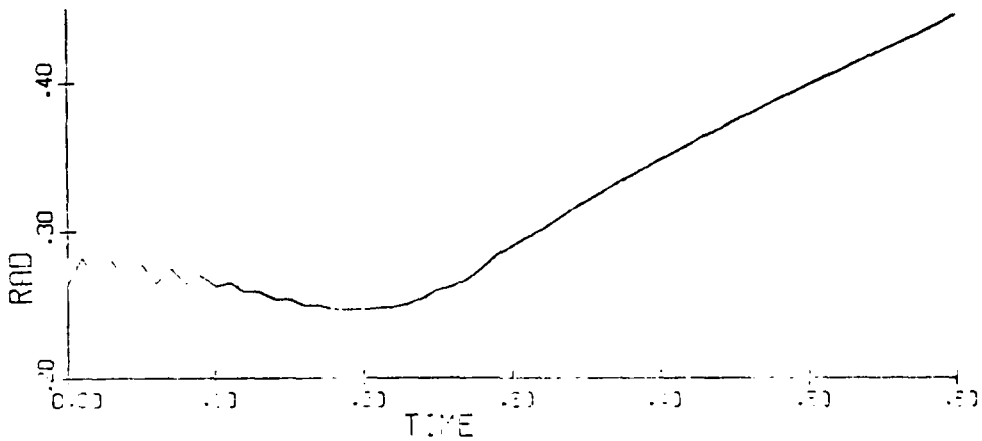

Fig. 3.8 (f)

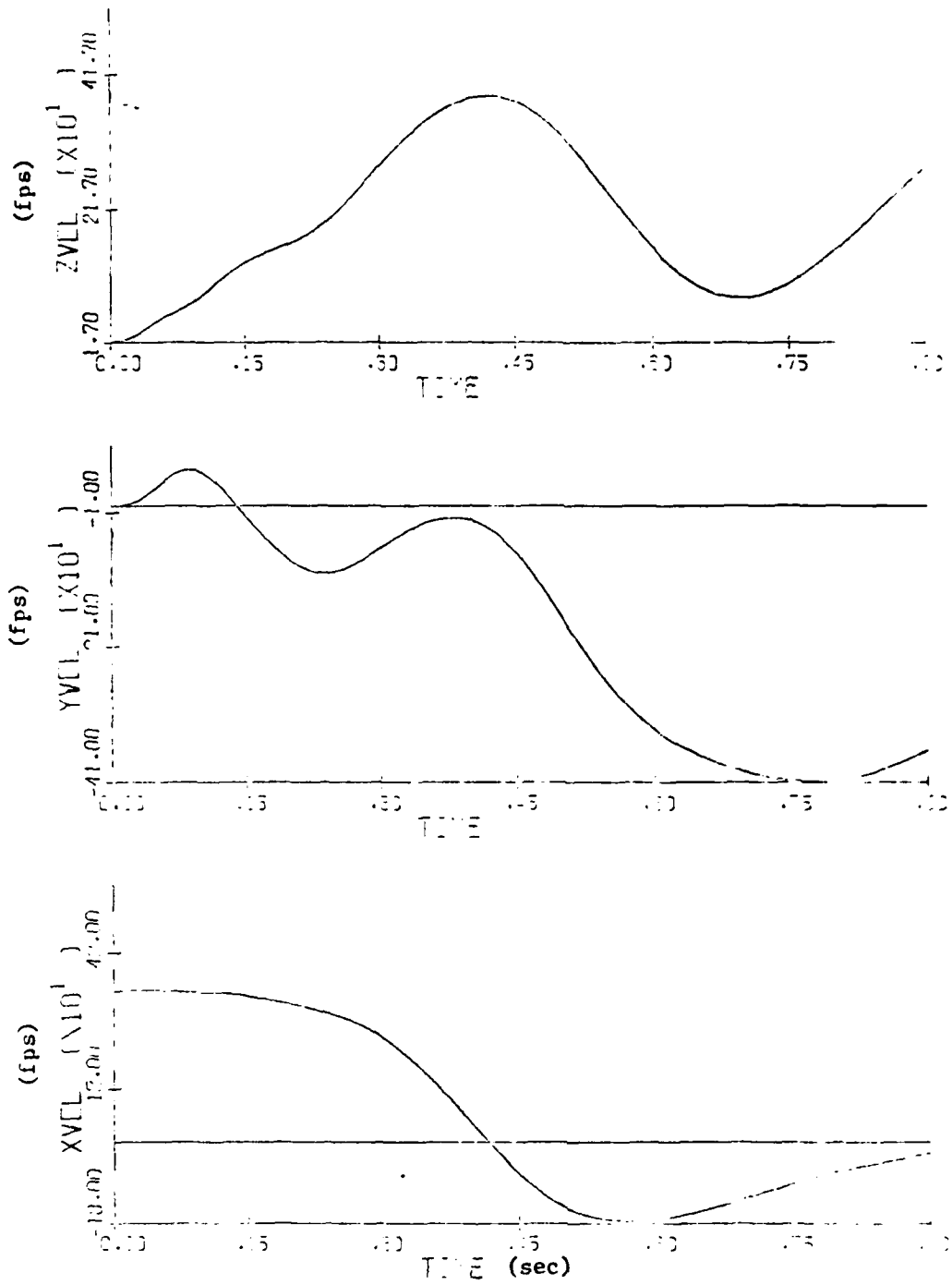

Fig. 3.9 (a)

MIL-S Case 1; Burn Time = 0.90 msec.

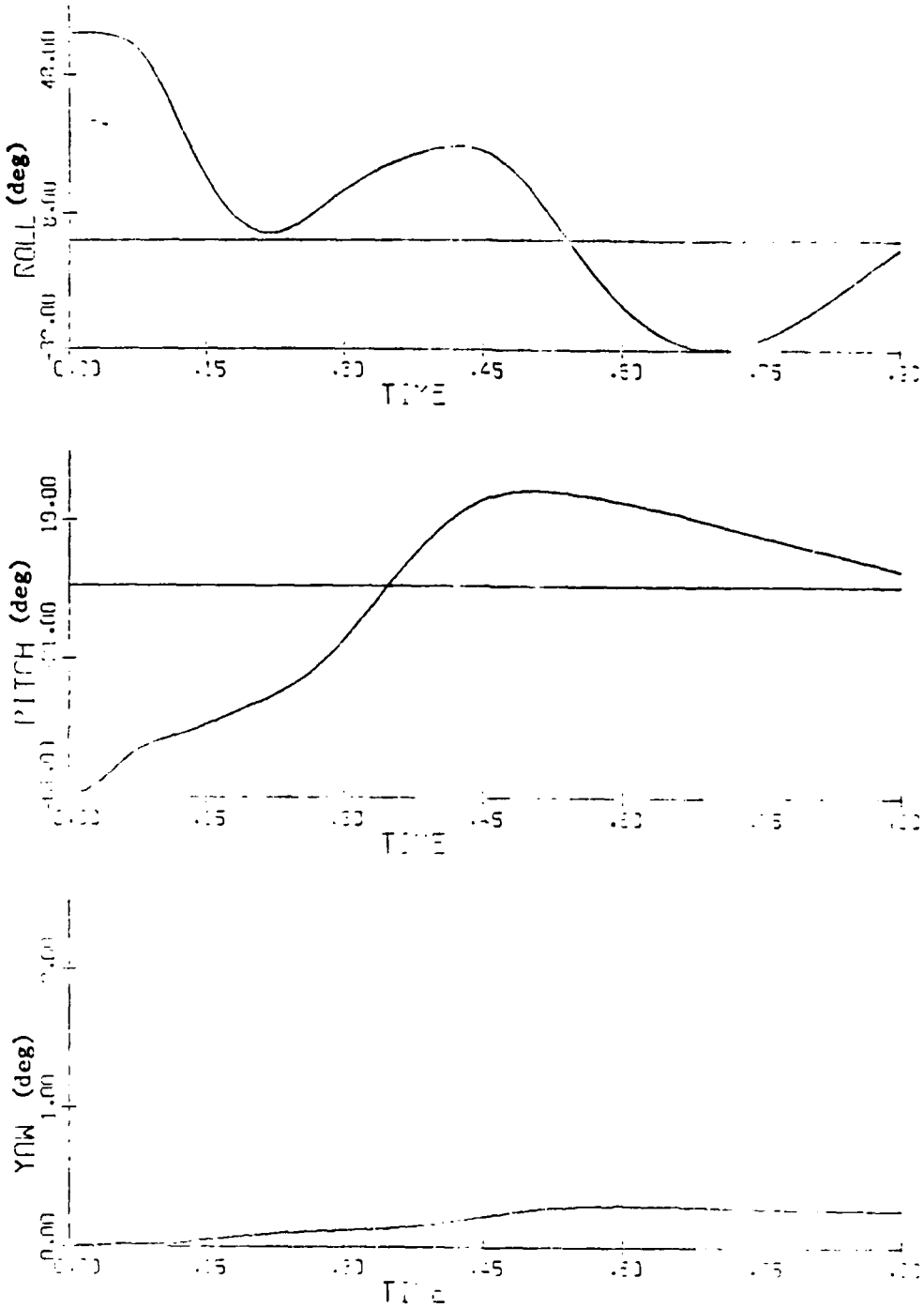

Fig. 3.9 (b)

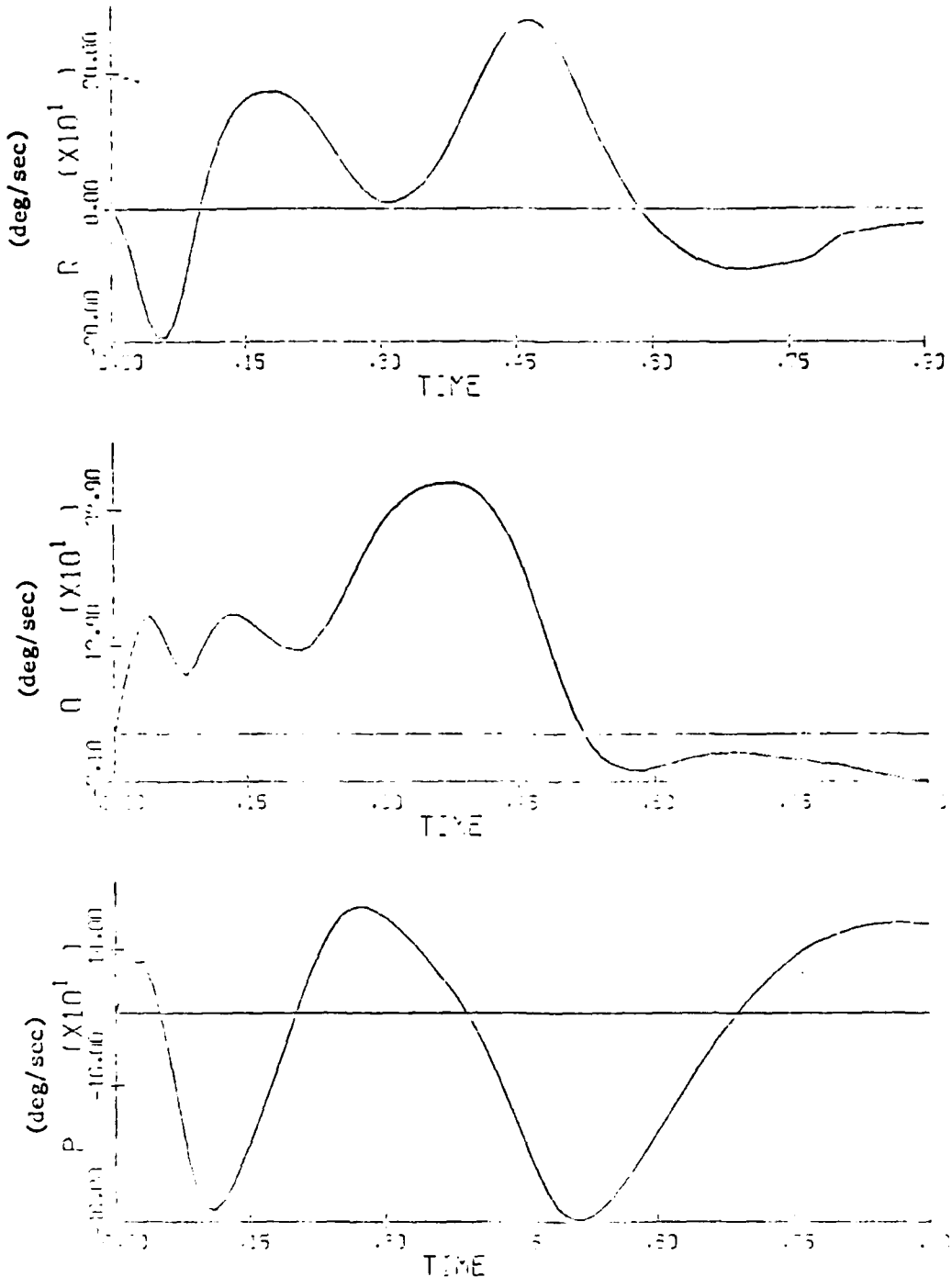

Fig. 3.9 (c)

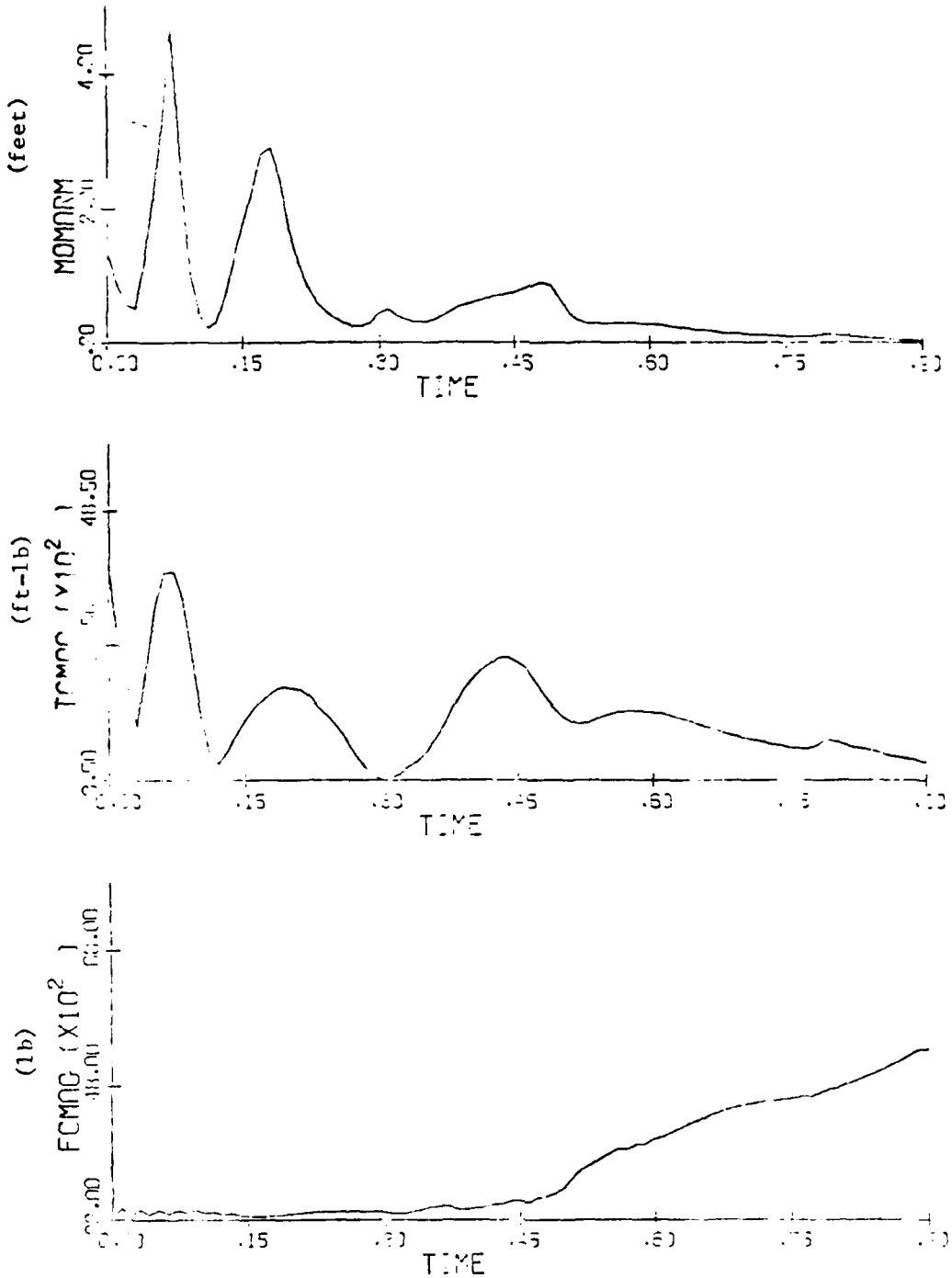

Fig. 3.9 (d)

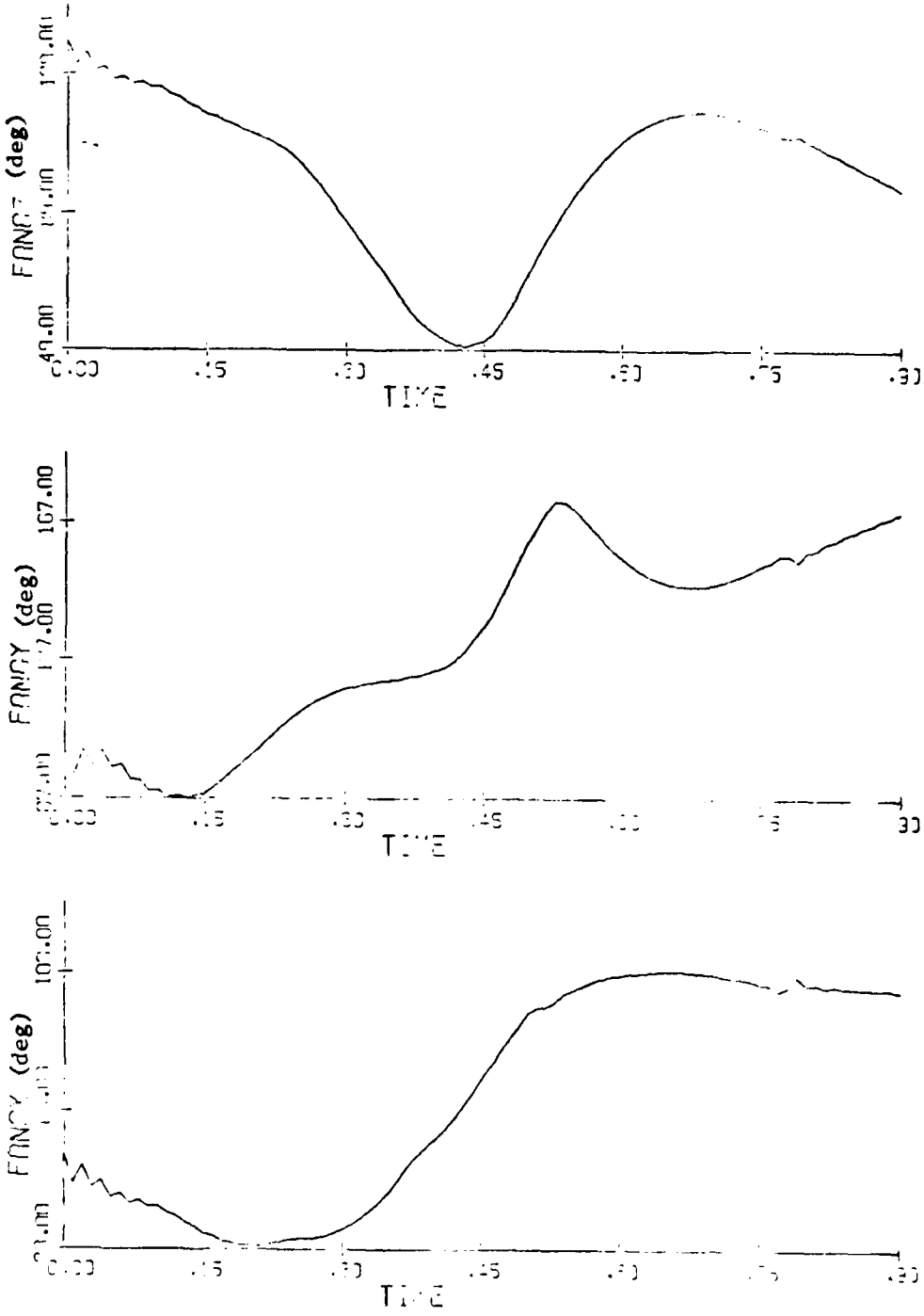

Fig. 3.9 (e)

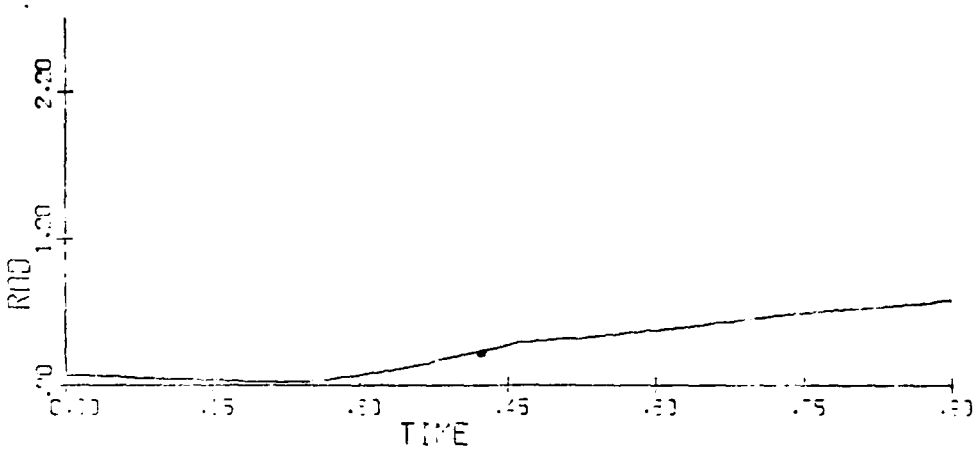

Fig. 3.9 (f)

The Figure 3.9 result shows that the extended burn time has induced more oscillatory behavior in the attitude variables, even at the early phase of the trajectory. A comparison of the roll plots in Figures 3.8 and 3.9 shows convincingly the nonlinear nature of the problem, since only the burn time was changed in the two runs.

3.3.4.2 Rocket Sizing Analysis. The study conducted in this subsection investigates the basic energy requirements for the escape conditions discussed in Section 3.3.4, along with the low altitude, high Q case originally presented in the Task 2 Interim Report (Figure 5.5). The data were computed by taking the commanded rocket force and torque at each control update time. The moment arm at each time was computed by dividing the torque magnitude by the magnitude of the force vector component perpendicular to the torque vector. Presented here are maximum values for the quantities force and torque magnitude, and moment arm. These values do not always occur siumultaneously, but they do tend to occur during about the first third of the rocket burn.

The cases in Table 3.1 generate the following energy requirements: for Condition 1, force = 2856 pounds, torque = 1597 ft-pounds, and moment arm = 7 inches; for Condition 2, force = 4166 pounds, torque = 2774 ft-pounds, and moment arm = 22 inches; for condition 3, force = 4998 pounds, torque = 3228 ft-pounds, and moment arm = 14 inches; and for Condition 4, force = 3029 pounds, torque = 1819 ft-pounds, and moment arm = 7.5 inches. Case 6 shows the highest energy demand of the seven MIL-S cases.

The high Q ejection condition is more appropriate for sizing the upper limits of the energy requirements, although inspection of adverse attitude cases is necessary to determine energy needed to gain sufficient altitude, as well as correct the attitude properly. For the high Q case presented as Figure 5.5 of the Interim Report, there is a maximum force requirement of 11,488 pounds, torque = 4492 ft-pounds, and moment arm = 11.5 inches. This has been improved with more detailed analysis of this condition, presented below.

Figure 3.10 shows the case in which there is no thrust magnitude limiting. Except for possibly excessive energy requirements, however, the results are very good. ZVEL, the body z-axis velocity component stays large and negative, which means altitude gain. The decrease in ZVEL's magnitude toward the end reflects control to the input desired final acceleration, a quantity which can also be "optimized". Similarly, XVEL decelerates for a while, but also responds to a(tf). Plots of CG motion, Figure 3.10(b), show the altitude gain clearly, and the basically planar motion which indicates that the controller is performing well. Attitude rates, shown in Figure 3.10(c) in deg/sec, are also very good, except perhaps for roll rate just before thrust cutoff. Roll angle is drifting a bit, but is not too tightly controlled anyway at these values. Yaw is very well controlled, which is critical at this speed, and the pitch response does not show quite enough control authority, although it has begun to correct itself. Particularly interesting about this run is that the controller gains were not greatly changed from those used in the low Q cases reported on earlier. Thus, a little more "tuning" of these gains, which are constant over a given run, as well as the nozzle and burn time parameters, will certainly lead to improvements.

Rocket motor results are plotted for this run in Figures 3.10(e-g). Nozzles 1 and 2 here are the "verniers", located off the pilot's shoulders in this case, and sized for about 2000 pounds thrust capacity apiece (see Figure 3.4). TMAG1 and TMAG2 plots show that lesser amounts are used. Pitch and roll angles are defined for each nozzle. The pitch direction is forward and back, and the roll is left-right. The plotted angles are values with respect to a nominal orientation, in a positive rotation sense in body axes. The nominal thrust direction for the verniers, nozzles 1 and 2, was arbitrarily set to be forward. Nozzle 3, located basically where the current ACES II nozzle is, but sized at about twice the energy, has pitch vectoring only. Its nominal direction is such that a pitch torque is generated which offsets the aerodynamic torque at 1600 Q. This offset is varied via input data to the program, for all nozzles, as well as their locations, nominal magnitudes, and thrust limits.

The verniers are now conceived as being basically fast responding, RCS-type thrusters, which can change thrust very fast in nearly all

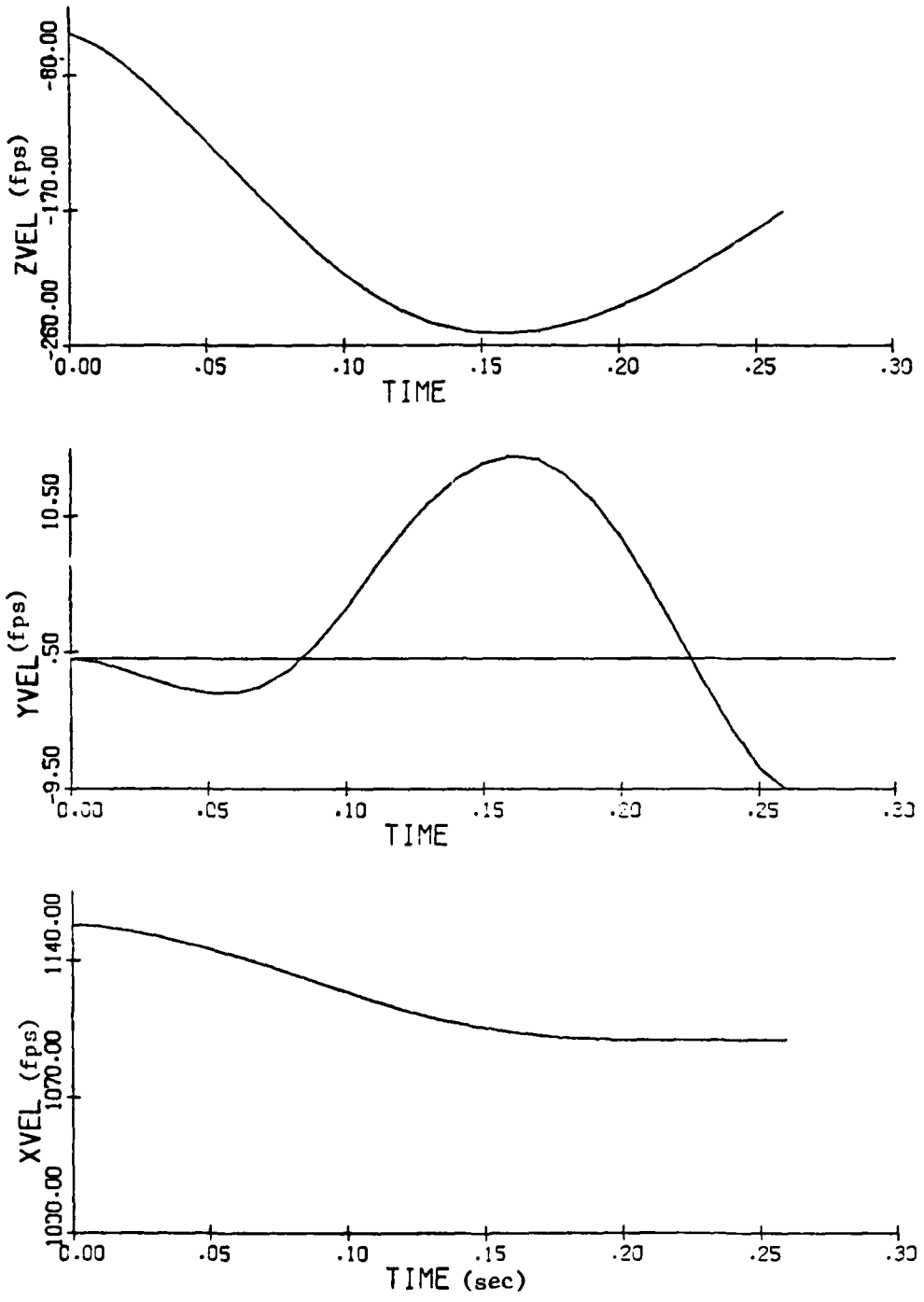

Fig. 3.10 (a)
High Q, Wings Level Case: No Thrust Limiting

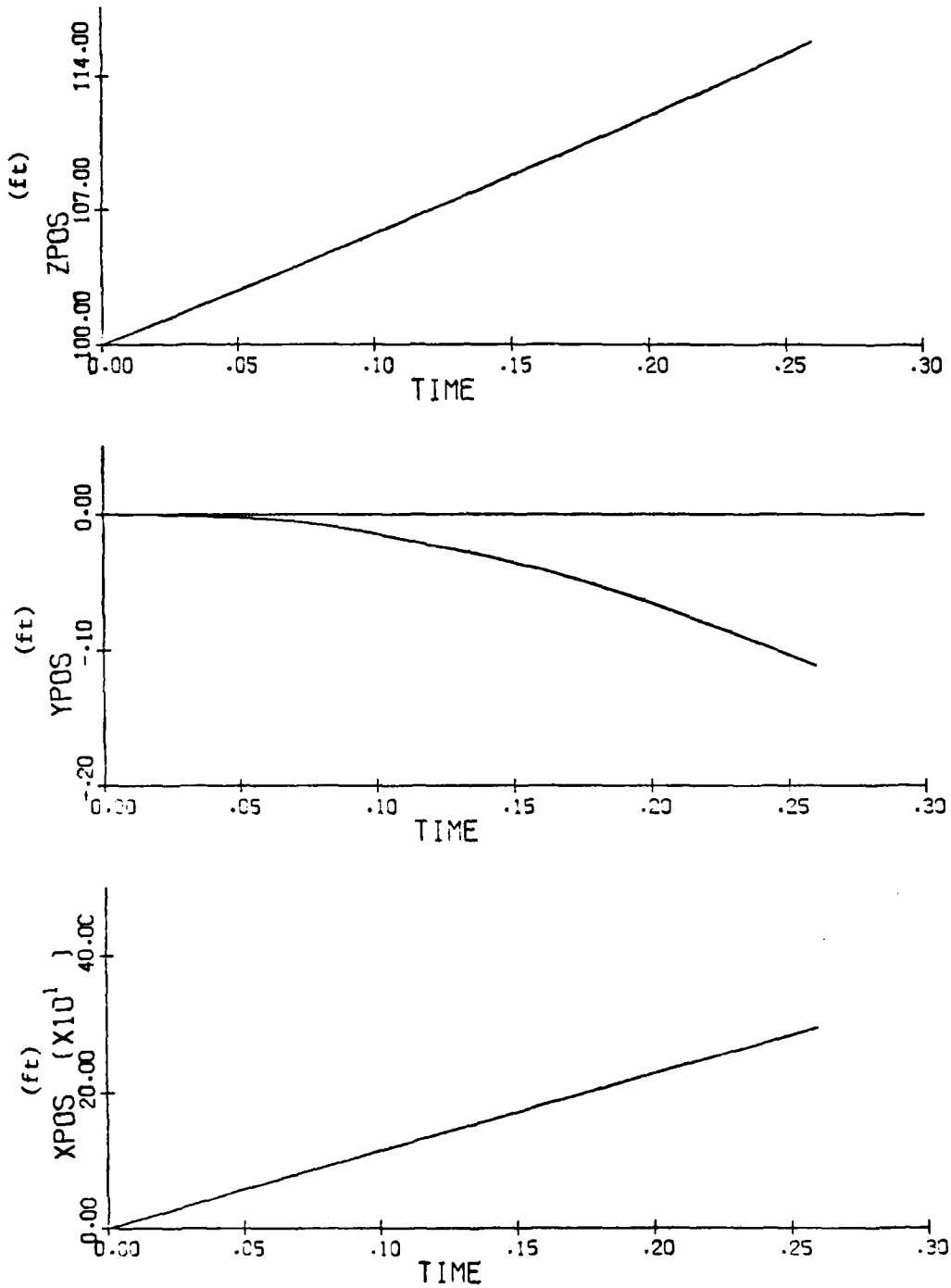
ZPOS (ft)
100.00
107.00
114.00
0.00
.05
.10
.15
.20
.25
.30
TIME
YPOS (ft)
0.00
-.10
-.20
0.00
.05
.10
.15
.20
.25
.30
TIME
XPOS (ft) (X10^1)
0.00
20.00
40.00
0.00
.05
.10
.15
.20
.25
.30
TIME

Fig. 3.10 (b)

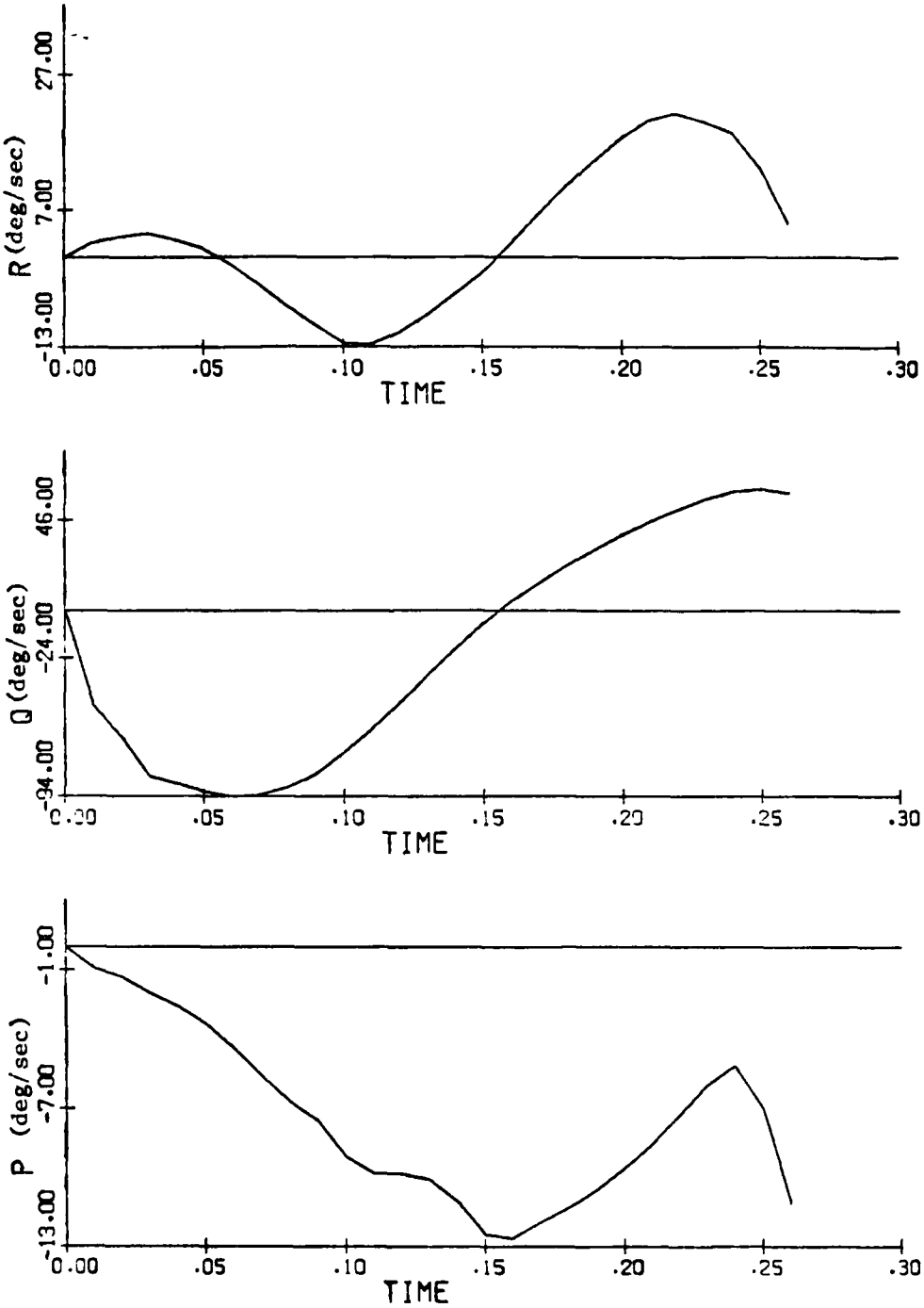
R (deg/sec)
27.00
7.00
-13.00
0.00
.05
.10
.15
.20
.25
.30
TIME
Q (deg/sec)
46.00
-24.00
-94.00
0.00
.05
.10
.15
.20
.25
.30
TIME
P (deg/sec)
-1.00
-7.00
-13.00
0.00
.05
.10
.15
.20
.25
.30
TIME

Fig. 3.10 (c)

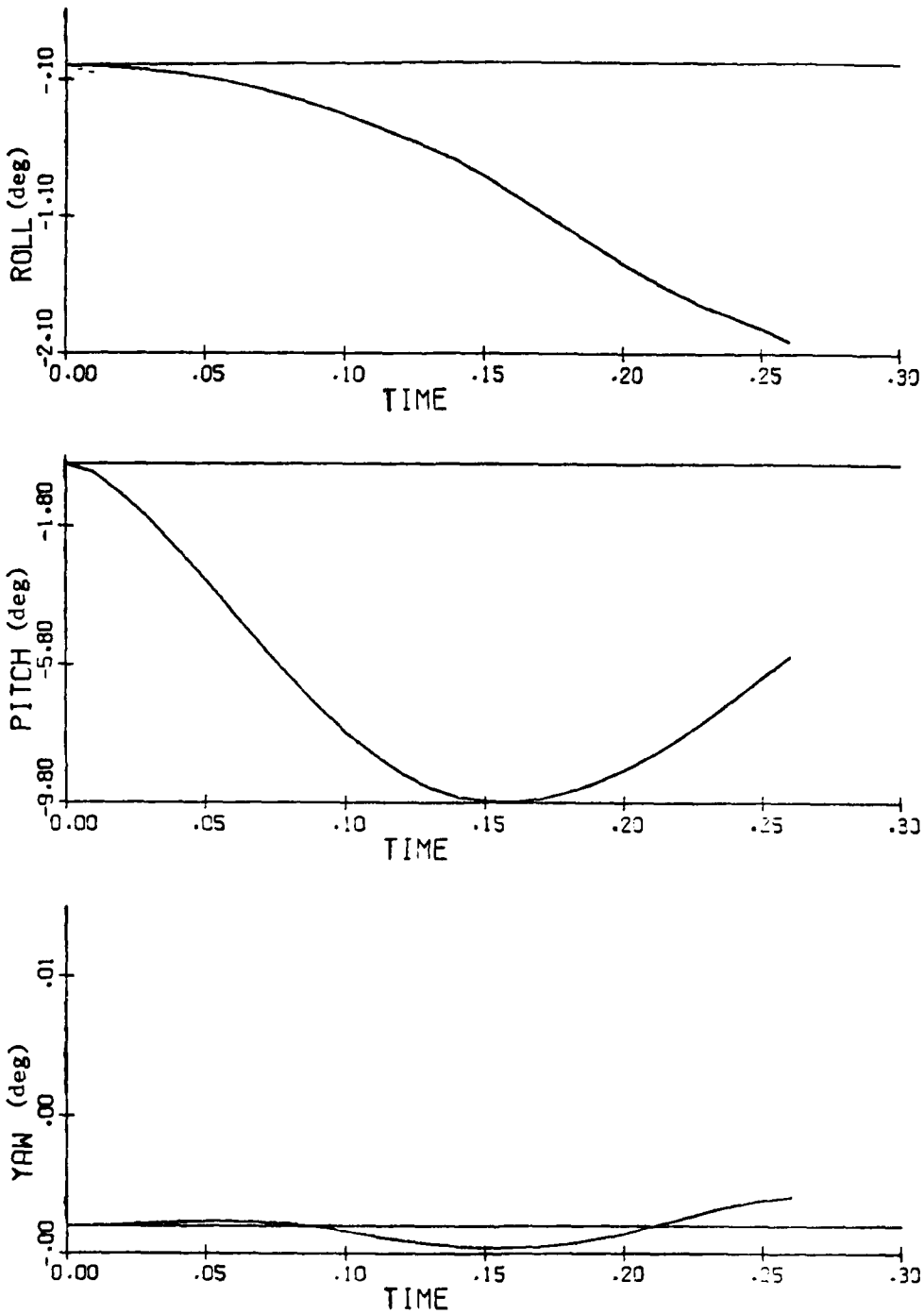
ROLL (deg)
-.10
-1.10
-2.10
0.00
.05
.10
.15
.20
.25
.30
TIME
PITCH (deg)
-1.80
-5.80
-9.80
0.00
.05
.10
.15
.20
.25
.30
TIME
YAW (deg)
.01
.00
-.00
0.00
.05
.10
.15
.20
.25
.30
TIME

Fig. 3.10 (d)

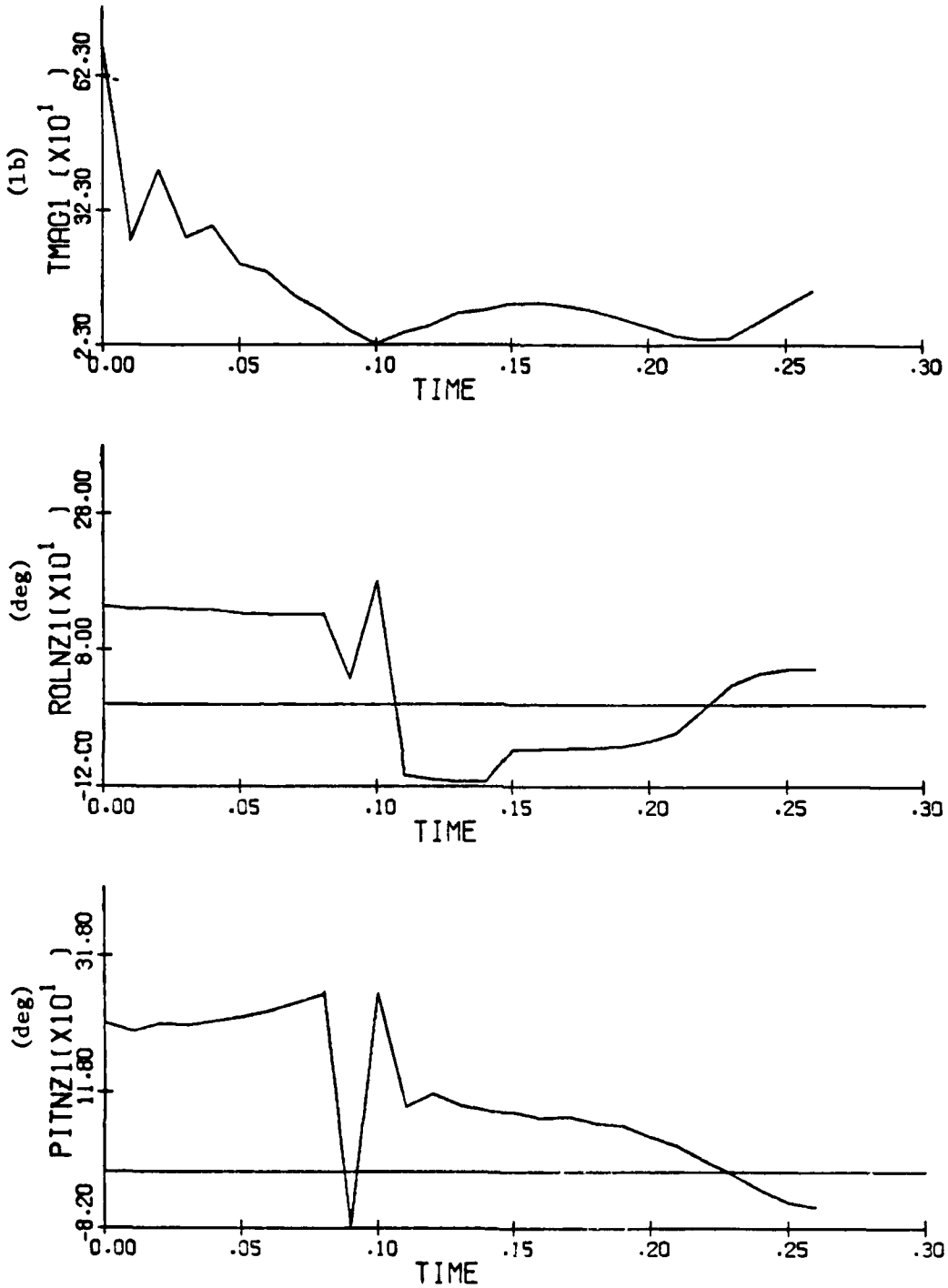
(lb)
TMAG1 (X10^1)
62.30
32.30
2.30
0.00
.05
.10
.15
.20
.25
.30
TIME
(deg)
ROLNZ1(X10^1)
28.00
8.00
-12.00
0.00
.05
.10
.15
.20
.25
.30
TIME
(deg)
PITNZ1(X10^1)
31.80
11.80
-8.20
0.00
.05
.10
.15
.20
.25
.30
TIME

Fig. 3.10 (e)

AD-A166 580 VECTORED THRUST DIGITAL FLIGHT CONTROL FOR CREW ESCAPE 2/3
VOLUME 1(U) SCIENTIFIC SYSTEMS INC CAMBRIDGE MA
J V CARROLL ET AL. DEC 85 AFWAL-TR-85-3116-VOL-1
UNCLASSIFIED F33615-C-82-3402 F/G 1/4 NL

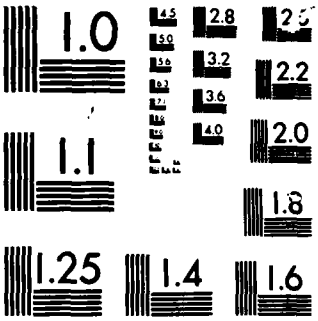

MICROCOPY CHART

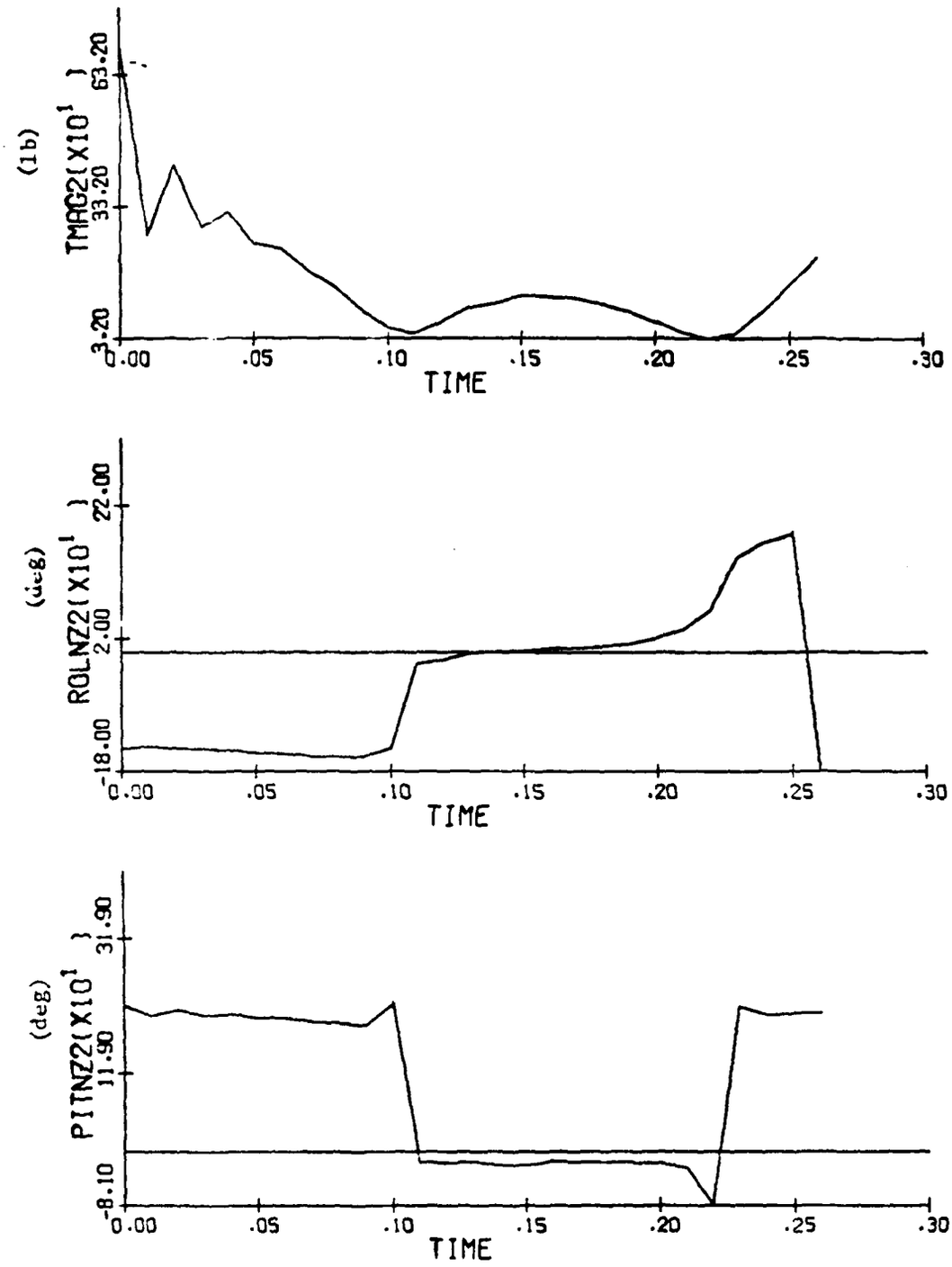
(lb)
TMAG2(X10^1)
63.20
33.20
3.20
0.00
.05
.10
.15
.20
.25
.30
TIME
(deg)
ROLNZ2(X10^1)
22.00
2.00
-18.00
0.00
.05
.10
.15
.20
.25
.30
TIME
(deg)
PITNZ2(X10^1)
31.90
11.90
-8.10
0.00
.05
.10
.15
.20
.25
.30
TIME

Fig. 3.10 (f)

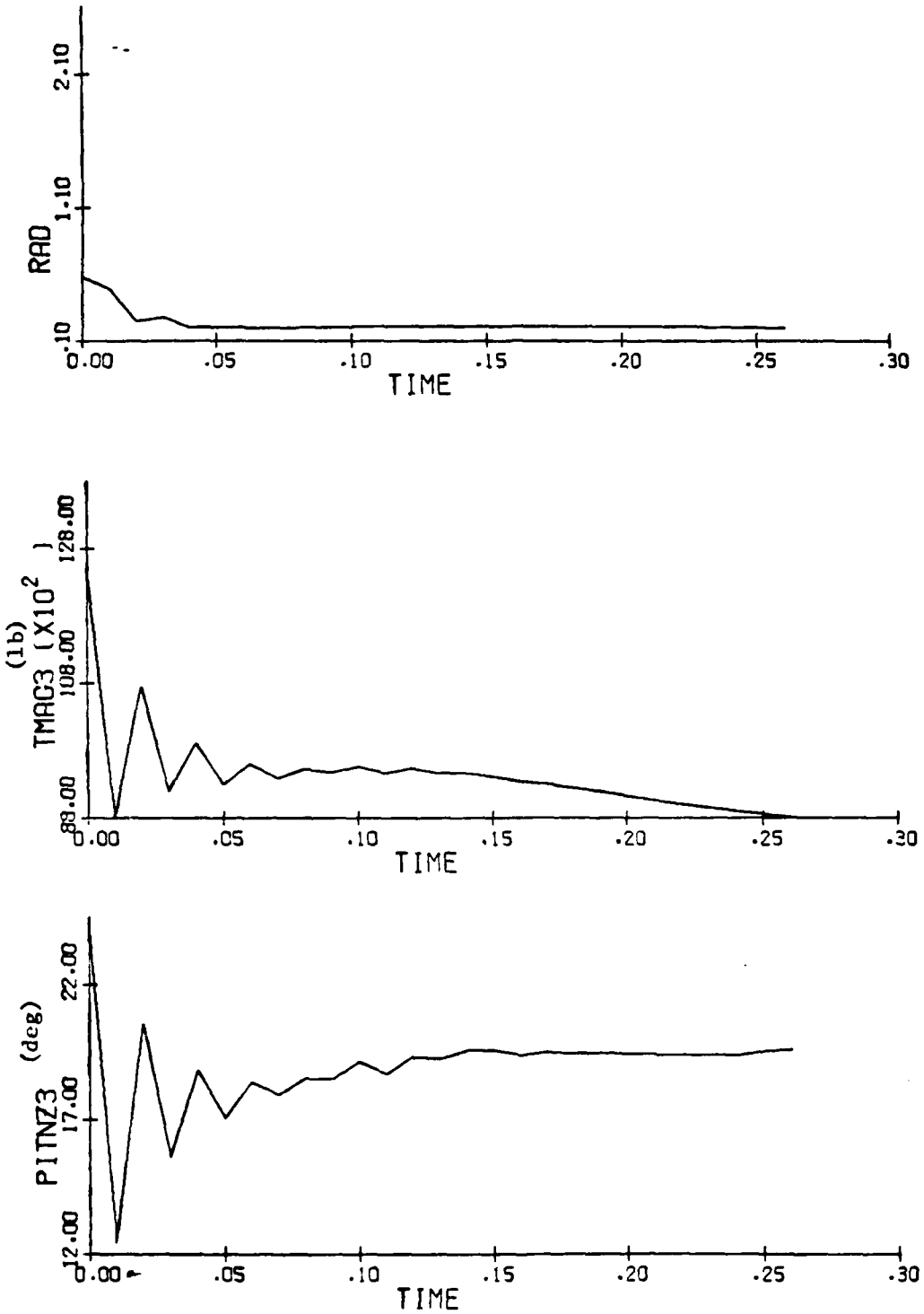
RAD
2.10
1.10
.10
0.00
.05
.10
.15
.20
.25
.30
TIME
TMAG3 (X10^2)
(lb)
128.00
108.00
88.00
0.00
.05
.10
.15
.20
.25
.30
TIME
PITNZ3
(deg)
22.00
17.00
12.00
0.00
.05
.10
.15
.20
.25
.30
TIME

Fig. 3.10 (g)

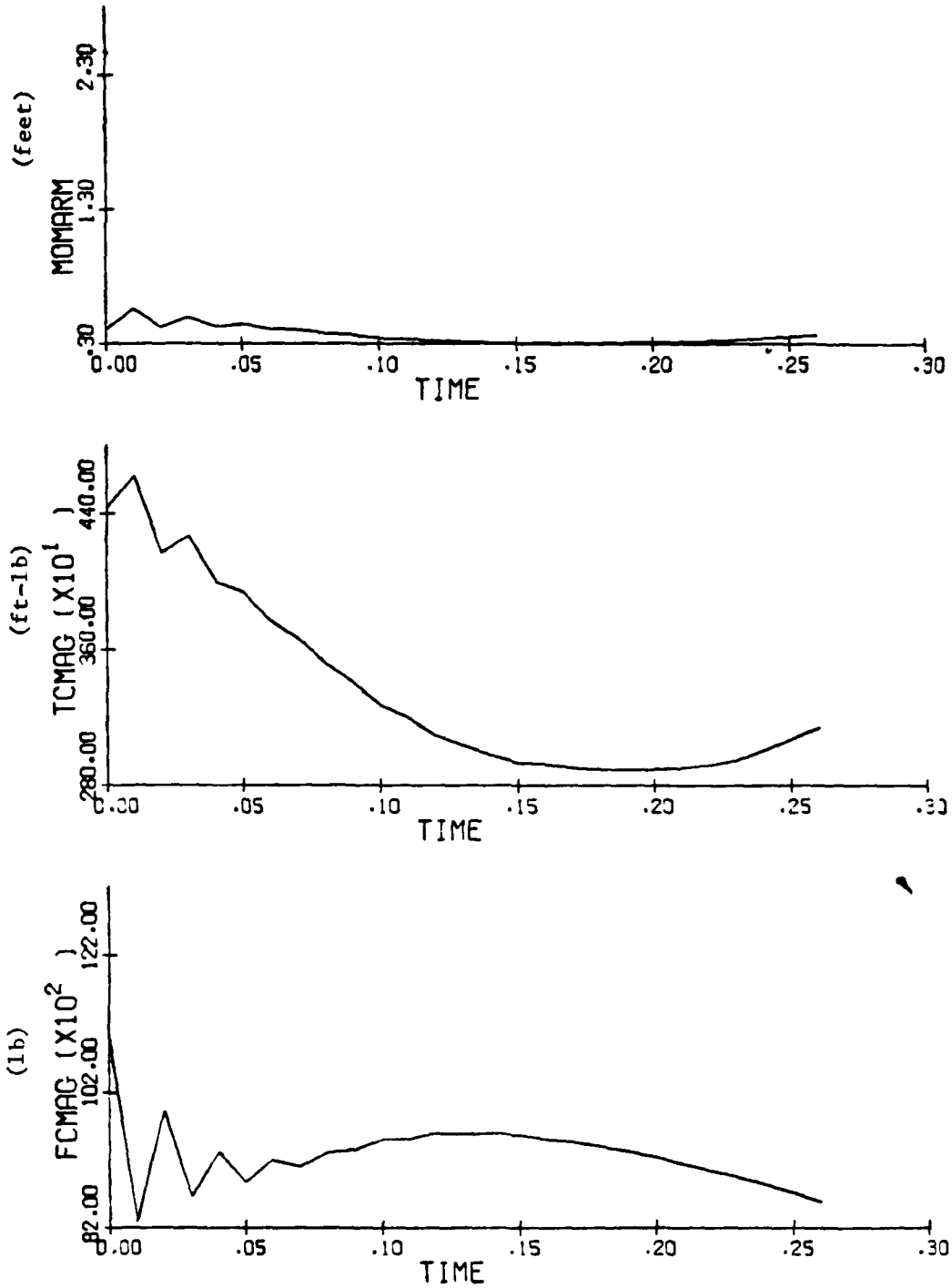
(feet)
MOMARM
2.30
1.30
.30
0.00
.05
.10
.15
.20
.25
.30
TIME
(ft-lb)
TCMAG (X10^1)
440.00
360.00
280.00
0.00
.05
.10
.15
.20
.25
.30
TIME
(lb)
FCMAG (X10^2)
122.00
102.00
82.00
0.00
.05
.10
.15
.20
.25
.30
TIME

Fig. 3.10 (h)

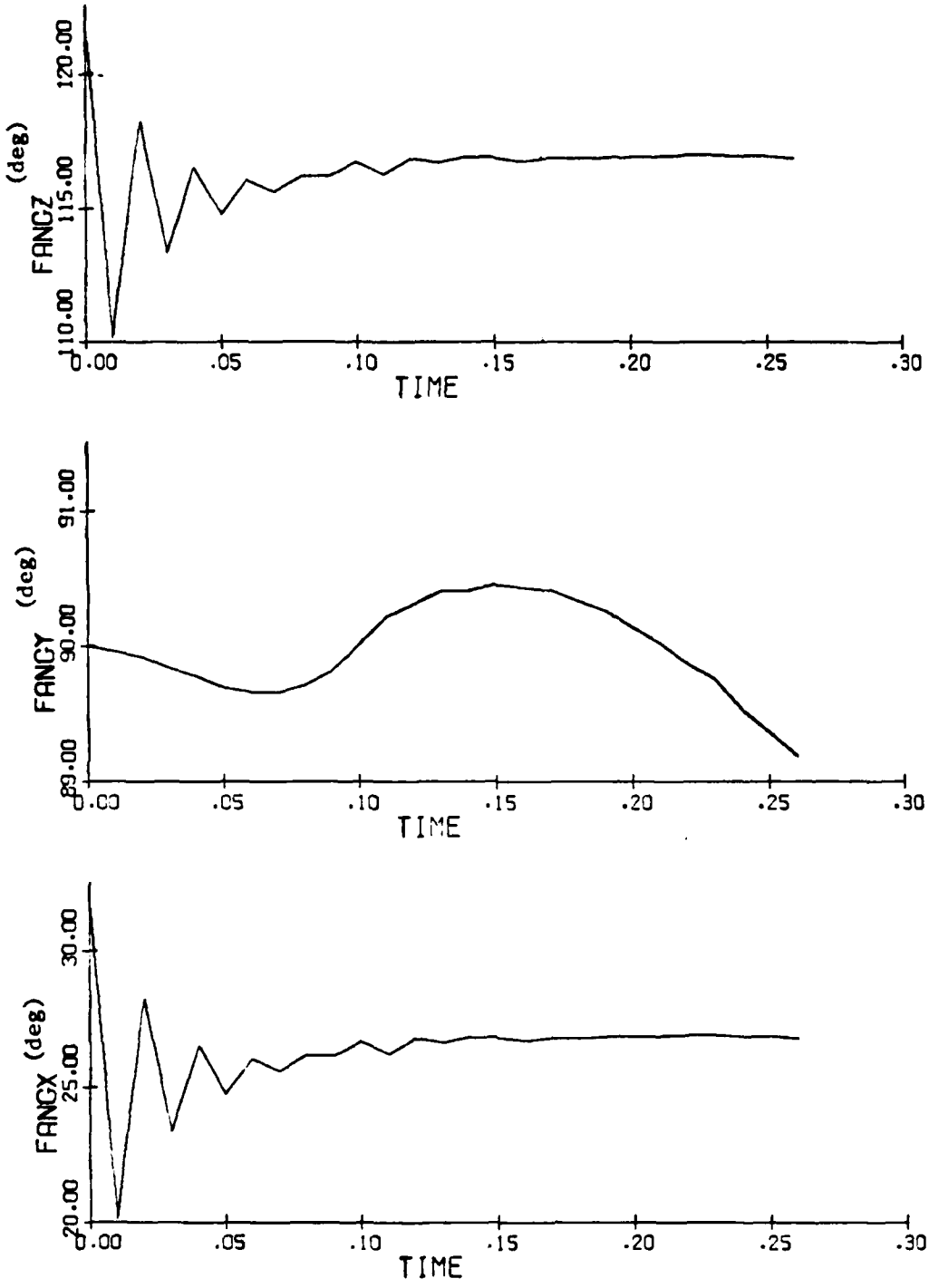
FANGZ (deg)
120.00
115.00
110.00
0.00
.05
.10
.15
.20
.25
.30
TIME
FANGY (deg)
91.00
90.00
89.00
0.00
.05
.10
.15
.20
.25
.30
TIME
FANGX (deg)
30.00
25.00
20.00
0.00
.05
.10
.15
.20
.25
.30
TIME

Fig. 3.10 (i)

directions. Rocket 3 can be considered to have a gimballed nozzle, whose cone angle is limited to about 30 degrees.

Summarizing, the controller module issues commanded (net) rocket force and torque vectors, (frc, trc). These are plotted in Figure 3.10(h,i) for this case. The actuator module converts (frc, trc) into nozzle angles and thrust magnitudes for a given configuration, e.g., Figures 4(e-g). There are 8 such quantities in this configuration, which become elements of the control vector, uc. System dynamics are a nonlinear function of uc.

CHAPTER 4

TASK 2: CONTROL LOGIC DESIGN

The main objective of Task 2 is to demonstrate the feasibility of vectored thrust control for the ejection seat by synthesizing a control methodology. The highly nonlinear and variable dynamics of the ejection seat, enlarged flight envelope and the lack of previous experience in applying the vectored thrust control concept to ejection seat makes the feasibility demonstration a challenging and key problem.

A review of a large number of control concepts by SSI revealed the fact that majority of the control design schemes cannot be applied directly to the ejection seat problem (Section 4.2). The highly nonlinear dynamics and short trajectory duration rule out the possibility of using purely linear design techniques such as LQG, frequency domain, pole placement, etc. It was realized that nonlinear reference trajectory methods, both real time and off-line optimal, need to be employed to determine feasibility under extreme ejection conditions such as high Q (dynamic pressure) and adverse attitude ejections. Therefore, a large part of the Task 2 effort was devoted to solving for optimal trajectories using ESOP (Ejection Seat Optimization Program). Then the issues of robustness and on-line implementation of optimal solutions were addressed. The results obtained (Volume II, Chapter 7) demonstrate the practicality of the vectored thrust control concept. Based on these results, one can assert with great confidence that an integrated design approach is capable of meeting all the specifications using near-term state-of-the-art hardware technologies.

In presenting the control law design, this chapter is broken into three main sections. Section 4.1 describes the special features and problems associated with control of ejection seats. Section 4.2 reviews candidate control approaches, and Section 4.3 describes in detail predictive acceleration control, the selected approach.

4.1 Unique Features, Problems in Ejection Seat Control.

There are many design issues which relate to vectored thrust control of ejection seats which must be addressed before the design can be finalized. For example, it is necessary to assimilate data on hardware components, model these into the system, and "fine tune" the controller. Other details relating to reliability issues, redundancy management and fault tolerance must be addressed by follow-on projects.

We have focused on control of the seat/pilot system once the rocket thrusters are on and it is free of the rails. The total control system must also address the catapult phase of the ejection - the portion of the trajectory from catapult ignition to rail separation. It is during this time that the system, fully activated, must sequence sensor start-up, detect the flight condition, establish the sequence for catapult operation, chute deployment, etc., set nominal thrust levels both for the rocket(s) and catapult(s), and compute/select the appropriate reference optimal trajectory.

As the sensors come on line (this must happen within 0.08 to 0.10 seconds after catapult ignition), they must provide relevant information from the environment so that the rocket nozzles can be gimballed (or appropriate RCS nozzles selected) to the proper settings for the escape condition. In this way, the system would be optimally configured to handle its environment once totally free of the rails. Sensor information will also be used to modulate the catapult thrust level, as required by the given condition. Closely related to these design issues is the effect of sensor noise on overall system performance. Sufficiently accurate, reliable sensors may result in a simpler design, with less need for redundancy and/or real time estimation.

When all but the last set of rail blocks are free, the seat/pilot system has a degree of freedom in pitch. The rocket should be on by this time, providing the required forces and restoring torques.

Event sequencing will be controlled from the microprocessor, aided by a clock and sensor input. There likely will be more than one sample rate,

the rates ranging from 50 Hz to as much as 500 Hz. With the capability for extremely high rates being generated, it is vital that aliasing be avoided. Control rates are thus an important design issue. The attitude control loop is the most critical; the system presented here does not require that the desired attitude at any instant be attained in order to issue appropriate steering commands. Control activity is decoupled, but it is recognized that the basic problem is a highly coupled 6 DOF problem. This is to say, for example, that success in attitude control has direct bearing on effectiveness of steering control.

4.1.1 Development of Control Design Methodology. In this chapter, we present the overall vectored thrust control requirements for crew escape, as well as the design methodology which we feel is most appropriate for developing an effective and efficient control system. The control requirements presented here are, in effect, qualitative control system specifications.

The control design approach must reflect the realities of the plant which is to be controlled. In the case of a detached ejection seat with crewperson ("seat/pilot") system, the extreme conditions of altitude, airspeed, and orientation can combine to pose a severely constrained optimization problem. In addition, it is a problem which does not readily lend itself to classic, or even classic/optimal design techniques, because in addition to the above constraints, the seat/pilot system in an airflow is highly nonlinear. The dynamic nonlinearity is further enhanced by nonlinearities due to energy source fuel consumption (mass change effect), and "discrete" mass changes due to deployment of various devices during the ejection sequence.

For these reasons, and they have been confirmed over the past few months by simulations and discussions with seat designers, the standard linear quadratic regulator (LQR) approach by itself is felt to be overly inadequate for this job , even assuming that it can be implemented at all. Our approach is, in summary, to use powerful techniques based on nonlinear acceleration control whose features are geared more appropriately to this type of control problem. The idea is to run several detailed off-line

solutions for optimal escape trajectories, the appropriate one of which could then be retrieved from storage and implemented in real time with linear perturbation optimal control augmentation; or, to generate suboptimal "on-line" trajectories, using sets of key pre-stored parameters to shape them depending on the condition.

4.2 Review of Candidate Control Synthesis Techniques.

Although we feel that the primary approach presented in this report is very capable of working efficiently throughout the MIL-S-9479 "escape envelope", it is also important to investigate other methodologies which offer potential for useful application instead of, or in conjunction with, the method presented. Such a survey has become increasingly more important as interest has grown in this project; however, a comprehensive effort in this direction is beyond the scope of the current effort. We do propose, however, to look closely at the more promising of the alternative approaches, and consider seriously their role as part of the overall design.

The common requirements which any method under consideration must have are: (1) an ability to work in a dynamic environment which is at best poorly modeled by an LTI (linear time-invariant) system; (2) predictive ability; (3) amenability to real time implementation; and (4) ability to adapt well in the presence of unanticipated disturbances, poor initial conditions, etc.

These requirements eliminate many of the standard classical and optimal design methods, and make quite difficult, if not impossible, the application of standard optimal control synthesis methods such as LQG (linear quadratic gaussian). The search focuses, then, to those methods capable of multivariable synthesis of systems whose system (Jacobian) matrix elements vary widely over the flight regime. Section 4.2.3 discusses briefly an appealing method of this type.

An inspection of escape trajectories reveals why standard linear control synthesis techniques would not be adequate for this problem. Uncontrolled trajectories show significant variation in the system Jacobian

LINEARIZATION MODE :
TIME = 0.0000

SYSTEM (JACOBIAN) MATRIX :

-1.42421	0.000000E+00	0.567874E-01	0.000000E+00	45.0000	0.000000E+00	
0.000000E+00	-32.1746	0.000000E+00	0.000000E+00	0.000000E+00	0.000000E+00	0.000000E+00
0.000000E+00	-0.912261E-02	0.000000E+00	-45.0000	0.000000E+00	-1000.00	
32.1746	0.000000E+00	0.000000E+00	0.000000E+00	0.000000E+00	0.000000E+00	0.000000E+00
0.000000	0.000000E+00	-0.233407E-01	0.000000E+00	1000.00	0.000000E+00	
0.000000E+00	0.000000E+00	0.000000E+00	0.000000E+00	0.000000E+00	0.000000E+00	0.000000E+00
-0.571924E-01	0.159028E-02	0.300056E-03	-0.550223	-0.209733E-01	-0.303573E-02	
0.000000E+00	0.000000E+00	0.000000E+00	0.000000E+00	0.000000E+00	0.000000E+00	0.000000E+00
-0.000017	0.228096E-03	0.150028E-01	-0.935063E-02	-1.04103	0.138593E-03	
0.000000E+00	0.000000E+00	0.000000E+00	0.000000E+00	0.000000E+00	0.000000E+00	0.000000E+00
0.120060E-1	-0.117206E-01	-0.267779E-02	-0.251184	0.377187E-01	-0.152202E-01	
0.000000E+00	0.000000E+00	0.000000E+00	0.000000E+00	0.000000E+00	0.000000E+00	0.000000E+00
0.000000E+00	0.000000E+00	0.000000E+00	1.00000	0.000000E+00	0.000000E+00	
0.000000E+00	0.000000E+00	0.000000E+00	0.000000E+00	0.000000E+00	0.000000E+00	0.000000E+00
0.000000E+00	0.000000E+00	0.000000E+00	0.000000E+00	1.00000	0.000000E+00	
0.000000E+00	-45.0000	0.000000E+00	0.000000E+00	0.000000E+00	0.000000E+00	0.000000E+00
0.000000E+00	1.00000	0.000000E+00	0.000000E+00	0.000000E+00	0.000000E+00	
0.000000	0.000000E+00	0.000000E+00	0.000000E+00	0.000000E+00	0.000000E+00	1000.00
0.000000E+00	0.000000E+00	1.00000	0.000000E+00	0.000000E+00	0.000000E+00	
0.000000E+00	-1000.00	0.000000E+00	0.000000E+00	0.000000E+00	0.000000E+00	0.000000E+00
0.000000E+00	0.000000E+00	0.000000E+00	0.000000E+00	0.000000E+00	1.00000	
0.000000E+00	0.000000E+00	0.000000E+00	0.000000E+00	0.000000E+00	0.000000E+00	0.000000E+00

Fig. 4.1 Systems Linear Matrix, Uncontrolled Run
(a) t=0 sec. (Rocket Ignition)

```
LINEARIZATION MODE :      2
TIME =      0.1000

SYSTEM (JACOBIAN) MATRIX, A :
-1.15971          0.261356          9.13450          0.000000E+00      565.823          -11.8134
        0.000000E+00      -25.7230          0.000000E+00      0.000000E+00      0.000000E+00      0.000000E+00

-0.244230         -0.231192E-02     -0.325353         -565.823          0.000000E+00      -802.376
        26.7196           -0.682254         0.000000E+00      0.000000E+00      0.000000E+00      0.000000E+00

-7.73554          0.319536          -0.417054         11.8134           802.376           0.000000E+00
        0.719769          17.7023           0.000000E+00      0.000000E+00      0.000000E+00      0.000000E+00

0.436909E-02      -0.252547E-02     -0.297072E-02     -1.79009          0.565816          -5.73980
        0.000000E+00      0.000000E+00      0.000000E+00      0.000000E+00      0.000000E+00      0.000000E+00

0.480[illegible]E-01      -0.990930E-03     -0.398624E-01     -0.227522         -1.02415          -0.100734
        0.000000E+00      0.000000E+00      0.000000E+00      0.000000E+00      0.000000E+00      0.000000E+00

0.744165E-02      -0.736407E-02     -0.470241E-02     1.45549           1.49538           1.24209
        0.000000E+00      0.000000E+00      0.000000E+00      0.000000E+00      0.000000E+00      0.000000E+00

0.000000E+00      0.000000E+00      0.000000E+00      1.00000           0.180423E-01      -0.669769


        5.56934           0.582059          0.000000E+00      0.000000E+00      0.000000E+00      0.000000E+00

0.000000E+00      0.000000E+00      0.000000E+00      0.000000E+00      0.999637          0.269284E-01
        -0.470744         0.000000E+00      0.000000E+00      0.000000E+00      0.000000E+00      0.000000E+00

0.[illegible]453          -0.124163E-01     -0.555950         0.000000E+00      0.000000E+00      0.000000E+00
        -0.445[illegible]         -[illegible]          0.000000E+00      0.000000E+00      0.000000E+00      0.140397

0.227727E-01      0.999573          0.116672E-01      0.000000E+00      0.000000E+00      0.000000E+00
        [illegible]          -0.535377         0.000000E+00      0.000000E+00      0.000000E+00      991.617

0.355623          -0.223711E-01     0.330454          0.000000E+00      0.000000E+00      0.000000E+00
        -[illegible]          -931.245          0.000000E+00      0.000000E+00      0.000000E+00      0.000000E+00

0.000000E+00      0.000000E+00      0.000000E+00      0.000000E+00      -0.324139E-01     1.20327
        -10.[illegible]          -0.377655         0.000000E+00      0.000000E+00      0.000000E+00      0.000000E+00
```

Fig. 4.1(b) t-0.1. Notice that elements are quite different from those in (a).

matrix elements even over periods as small as 0.01 seconds, as seen in Figure 4.1, where the system matrix is compared at t=0.0 (Figure 4.1a) and t=0.1 seconds (Figure 4.1b). There is improvement when the trajectory is "controlled", as seen in Figure 4.2, but robustness is always a concern with such designs.

4.2.1 LQR Design. The purpose of LQR design is to stabilize the seat around a nominal trajectory using vernier rocket thrust via feedback from sensed angular rates, attitude, accelerations, etc., for disturbance rejection and pilot load minimization. LQR design is based on the linearized models developed in Section 3.2 and a performance index based on the minimization of deviations from the nominal trajectory. LQR designs can be computed using OPTSYS III software described in section 4.3.3. The purpose of LQR design is to place all the poles of the system in the left-half plane for different flight conditions to achieve stability and robustness. This would most likely require time varying gains which will be computed off-line and stored in the microprocessor memory for online retrieval.

The LQR design process begins with the deterministic first order linear constant coefficient set of equations, (A.2), which are rewritten here in compact form

$$\dot{x} = Ax + Bu \tag{4.1}$$

Disturbance and other random effects are modeled by adding to Equation (4.1) process noise terms of the form Γw where w is a vector of random variables with quantifiable statistics, and Γ is an appropriate constant matrix. Continuous or sampled measurement equations of the form

$$y(t) = Cx(t) + v \tag{4.2}$$

complete the dynamic representation of the system (v is measurement noise. See Appendix E for a treatment of estimating x in the presence of w and v).

In our application, the LQR optimization process would be done about a reference optimal solution, (x,u), generated off-line by means of a

```
LINEARIZATION MODE :      2
TIME =      0.0000

SYSTEM (JACOBIAN) MATRIX, A :
-1.48621          0.000000E+00      0.567894E-01      0.000000E+00      45.0000           0.000000E+00
        0.000000E+00      -32.1740          0.000000E+00      0.000000E+00      0.000000E+00      0.000000E+00

0.000000E+00      -0.912261E-02     0.000000E+00      -65.0000          0.000000E+00      -1000.00
        32.1740           0.000000E+00      0.000000E+00      0.000000E+00      0.000000E+00      0.000000E+00

0.513681          0.000000E+00      -0.233437E-01     0.000000E+00      1000.00           0.000000E+00
        0.000000E+00      0.000000E+00      0.000000E+00      0.000000E+00      0.000000E+00      0.000000E+00

-0.671924E-02     0.159502E-02      0.302356E-03      -0.550220         -0.209733E-01     -0.303673E-02
        0.000000E+00      0.000000E+00      0.000000E+00      0.000000E+00      0.000000E+00      0.000000E+00

-0.333517         0.228209E-03      0.150032E-01      -0.908943E-02     -1.04103          0.188593E-03
        0.000000E+00      0.000000E+00      0.000000E+00      0.000000E+00      0.000000E+00      0.000000E+00

0.120840E-01      -0.117227E-01     -0.343779E-03     -0.253184         0.377187E-01      -0.162202E-01
        0.000000E+00      0.000000E+00      0.000000E+00      0.000000E+00      0.000000E+00      0.000000E+00

0.000000E+00      0.000000E+00      0.000000E+00      1.00000           0.000000E+00      0.000000E+00
        0.000000E+00      0.000000E+00      0.000000E+00      0.000000E+00      0.000000E+00      0.000000E+00

0.000000E+00      0.000000E+00      0.000000E+00      0.000000E+00      1.00000           0.000000E+00
        0.000000E+00      0.000000E+00      0.000000E+00      0.000000E+00      0.000000E+00      0.000000E+00

1.00000           0.000000E+00      0.000000E+00      0.000000E+00      0.000000E+00      0.000000E+00
        0.000000E+00      -45.0000          0.000000E+00      0.000000E+00      0.000000E+00      0.000000E+00

0.000000E+00      1.00000           0.000000E+00      0.000000E+00      0.000000E+00      0.000000E+00
        45.0000           0.000000E+00      0.000000E+00      0.000000E+00      0.000000E+00      1000.00

0.000000E+00      0.000000E+00      1.00000           0.000000E+00      0.000000E+00      0.000000E+00
        0.000000E+00      -1000.00          0.000000E+00      0.000000E+00      0.000000E+00      0.000000E+00

0.000000E+00      0.000000E+00      0.000000E+00      0.000000E+00      0.000000E+00      1.00000
        0.000000E+00      0.000000E+00      0.000000E+00      0.000000E+00      0.000000E+00      0.000000E+00
```

Fig. 4.2 System Linear Matrix, Controlled Run
(a) t=0. sec. (Rocket Ignition)

```
LINEARIZATION MODE :     2
TIME =      0.1000
SYSTEM (JACOBIAN) MATRIX, A :
-1.41622          -0.951676E-02        0.654251          0.000000E+00        58.5250          0.265044
        0.000000E+00        -32.1512          0.000000E+00        0.000000E+00        0.000000E+00        0.000000E+00

 0.964269E-02      -0.872045E-02        0.641134E-02       -58.5250          0.000000E+00       -957.009
        32.1512          0.223993E-03        0.000000E+00        0.000000E+00        0.000000E+00        0.000000E+00

 0.127297          -0.398632E-02       -0.302676E-01       -0.265044          957.009          0.000000E+00
       -0.638085E-02        1.21075          0.000000E+00        0.000000E+00        0.000000E+00        0.000000E+00

-0.635745E-02       0.155622E-02        0.388734E-03       -0.579338         -0.132024E-02       -0.258234
        0.000000E+00        0.000000E+00        0.000000E+00        0.000000E+00        0.000000E+00        0.000000E+00


-0.317842          0.605929E-03        0.194374E-01       -0.132681E-01       -0.994948         -0.215664E-01
        0.000000E+00        0.000000E+00        0.000000E+00        0.000000E+00        0.000000E+00        0.000000E+00

 0.111621E-01      -0.111556E-01       -0.582605E-03       -0.171691          0.991327E-01        0.391089E-01
        0.000000E+00        0.000000E+00        0.000000E+00        0.000000E+00        0.000000E+00        0.000000E+00

 0.000000E+00       0.000000E+00        0.000000E+00        1.00000          -0.712238E-05       -0.376580E-01
        0.136445E-01       -0.100020E-01        0.000000E+00        0.000000E+00        0.000000E+00        0.000000E+00

 0.000000E+00       0.000000E+00        0.000000E+00        0.000000E+00        1.00000          -0.189133E-03
        0.998782E-02        0.000000E+00        0.000000E+00        0.000000E+00        0.000000E+00        0.000000E+00

 0.999292          0.400731E-03       -0.376314E-01        0.000000E+00        0.000000E+00        0.000000E+00
        0.134785E-01       -22.4700          0.000000E+00        0.000000E+00        0.000000E+00        0.116824

-0.407560E-03       1.00000          -0.173735E-03        0.000000E+00        0.000000E+00        0.000000E+00
        58.5250          0.915435E-02        0.000000E+00        0.000000E+00        0.000000E+00        958.534

 0.375313E-01       0.138999E-03        0.999292          0.000000E+00        0.000000E+00        0.000000E+00
        0.275917          -958.534          0.000000E+00        0.000000E+00        0.000000E+00        0.000000E+00

 0.000000E+00       0.000000E+00        0.000000E+00        0.000000E+00        0.189267E-03        1.00071
       -0.357902          0.375356E-03        0.000000E+00        0.000000E+00        0.000000E+00        0.000000E+00
```

Fig. 4.2 (b) t=0.1 sec. Notice that the degree of change from (a) is much less than in Fig. 4.1

nonlinear programming technique such as ESOP (Subsection 4.2.4). Equations (A.2) are designed to be formulated about a general reference trajectory. The cost function for the off-line nonlinear solution may be of the form

$$\min_{u} \quad J = \int_{t_0}^{t_f} [(\text{Radical})^2 + 1/2\ x^T Q x + 1/2\ u^T R u] \tag{4.3}$$

where the event times t_0 and t_F represent the initiation and termination, respectively, of the sustainer rocket phase, and the acceleration radical is given in Equation (3.34). Minimization of (4.3) is done subject to equality and inequality constraints of the form

$$\text{(Equality)} \qquad g(X,U) = 0. \tag{4.4}$$

$$\text{(Inequality)} \qquad h(X,U) < 0. \tag{4.5}$$

$$X_\ell < X < X_u \tag{4.6}$$

$$U_\ell < U < U_u \tag{4.7}$$

where X is the string of state variables at each sample time, i.e, $[x_0, x_1, , , x_N]$, and U is similar for the control vectors. The equality constraints (4.4) are the dynamic equations (A.1), and the inequality constraints quantify requirements such as altitude, seat-aircraft separation and TVC constraints. These constraints are presented in Section 3.3. Subscripts in Equations (4.6) and (4.7) refer to appropriate lower and upper bounds for state and control variables.

The cost function is itself a function of the spinal compression deflection and rate, as given in the DRI expression in MIL-S-9479B, and also of the seat/pilot load factors, Equations (A.1), and finally, of specific, condition-dependent state and control quadratic elements.

The LQR cost and constraints are obtained by linearization of Equations (4.3 to 4.7) around the off-line-generated optimal solutions using the ESOP approach. The LQR phase in the design process effectively closes the loop, so that control is stable in the presence of process and measurement disturbances for a specific escape trajectory.

A major object of the LQR design is that it ensure a stable closed loop system for the combined MAC-MINOS based outer loop control to operate on. One technique for assuming stability is left half plane pole placement which can be achieved by minimizing a quadratic cost function which goes to zero when the eigenvalues of the closed loop system are at the desired stable locations. The technique reduces to the solution of an n(n-m) th order linear algebraic system, where n is the state dimension, and m is the control variable dimension.

Linear Operating Points. The very nonlinear nature of the seat/pilot dynamic system requires great care whenever linearization assumptions are made. We have therefore presented a very general set of linear equations (A.2). These are designed to be used about any nominal trajectory, stable or not (although the latter will work only for a brief time interval). It is necessary, however, to choose carefully the points along a given trajectory where linearization makes most sense. From our experience, a single linearization will not suffice over a given trajectory. Fortunately, EASIEST or the SSI-developed control design software can perform numerical system linearization at any desired point(s).

4.2.2 Model Algorithmic Control (MAC) Design. It is possible to consider a MAC design approach for modulating the main thrust on-line to keep the seat on the preselected optimal trajectory while minimizing pilot acceleration loads. The MAC design approach has been described in Mehra et al. (1980) and consists of predicting the future motions of the system and taking corrective actions to keep all the constraints satisfied. In essence, the MAC approach implements the trajectory optimization procedure on-line to compensate for stochastic deviations from the open loop optimal trajectories. MAC design is more appropriate for this application compared to LQR since hard constraints on states and controls have to be kept satisfied.

The following description is intended to provide background information on the MAC philosophy. With this information, it can be seen how critical MAC concepts relate to the crew escape control logic design actually developed. In particular, ideas common both to MAC and

acceleration control include: (i) internal model of the system; (ii) hierarchical structure; and (iii) use of reference trajectories. The main features and philosophy of MAC are discussed. Next, MAC implementation and algorithms are outlined. A fairly complete bibliography is included for further information.

Historical Overview. Model Algorithmic Control was first conceived by Adersa/ Gerbios in the late 1960's. (Richalet and Gimoret 1968, Lecamus and Richalet 1968; Richalet, Lecamus and Hummel 1970; Richalet, Rault, Pouliquen 1971). The method was subsequently developed and applied successfully to several industrial processes involving multivariable plant dynamics. With the growth of digital technology in the 70's and particularly the availability of powerful microprocessors with large memories, the application of MAC to industrial processes became more practical and economical. For instance, in the past five years, MAC has been successfully used for Aircraft Flight Control (Rault et al. 1975), Superheater Control (Testud 1977), On-Line Control of Steam Generator (Lecrique et al. 1978), European Transonic Wind Tunnel Control (Mereau and Littman, 1978), F-100 Jet Engine Multivariable Control (Mehra et al. 1977), Adaptive Flight Control (Mehra et al. 1978) and Electric Plant Control (Mehra et al. (1980)). Recently attention has also been focused on theoretical properties of MAC to gain a better understanding for design purposes. These theoretical results are reported in Richalet et al. (1978), Mehra et al. (1979), Praly (1979), Mehra et al. (1980), Mehra and Rouhani (1980) and Reid et al. (1980).

Basic Principles of Model Algorithmic Control (MAC). The MAC strategy relies on the following four features: (i) internal model of the system; (ii) hierarchical decomposition; (iii) reference trajectory and output constraints; and (iv) control trajectory computation.

Internal Model of the System. The multivariable system to be controlled is represented by a mathematical model in time-domain of the input-output type (see Figure 4.3). For linear systems, the model may be of the impulse response type, a representation which has certain distinct advantages over the state space representation or the transfer function

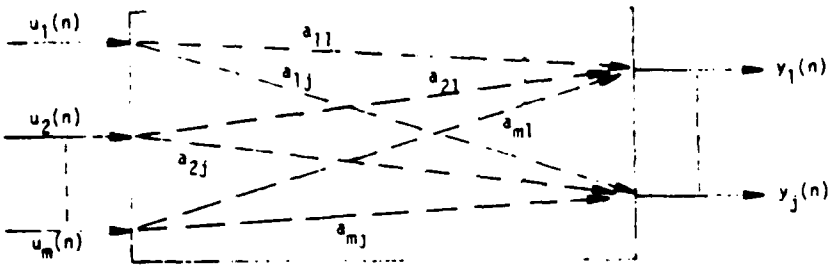

Figure 4.3 Impulse Response Representation of a Linear System.

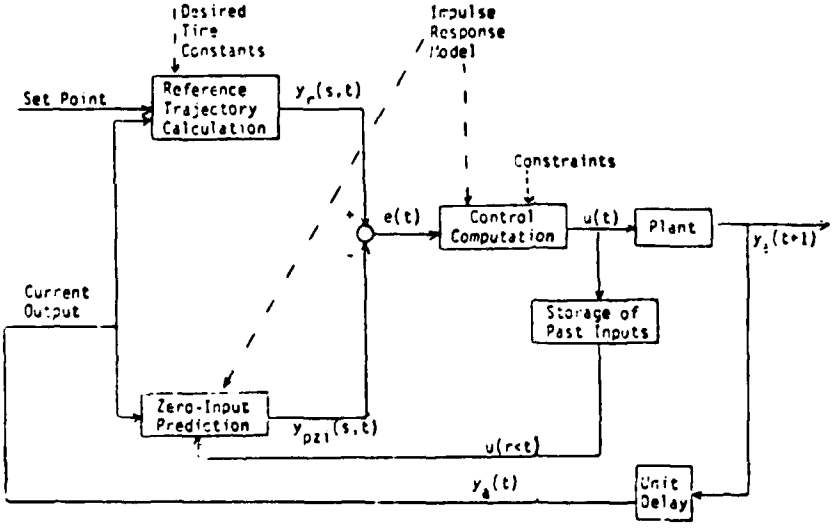

Figure 4.4 IDCOM Components.

representation for multivariable control. For nonlinear systems, both the state space and the input-output representations have certain advantages and disadvantages. In applications, one may use either or both depending upon the nature of nonlinearities and the complexity of the resulting controller. The purpose of the internal model is to have a flexible representation of the controlled system stored in the computer memory, which can be updated as the system changes and which can be used at any instant to predict the future behavior of the system under different control inputs. The internal model of the system is used to compute optimal inputs, to detect process changes, sensor malfunctions and severe faults. The inputs and current output of the internal model are updated according to the actual observed values of these variables, but any large difference between the computed and the actual values gives important clues as to the malfunctioning of sensors and actuators.

The internal model of the system is generally obtained via off-line identification, using either a physical model structure when one is easily available or an input-output representation model such as the impulse response model, which may change with the operating point. Some form of on-line parameter identification may also be done in those cases where large random variations of system parameters are expected. It has been found from experience that the robustness of MAC is sufficient to take care of small parameter changes.

Reference Trajectory and Output Constraints. The desired response of the closed-loop system is specified in the form of a reference trajectory and constraints which are updated on-line using the actual output of the system. It is possible to handle state-dependent constraints in this fashion and to eliminate the steady state offset error. It should be noticed that the specification of reference trajectories and constraints is much easier and natural than the specification of a scalar performance index. Typically, the requirements on controlled outputs are stated as "no overshoot," "fast response," "within maximum and minimum limits," etc. These requirements are difficult to express in a scalar quadratic performance index, but they are easily converted into desired trajectories and constraints which can also be explained to the operators without any difficulty.

The concept of using reference trajectories is more general than model-following. First, it may not be possible to represent a reference trajectory by a simple model, and second, under sensor or actuator fault conditions, one may have to relax the system requirements to control within a band. Certain control problems such as water level control involving inexact measurement of the water level are formulated more naturally as band-control problems rather than model-following or scalar performance index problems.

Control Trajectory Computation. Controls are computed, in general, for a number of future time points using an iterative optimization technique which minimizes the distance between the desired reference trajectory and output trajectory predicted by the internal model, while keeping all the output, state and control constraints satisfied. The complexity of the control algorithm is directly dependent on the structure of the internal model, the number of inputs and outputs and the constraints. For linear systems, the impulse response representation results in a simple projection-type quadratic programming solution which can be implemented quite fast in micro/mini-computers of the present generation. The actual dimensionality of the state does not increase the complexity of the algorithm as it would in a state vector representation. In order for this approach to be feasible, a countable number (say, 50) of impulse response delays must be stored. This implies that the plant to be controlled should be stable, so that a finite representation of the impulse response function is valid.

The MAC design approach has been found to be flexible and robust. It is well suited for the evolving microprocessor technology providing high speed memory and fast computation times for basic calculations such as convolutions. The universality of the impulse response representation leads to a unified design approach for systems of all orders. Furthermore, the parameter-linearity of this representation leads to a duality between identification and control.

The MAC is implemented by a program called IDCOM. The special features of IDCOM are: (i) no model order reduction is required since an

impulse response representation is used. (ii) Input magnitude and rate constraints are handled directly and exactly. (iii) The control law is time-varying and the closed loop response is robust to parameter changes. (iv) Gain scheduling is replaced by on-line updating of the internal model using operating data and parameter estimation techniques, thereby reducing reliance on theoretical models of the system. (v) Same algorithm is used for impulse response identification and for control law computation, thereby simplifying the hardware requirements. (vi) Different sampling rates can be used for controlling different outputs. (vii) The control laws can be modified on-line in case of sensor failures or degraded system performance.

IDCOM Implementation. A block diagram of IDCOM is shown in Figure (4.4). As indicated in the figure, when a new measurement is made, it is fed to two IDCOM modules which compute a reference trajectory and a "zero output" prediction of the future outputs over a short horizon (for optimization). The reference trajectory is usually a first-order exponential drawn from the current (measured) output to a given set point. The designer supplies a time constant (τ_1) for this exponential for each output i. The "zero-input" prediction uses the past inputs, measurements, and internal impulse-response model to predict the future outputs in the absence of future control inputs.

These two trajectories (reference and zero-input prediction) are differenced to obtain an error trajectory to be minimized by the future controls. The control calculation block then performs this minimization in one of several ways. Once an input sequence has been computed, the first input is applied to the plant, and the cycle starts again after the next measurement.

Similar Approaches. Some of the other modern control approaches which are closer to MAC are Dynamic Matrix Control (Cutler et al. (1980) Model Reference Adaptive (Landau (1974)) and Self Tuning Regulators (Astrom (1980)). They are, however, not exactly similar since the specification of models (reference, prediction, control) and algorithmic computations are done differently. Model Reference Adaptive (MRA) techniques try to reduce

the error between the system output and the model output by using error feedback. No computation of predictive controls is done and no reference trajectories are specified. The extensions of these techniques to nonlinear systems and to hierarchical levels of control are much more difficult both from a conceptual and an algorithmic viewpoint. Furthermore, by on-line adaptation of the internal model in MRA and STR the ability to detect failures is lost. The Dynamic Matrix Control approach is conceptually similar to MAC, but lacks proper use of reference trajectories and internal models which are especially important for nonminimum phase systems. Similar problems exist with the use of other Inverse Control type of methods (Meyer (1980)).

4.2.3 Frequency Domain (Classic) Methods. There are few methods known to us which are capable of being applied successfully to the ejection seat control problem. The work of Horowitz (see Horowitz et al, 1980 for a presentation of this approach and support literature) seems at this time to offer the best hope as an alternative. This method works primarily in the frequency domain and with linear representations, but combines the latter in a way which produces an LTI equivalent set to the nonlinear system being approximated. Elements of the LTI set are adjusted by compensation (primarily forward loop) to operate within specified bounds over all variations (of up to several orders of magnitude) in the system matrix elements. The equivalence has been demonstrated rigorously using functional analysis, under not very restrictive assumptions on the system. It is, then, a quantitative nonlinear technique, which does directly address the "plant ignorance" problem. It is thereby claimed to be very good at disturbance rejection, particularly the amplification of sensor noise.

The technique is now briefly described. If w is a nonlinear plant or element, an LTI-equivalent element p usually exists which, for a specific input x(t), matches the (assumed unique) output of w, y(t) (y(t) = w(t;x(t))). p can be found via the inverse Laplace transform of [Y(s)/X(s)] under the conditions that w has a unique inverse (which excludes direct modeling of saturation dynamics), and that x and y are Laplace transformable. An LTI set P equivalent to a set of nonlinear

plants W with respect to a given output y (t), can thus be generated. By extension, a larger set P can then be found which is equivalent to W with respect to a set of outputs Y (which can be selected to bound the allowable response region). In general, the sets Y, W and P are uncountable. A finite and countable subset of each which is developed from the system performance bounds can usually be developed. The approach has been extended to multivariable systems.

Adaptation of this approach to the ejection seat synthesis problem would require great care, and quite possibly, strenuous effort beyond available resources. The need to look at all combinations of extreme values of elements of A, the system matrix, could lead to a prohibitively high number of cases to be run in the available time. In addition, more software would have to be developed or obtained, in order to perform this design in the multidimensional environment of the ejection seat system. Because the approach has worked with nonlinear, high performance aircraft systems, and possesses adaptive and robustness characteristics, it merits consideration.

Another approach with adaptive features and flight vehicle control applications has been proposed by Porter (see, e.g., Porter and Bradshaw, 1982). The approach is to use fast-sampling error-actuated digital adaptive controllers. It is claimed that the controllers are simple to implement and can track well over a wide flight envelope.

The fast-sampling feature of the adaptive controllers is necessary to remove major restrictions on the underlying synthesis technique that the model be LTI and rather accurately known. In addition, singular perturbation analysis is used to remove a restriction to "matchable" plants.

The control law generates a control input vector u which causes the output vector y to track any constant (over the sampling interval) command input vector v so as to drive the difference (v(k) - y(k)) to zero, as sample time k goes to (tracking condition). The singular perturbation analysis generates specific conditions for stability. The technique uses a

PID structure for loop closure, using, as we do, only proportional and integral gains. The integrator gain is related to the proportional gain via a positive real scalar, and the proportional gain is generated in real time via an iterative process. It is shown that, as sample period T goes to zero, the behavior of the adaptive system asymptotically approaches that of the fixed structure discrete time tracking system at the asymptotic limit. The accuracy of the system is thus directly and proportionally related to the controller sample frequency.

This approach appears to have the necessary features required, but it is unknown at this time if what it offers is sufficient for ejection seat applications. Robustness is a key concern, particularly in view of the short duration of the seat control activity, vis-a-vis the asymptotic accuracy requirement. The scheme seems to be very easy to implement, however.

There are other promising concepts and approaches, all covering multivariable control and offering robustness and sensitivity reduction. A technique not yet well enough developed for this project but a very promising one for eventual investigation is the stable rational factorization approach developed by Youla, Sain, MacFarlane, and M. Vidyasagar. The latter is a consultant to SSI. Multivariable performance and robustness analysis for systems with structural uncertainty is also dealt with in a series of papers by Doyle and Stein (see in particular Doyle and Stein (1981) and Doyle et al (1982)). This theory, if implemented, may offer a way to accomodate the serious objection to optimal and even adaptive methods that they require accurate models. The main drawback to all of the above approaches for ejection seat application are assumptions of linear or linearizable dynamics.

4.2.4 <u>Computation of Optimal Trajectories Using ESOP (Escape System Optimization Program)</u>. This large scale nonlinear programming code has been developed at Stanford University by Murtaugh and Saunders (1981) and has been used by SSI for solving optimization problems with over 2000 constraints. We also used this code for obtaining optimal thrust vector profiles for the ejection seat to keep all the flight and human tolerance

constraints satisfied. We give a brief description of the algorithm in this section.

The approach in using ESOP is to consider a general optimization problem, where the nonlinearity is separated from the linear part in the following form:

$$\text{Minimize } F(x) + c\,x + d\,y \tag{4.8}$$

such that

$$g(x) + A_1 y = b_1 \tag{4.9}$$

$$A_2 x + A_3 y = b_2$$

$$\ell \leq \begin{bmatrix} x \\ y \end{bmatrix} \leq u \tag{4.10}$$

where x, y, ℓ, u, d, b_1 and b_2 are vectors and A_1, A_2, A_3 are matrices of consistent dimensions. F(x) is a scalar function and g(x) is a vector valued nonlinear function. The vector (x, y) in (4.10) represents all state and control variables over the flight trajectory at discrete time points. That is, x is the string $[x_0(t_0), x_1(t_1), \ldots, x_N(t_N)]$.

The solution technique consists of solving a sequence of linearly constrained subproblems ("major iterations"). At the start of each iteration, the nonlinear constraints are linearized and the objective function is modified, actually augmented with a penalty term to prevent large excursion of variables from the current point. The subproblem is then:

$$\text{Minimize } F(x) + c\,x + d\,y - \lambda^T(g-\tilde{g}_k) + \frac{\rho}{2}(g-\tilde{g}_k)^T(g-\tilde{g}_k)$$

$$\text{s.t.:} \quad \begin{bmatrix} J_k & A_1 \\ A_2 & A_3 \end{bmatrix} \begin{bmatrix} x \\ y \end{bmatrix} = \begin{bmatrix} b_1 - g(x_k) - J_k\, x_k \\ b_2 \end{bmatrix} \tag{4.11}$$

$$\ell < \begin{bmatrix} x \\ y \end{bmatrix} < u$$

where $\tilde{g}(x)$ is the linear approximation to $g(x)$ at x :

$$\tilde{g}_k(x) = g(x_k) + J_k\,(x - x_k)$$

J_k = Jacobian of $g(x)$ with respect to x at x_k.

λ_k is a multiplier vector corresponding to the nonlinear constraints $g(x)$ and the scalar ρ is positive.

The above subproblem is linearly constrained with a nonlinear objective function. A particular version of the Generalized Reduced Gradient method is then developed which, for the sake of notational simplicity, is formulated in terms of the following optimization problem

$$\begin{array}{lll} \text{Minimize } F(x) + c\,x & & F : \text{nonlinear},\ x,\ c \in R^n \\ \text{s.t.} \quad Ax = b & & A : m \times n,\ x,\ b \in R^n \\ \qquad \ell < x < u & & \end{array}$$

The matrix A is divided in three blocks corresponding to:

$$A = [B \quad S \quad N]$$

The mxm matrix B corresponds to basic variables, as in the simplex method. The basic variables take values anywhere between the lower and upper bounds. The n-m remaining variables are divided into nonbasic (N) and superbasic (S) variables. The nonbasic variables are always equal to one of their bounds, but the superbasic variables can take values within their bounds. The basic and nonbasic variables are eliminated and the problem reduced to the optimization over superbasic variables only. In terms of the matrix Z, the choice is:

$$Z = \begin{bmatrix} -B^{-1} S \\ I \\ 0 \end{bmatrix} \begin{matrix} m \\ n_s \\ n-n_s-m \end{matrix}$$

The reduced gradient is then computed as

$$\nabla_r = Z^T \nabla F(x)$$

and the optimization is done over n_s superbasic variables. Once it appears that no improvement can be achieved with the current set of superbasic variables, one or more basic variables are selected to become superbasic and the minimization is done with respect to the new set.

For large scale sparse problems, sparsity techniques are used both in constructing the matrix Z, and in bypassing the computation of B^{-1}. To apply to the ejection seat trajectory optimization problem, the following steps are taken:

(i) The ejection seat trajectory is divided into various segments and equations of motion and constraints are specified as in Section 3.2.

(ii) The equations of motion are discretized based on the bandwidth of control actuators which determine the rates at which the magnitude and direction of thrust vector can be changed.

(iii) A performance index based on minimization of the radical over the flight trajectory is specified.

(iv) The equations from steps (ii) and (iii) are expressed in the form of Equations (4.8 to 4.10). Notice that vectors x and y consist of both the state and the control variables over the trajectory and are, therefore, of a fairly high dimension. For example, if a discretization step of 0.01 sec. is used, then during the rocket burning phase of approximately 0.3 sec., there will be 30 values for all the states and controls, which would typically result in a vector [x,y] of dimension around 900. Since ESOP is capable of handling such vectors of dimension 4000 to 5000, this would not cause any difficulty. Notice that ESOP allows for very general constraint

and performance index specification (cf. Equations 4.8 to 4.10)) and exploits effectively the sparsity in these constraints. Since in an optimal control problem, the equality constraints come from a set of differential equations, the constraints (4.9) will have a triangular structure.

ESOP can be used for a number of ejection conditions to cover the complete flight envelope. The real-time, suboptimal, method of generating reference accelerations continues to offer much promise as a reliable scheme, in view of the excellent robustness of the basic design.

4.2.5 Other Related Programs (MPES).

Investigation into onboard, feedback controllers for escape systems did not originate with this project. In the late 1970's, the Naval Air Systems Command initiated a program at the Naval Air Development Center to improve aircrew escape safety and survivability (Arrone et al, 1981). This program developed the Maximum Performance Ejection Seat concept, which demonstrated advances in propulsion control, pilot restraint technology, survival equipment, and maintainability (Stone and Bishop, 1980). The baseline system was the Martin-Baker GRU-7A ejection seat and its operation within the F-14A aircraft. The program was contracted to Grumman Aerospace Corporation, Bethpage, NY.

One of the key technologies related to automatic control of the seat involved design and test of a vertical seeking capability. Incorporating the vertical seeking technology into the GRU-7A seat required design of a vectored thrust control system which could utilize the vertical seeking function for the critically needed attitude reference. Upgrading current systems with such a system offers dramatic improvements in minimum altitude performance capabilities.

The project which is the subject of this report represents an extension of the MPES technology primarily in that multi-nozzled, thrust modulation propulsion systems are utilized in the design. By doing so, a fully integrated, comprehensive attitude and trajectory control scheme can be mechanized. The MPES program considered single and twin rocket systems,

but these have restricted flexibility in full 6 DOF applications. See Section 3.2.2 for further details on single vs. multiple nozzle configurations. See also Chapter 5 for a components trade analysis of the micrad altitude sensor, which was utilized in MPES as the verticle seeking sensor.

4.3 Acceleration Control.

This section presents a detailed description of the control concept selected for the vectored thrust digital control law design for ejection seats. It is a nonlinear, predictive, multivariable scheme which relies heavily on translation and rotation accelerations, both for the quick response properties and because of the acceleration constraints (e.g., the acceleration radical) which are peculiar to the ejection seat problem.

4.3.1 Evolution of Design

The unique control requirements imposed by the crew escape mission require a control structure uniquely suited to implement these requirements. After careful analysis, we have chosen a predictive, nonlinear, multivariable scheme which we shall in this report call "acceleration control". This approach follows closely the work of Meyer and Cicolani (1975), although certain modifications specific to ejection seat control applications have been implemented. The discussion in this section follows that of the above reference. This section presents the rationale behind the selection of the acceleration control approach, and describes the modifications made for ejection seats.

Earlier sections have examined the basic control requirements and other control approaches, and have presented their various shortcomings for this application. Acceleration control has been selected for this problem because its shortcomings are fewer by comparison with the other approaches.

Acceleration control works directly with nonlinear, multivariable models. As we shall show, it can be made to work in rapid response situations in real time, especially when the design is hierarchical, and can adjust properly for a broad spectrum of escape conditions.

Due to the recent technological explosion in practical sensing devices and computational capacity, the designer is limited now primarily by the available methodology for the design of automatic flight control systems, and by the propulsion system hardware. The latter limitation is not a direct focus of this report, although we recognize its critical role in the overall control design effort.

In the area of control design methodology, the most severe limitation of most existing design techniques is their extreme reliance on linear perturbation models of the physical plant being controlled. Such models are usually a key to whatever control design process is used. We have demonstrated in this report the high degree of nonlinearity which is a feature of the dynamics of open ejection seats. For schemes dependent on linearization, a highly nonlinear plant leads to the requirement for many perturbation models to cover the flight envelope adequately. Logic then must be provided in the flight computer for switching the perturbation control gains and reference controls as the seat leaves the domain of validity of one perturbation and enters another. The result would be a design that is complex both in concept and implementation so that analyses of closed-loop sensitivity to modeling errors and subsystem failures are exceedingly difficult and not very convincing.

Design techniques are needed of sufficient generality to be applicable to a large set of escape conditions with nonlinear dynamics and multiple controls. The techniques must be nearly algorithmic to allow for ready adaptation to many alternative configurations early in the design cycle. Of great importance, these techniques must result in designs sufficiently simple to achieve the critical reliability requirements for operational escape systems.

4.3.2 Features of the Final Design

The acceleration control concept is responsive to the above requirements. The proposed logic structure for the controller (Fig. 4.5) consists of four major subsystems: (1) translational acceleration control; (2) attitude control via tracking of angular acceleration trajectories;

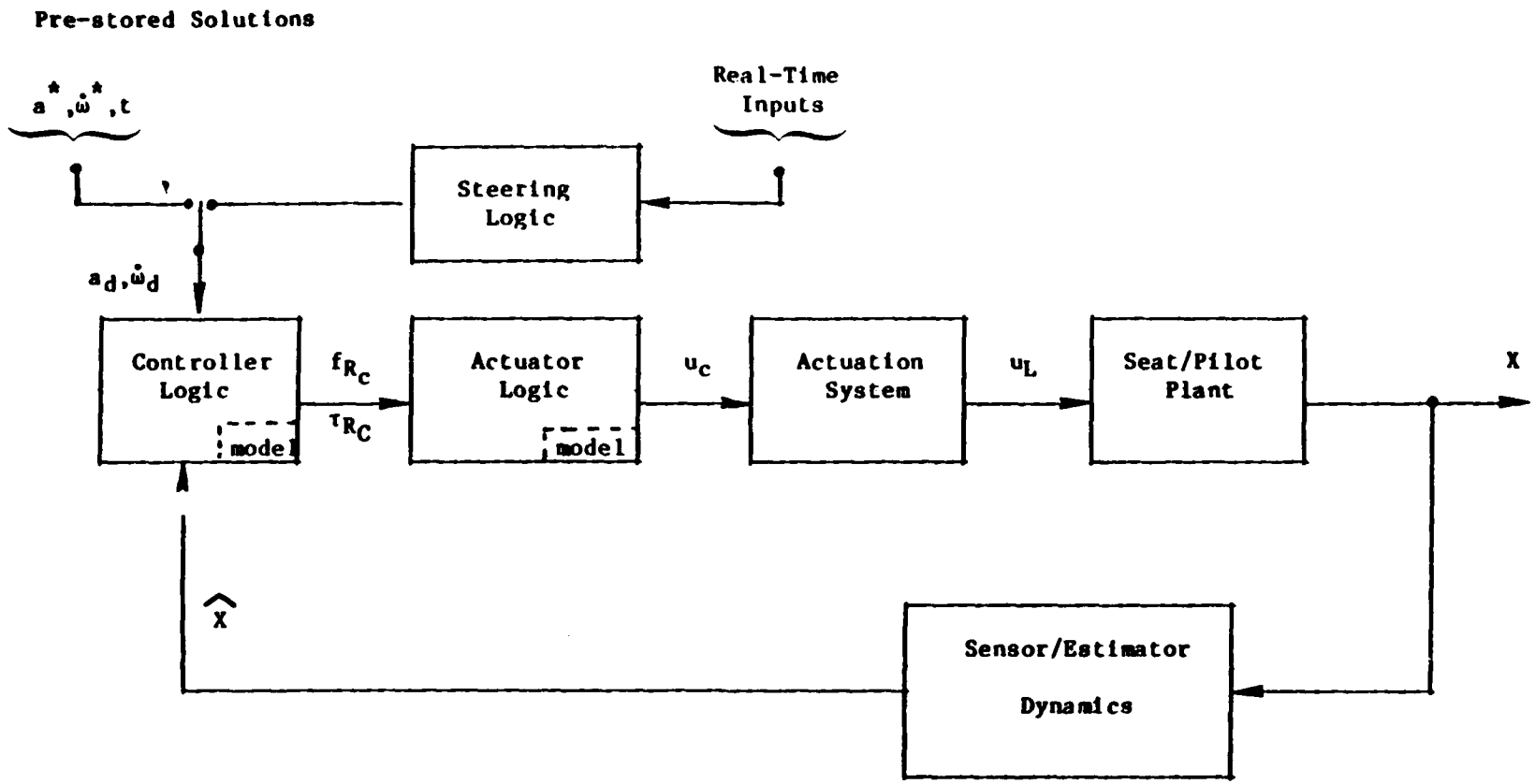

Figure 4.5. **BASELINE CONTROL SYSTEM OVERVIEW**

(3) trajectory perturbation controller which closes the loop around the inaccuracies of the tracking control activities. The result is a trajectory acceleration controller whose input-output relation between commanded and actual acceleration is essentialy an identity--provided the input is flyable and its bandwidth is suitably restricted; (4) the trajectory command generator develops translational and rotational accelerations which are consistent with the capabilities of the overall system ("achievable" commands).

The basic input to the control logic is the trajectory to be followed by the seat, from the time of complete departure from the cockpit of the stricken aircraft. Prior to this time, the seat has been moving up guiderails inside the aircraft, accelerated by a catapult device. During this period, which lasts approximately 120 to 150 milliseconds, the control system should be in operation, turning on sensors, determining the escape condition (speed, altitude, attitude), positioning the sustainer rocket system's control effectors, deciding on reliability of data from the aircraft aironics systems, selecting parameters and (if needed) reference trajectories appropriate to the escape condition; and conducting self-examinations (e.g., built in test and evaluation -- BITE) of its sub-systems.

Proportional plus integral control in the error control loop provides velocity and acceleration vectors to the control logic continuously. Moreover, since ultimately the seat's motion is in inertial space (for this problem, a flat nonrotating earth is an adequate inertial reference), inertial vector quantities are considered as fundamental. As stated above, it is important that the control logic contains a trajectory command generator that synthesizes "flyable" trajectories -- that is, trajectories amenable to the capabilities and limitations of the full control system.

Because tracking accuracy in the usual sense is not a tight requirement for crew escape, beyond achieving attitudes for crewperson survival and minimum discomfort/injury, a relatively simple seat/pilot model may be used. Increasing accuracy requirements usually adds complexity to the control logic, and with it extra computer operations in the duty cycle.

The sustainer rocket configuration provides the thrust vectoring capability needed to track the reference trajectories. Vectored thrust refers both to magnitude and direction changes in the resultant rocket thrust brought about by active control commands. Our control logic design and analysis quite naturally points to the need for a flexible, fast-reacting configuration. The preferred means of realizing this appears to be to locate several nozzles at the seat extremities for attitude or "vernier" control, and retain a larger, main thruster roughly where current rockets now are.

The "trim problem" refers to the "inverse" operation of converting the control logic output - rocket force and torque commands - into throttle levels, gimbal angles, valve settings, etc., of each nozzle control device. Each quantity is an element of the control vector. A complication to the trim problem arises when the actuator configuration admits redundant control. The trim problem is said to be overdetermined. This happens when the dimension of the full control vector exceeds six, which is the number of force and torque vector components to be realized. The "trimmap" is the section of the control logic in which the control redundancy is resolved and commands are generated continuously. In practise, for overdetermined problems this logic typically involves introduction of constraint and optimization criteria to generate a unique command.

When the trim logic is adequately constructed, it provides a priori open loop information to the full control system, relative to performance limitations. Ideally, this reduces the role of the perturbation controller to control of uncertainties in the dynamic model or environment. Thus, there is again a tradeoff between accuracy of performance and logic complexity (e.g., detail of models).

During the course of this project, we have analyzed two major thrust actuation configurations. One, developed at SSI, consists of a main thruster and two verniers with full vectoring capability. The main thruster gimbals in pitch only. This configuration is "generic" in the sense that its primary purpose is to allow study of the interaction of the control logic outputs with dynamic control elements, in order to quantify

performance requirements of the latter. Less attention has been given to possible unrealistic or harmful gimbal orientations which may arise in certain situations. See Section 3.2.2.3.

The second design, proposed by Martin Marietta (Section 3.2.2.4), is more realistic, consisting of a total of seven nozzles, three pairs of which are primarily dedicated to attitude control. Considerations of a proprietary nature prohibit us from explaining this concept in detail. However, the purpose for analyzing this configuration was primarily to investigate the effect of a more realistic configuration on the structure of the control logic.

The perturbation controller acts in a closed loop manner to eliminate acceleration and velocity departure, from the reference generated trajectories. This amounts to feedback control over details of the physical process that are not accounted for in the open loop, feedforward trim control either because they are unknown or because adding them would unnecessarily complicate the open loop control. Consider a nonlinear system governed by the vector equation

$$\dot{x} = f(x,u) \tag{4.12}$$

where x is the n-dimensional state vector and u is the m-dimensional control vector. In addition consider that u is restricted to a set U which could depend on x, but more typically is defined primarily by the rocket configuration and thrust capability of the rocket. A trajectory $[x_o(t), t\varepsilon T]$ is <u>achievable</u> if, for all $t\varepsilon T$, where T defines the time period during which the sustainer rocket are ignited, there is a control $u_o(t)\varepsilon U$ such that

$$\dot{x}_o(t) = f[x_o(t), u_o(t)] \tag{4.13}$$

The trim problem is defined in terms of equation (2) as that of finding a control u_o satisfying (4.13), given that the trim (nominal) trajectory $x_o(t)$ is achievable. The solution is the inverse of the state equation namely the trimmap (g,E), so that for all $(\dot{x},x)$ in the escape envelope E,

$$\dot{x} = f[x, g(\dot{x}, x)].$$

The corresponding trim control is

$$u_o = g(\dot{x}_o, x_o)$$

Trim usually referes to fixed u_o, which is allowable subset of controls for the crew escape problem also. However, the concept is generalized here to include time-varying open loop controls. As noted above, when controls are redundant, that is, $m > 6$, equation (4.12) alone does not define the trimmap (g,E), and additional conditions (eg. cost criteria) must be introduced.

After the trim problem is solved, the next step has usually been to design feedback control systems based on perturbation models derived from equation (4.12). Methods of linear and optimal control theory produce a perturbation control law

$$\delta_u = K_o \delta_x$$

where the matrix gain K_o is appropriate to the reference trajectory. Complete coverage of the escape envelope E requires offline development of a scheduled gain matrix $K(\dot{x}_o, x_o)$, resulting in the complete control law

$$u = g(\dot{x}_o, x_o) + K(x_o, x_o)(x - x_o)$$

The structure such a controller is depicted in Figure 4.6. The above LQ-type process (this is how K is usually derived) has appreciable difficulty when the system (4.12) is very nonlinear. The procedure for choosing the proper set $\{x_{oi}, x_{oi})\}_N$ of nominal trajectories to cover adequately the envelope E and switch among perturbation models is for now rather unclear. In addition, LQ methods require extra complexity even to deal approximately with state and control constraints. For the crew escape problem in particular, this is a serious limitation. Excessive nonlinearity may force the perturbation trajectory outside the envelope, from a nominal $x_o \varepsilon E$. If envelop limiting is achieved by limits δU on δu,

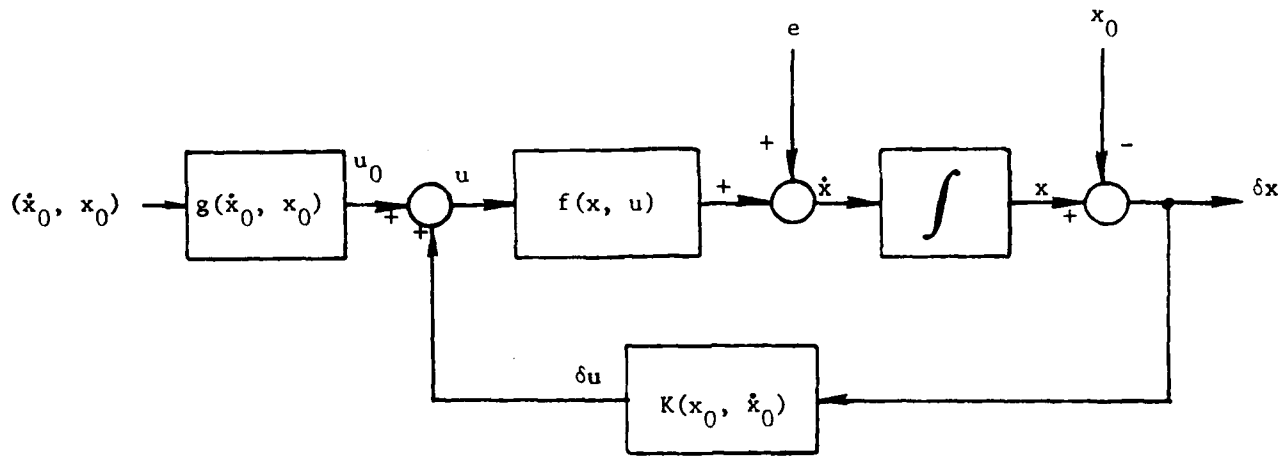

Figure 4.6. Selected structure in conventional design.

The nonlinear function $g(\dot{x}_0, x_0)$ is the trim control function, generating trim control u_0. Latter is augmented by LQ feedback correction control, du, to produce complete control, u. State variable rates of change $\dot{x}$ are a function of f(x, u), the system nonlinear model, plus disturbances, e. $\dot{x}$ is integrated to obtain x, which is compared to nominal x.

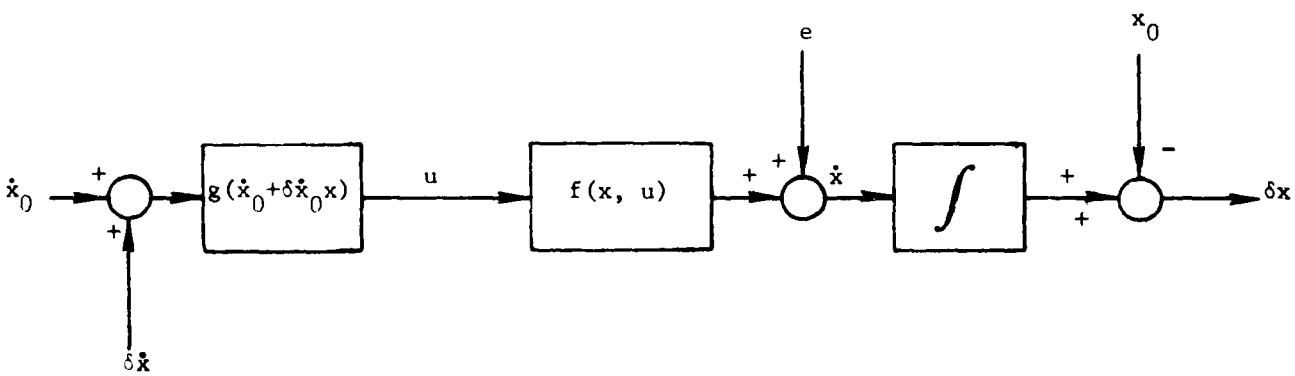

Figure 4.7. Stucture of proposed perturbation controller.

By passing feedback (error) signals through the trim logic, effects of uncertainties are controlled better. See accompanying text.

then questions concerning the stability of the resulting nonlinear perturbation controller must be resolved for each of the N perturbation models. Since these limits on δu are likely to depend on $(\dot{x}_o, x_o)$, $\delta U(\dot{x}_o, x_o)$ must be stored in the control logic in addition to $K(\dot{x}_o, x_o)$ and the trimmap $g(\dot{x}_o, x_o)$. Also, the dynamics of switching from one case to the next must be designed, including some accounting for the possibility of using hysteresis to prevent chatter if the seat is to fly along a boundary between two models. Switching logic and dynamics add further to computational burden and complexity. Finally, there are reliability issues. Is stability maintained when a column (sensor) or a row (control) of K is lost?

Such questions are difficult to deal with in the framework of modern control or the LQ approach. Older classical techniques based on sequential loop closures that result in a nesting (hierarchy) of subsystems with decreasing bandwidth are more effective for designing fail-safe (robust) systems. The acceleration control concept presented here has these features, and in addition is much less effected by the nonlinearity of equation (4.12) or by state and dynamic constraints. See also Section 4.2.1.

In contrast to the standard design approach exemplified in Figure 4.6, the acceleration control structure for the automatic flight control system consists of feedback achieved through the automatic trim logic. This is seen in Figure 4.7. Here, the feedback is through the perturbation $\delta\dot{x}_o$ on the (nominal) trim condition $\dot{x}_o$. The open loop reference trajectory accelerations generate an open loop control u which is capable of maintaining $x = x_o$ if: (1) initially, $x = x_o$; (2) the trajectory is feasible, and (3) there are no systems modeling errors.

In these conditions are met, the tracking will be perfect, even in the presence of nonzero δx_o (which arises from distribances, or process noise), as long as $(\dot{x}_o + \delta\dot{x}_o)$ falls within E, the achievable escape region. The control

$$u = g(\dot{x}_o + \delta\dot{x}_o, x)$$

then takes $x(t)$ into $x_o(t)$, that is, the feedback for controlling process uncertainties is closed through the automatic trim logic (assuming feasbility) Figure 4.7, rather than after the trim logic, Figure 4.6, the LQ approach.

The structure allows for envelope limiting and use of dynamic constraints within the trimmap. Admissable perturbations $\delta\dot{x}_o$ are directly handled by this structure. Thus, the emphasis is shifted from the several linear perturbations models required to cover E to the construction of achievable perturbations in the commanded trajectories. When emphasis is made of hierarchical design, this latter task is simplified.

We note here that the envelope limiting within the trimmap, predictive control based on reference trajectories, use of the plant model in the control logic and incorporating explicit limiting within the control logic (trimmap) are also features of Model Algorithmic Control (Section 4.2.2). The hierarchy consists of slower varying (command) processes at higher levels, and fast-reacting processes at lower levels. The hierarchical structure for the crew escape control logic is centered on the rotational and translational acceleration controllers. In more common systems, e.g., the VSTOL controller discussed in Meyer and Cicolani (1975), the attitude controller is at a lower (faster) level than the translational acceleration controller. We don't allow the "luxury" of seperate levels for attitude and translation in the crew escape problem, because in many scenarios there is no time to allow for attitude transients to grow sufficiently small before issuing acceleration commands.

The ejection seat acceleration controller, then, solves simultaneously the 6 DOF attitude and trajectory problem. This is done by accepting commands from the command generator, at one level higher, which produces, in real time, $a_c(t)$ and $\dot{\omega}_c(t)$. They are sent as commands to throttle and nozzle acuators, which are one level lower. From the controller level, acuator models may be relatively simple input-output relations, which are treated as specifications to be met in the design of these subsystems. The overall design can proceed one level at a time, at each level assuming acceptable inputs from the other levels. Sensor dynamics are treated simi-

larly, and are also one level below the acceleration controller. The trimmap is the major logic activity of the acceleration controller. The inertial coordinates of the acceleration commands $(a_c, \dot{\omega}_c)$ are converted by the acceleration control logic first, to force and torque commands (frc,trc) to be realized by the propulsion system, in seat/pilot (Body) coordinates; and secondly, to commanded thrust levels and (where appropriate) nozzle gimbal angles or value settings-the elements of u. The realized acceleration, $(a, \dot{\omega})$ compares to the command $(a_c, \dot{\omega}_c)$ to within the inaccuracies of the trimmap. Much of these relate to the detail of the model used in the controller. While there is no inherent, structured limit to be associated with the detail, or complexity, of this model- as, for example, the requirement that it be linear - it is typically wisest to use as simple a model as possible which produces adequate performance.

The discrepancies between commanded and actual accelerations are resolved by the perturbation controller. Inertial acceleration and velocity errors are weighted by the constants K1, K2, K3, and K4 to generate commands commensurate with the rocket acceleration capabilities:

$$dfr = m[K_1(a_d - a) + K_2(v_d - v)]$$

$$dtr = I[K_3(W_d - W) + K_4(W_d - W)]$$

Note that the combination of acceleration and velocity error signals is equivalent to processing acceleration errors through a proportional-plus-integral feedforward filter. This type of compensator in closed loop error control is commonly and successfully used for steady state error control.

The trajectory command generator must provide admissible acceleration commands to the acceleration controller. In the hierarchy of the central logic the command generator is one level above the acceleration controller. The set of admissible (inertial) commands of total seat/pilot CG and rotational accelerations have been arrived at by several schemes in our work. For example, attitude commanded accelerations have been supplied by off-line optimal programs (see 4.2.4), cross product steering, and Euler steering. By setting up a general structure, as we have done, other variations within the three classes can be achieved by zeroing a parameter.

And there are certainly other schemes not tried in our current work which should also do very well.

4.3.2.3 Details; Summary Considerations of reliability and simplicity motivated the decision to use hierarchical acceleration control. The control logic works simultaneously on the six rigid body degrees of freedom. Process uncertainties are controlled by means of a perturbation controller which closes the loop around the acceleration controller and the control select (trimmap) logic. The design and implementation of the perturbation controller are greatly simplified by the decision to close the feedback through the trimmap.

The idea is an acceleration controller whose input-output relationship is approximately an identity everywhere within the escape envelope (E) for suitably restricted acceleration commands. The function of the command generator is to give only admissible commands to the accelerator controller.

A specific seat rocket configuration geometry, part of the 6 DOF simulation model, converts the control vector u_c into seat-referenced rocket forces and torques via the relationship

$$\begin{bmatrix} f_R \\ \tau_R \end{bmatrix} = B(u_c) \tag{4.14}$$

where B is a (6 x 1) vector and f_R and τ_R are the 3-dimensional forces and torques due to rocket thrust.

The control design presented in this report answers affirmatively the concerns about overall feasibility of self-contained, active control of an ejection seat, using state- or near-state-of-the-art hardware. The complexity of the controller is flexible, from being able to handle the highly constrained high-Q ejections by utilizing increased energy source and microprocessor capability, to reliance on very simple control strategies where physiological limits are not threatened, to shaping appropriate trajectories for impact avoidance of either moving or still objects. For example, in a moderate altitude low-Q ejection, the prestored

solution is much simpler, and not necessarily "optimal", since safe egress can be effected by any number of trajectories. For such ejections low speed, near nominal attitude, rocket thrust is reduced but fixed, and attitude is set for safe main chute deployment.

Currently, seat dynamics are being generated by a 6 DOF simulator. For this function, we are now using, as appropriate, one of four basic simulation systems: EASIEST (West, Ummel and Uyrczyk, 1980), SAFEST (Jines, 1982), plus our own specialized 6 DOF program, THIST, developed specifically for generalized control synthesis of the type required for this project. THIST and its support software are described in Appendix C. The fourth simulation system is, of course, the real time hybrid system which uses the breadboard controller (Volume II, Chapter 6).

Referring to Figure 4.5, the 6 DOF simulator (which now has the role of the physical plant, the ejection seat) generates the plant output vector x, the system or state variables. We are using the 12th order set

$$x = (u,v,w,p,q,r,\phi,\theta,x_E,y_E,z_E,\psi) \tag{4.15}$$

where notation follows standard aeronautical usage, except that x_E, y_E and z_z are position components in the reference inertial (local horizontal) frame. The linear and angular velocity variables are inertial quantities, but coordinalized in body-fixed areas.

Components of the state vector x are sensed or estimated on board in real time, as the vector $\hat{x}$. In order to have available the appropriate quantites for the controller, such as local vertical, it is necessary that the seat have on-board rate gyros and accelerometers for all three axes. For the remainder of this chapter, we shall use elements of x and $\hat{x}$ interchangeably, the assumption being that we are specifically referring to the measured elements $\hat{x}$.

The internal model block of Figure 4.5 solves the following set of equations for τ_R and f_R

$$\dot{v} + \omega x v = (f_g + f_a + f_r)/m \tag{4.16}$$

$$I\dot{\omega} + \omega x(I\omega) = \tau_a + \tau_r \tag{4.17}$$

The elements of x needed for these computations are $\omega = (p, q, r)$, θ, ϕ, (for f_g, gravity force), u, v and w (for f_a and τ_a, aero force and torque), and $a = (\dot{u}, \dot{v}, \dot{w})$. To these computed rocket forces and torques must be added correction forces and torques of the form:

$$\Delta f = m[k_1(a_d - a) + k_2(v_d - v)] \tag{4.18}$$

$$\Delta\tau_r = I[k_3(\dot{\omega}_d - \dot{\omega}) + k_4(\omega_d - \omega)] \tag{4.19}$$

In equations (4.18) and (4.19), a_d, $\dot{\omega}_d$, v_d and ω_d are the reference, or the desired translational and rotational accelerations and their integrals, respectively. These quantities are obtained either from the prestored files, generated off-line for a similar case, or from real-time, suboptimal logic, such as cross product steering logic.

We are currently obtaining success implementing Equations (4.18) and (4.19). More generally, the $\Delta v = (v_d - v)$ and $\Delta\omega$ terms come from the integral feedforward compensator, e.g.,

$$\Delta a = (k_1 + \frac{k_2}{s})\Delta a(s) \tag{4.20}$$

The measurement/estimation process typically has an implied integration, so there is no loss of generality in this regard.

The required forces and torques for the next cycle are then given by

$$f_r(t) = f_r(t-1) + \Delta f_r(t) \tag{4.21}$$

$$\tau_r(t) = \tau_r(t-1) + \Delta\tau_r(t) \tag{4.22}$$

where $f_r(t-1)$ and $\tau_r(t-1)$ are found from Equations (4.16) and (4.17). The actuator controller mechanizes the specific configuration geometry - that is, the current rocket and force commands are converted into thrust magnitudes and nozzle deflection angles. Another loop around this controller represents "actuator" dynamics for the propulsion system.

Algorithmically, Equations (4.21) and (4.22) are implemented as follows:

$$\begin{bmatrix} f_r \\ \\ \tau_r \end{bmatrix} = M[Ax + \binom{B}{0}u] + \begin{bmatrix} f_{r_0} \\ \\ \tau_{r0} \end{bmatrix} \tag{4.23}$$

where

$$M = \left[\begin{array}{c|c|c} mI_{3x3} & 0_{3x3} & \\ \hline & & 0_{6x6} \\ \hline 0_{3x3} & I & \end{array}\right] \tag{4.24}$$

and f_{r_0}, τ_{r_0} represent zero-deflection, nominal thrust forces and torques. In our algorithm, $\tau_{r_0} = 0$ for a 50%-ile pilot, and we are for the moment specifying that each nozzle direct its nominal thrust line through the 50% pilot's CG. In Equation (4.24), 0_{3x3} and 0_{6x6} are matrices of zeros, I_{3x3} is the 3-by-3 identity matrix, m is the seat/pilot mass, and I its inertia.

Working with accelerations, the submatrix B performs the transformation between commanded rocket accelerations, a_r and $\dot{\omega}_r$, and control vector u as follows:

$$\begin{bmatrix} a_r \\ \dot{\omega}_r \end{bmatrix} = Bu \tag{4.25}$$

Thus

$$u = (B^TB)^{-1} B^T \begin{bmatrix} a_r \\ \dot{\omega}_r \end{bmatrix} \tag{4.26}$$

Equations (4.18) and (4.19) are divorced from the (simulation) dynamic system update cycle by means of discretization. If t represents the current time sample (ie, t = T), where T is the sample period, we have

$$a(n+1) = a_d(n+1) + \Delta a(n+1) \tag{4.27}$$

where

$$\begin{aligned}\Delta a(n+1) &= a_d(n+1) - a(n+1) \\ &= k_1(a_d(n) - a(n)) + k_2(v_d(n) - v(n))\end{aligned} \tag{4.28}$$

Z-transforming (4.28) yields

$$(a_d - a)\left(z - k - \frac{k_2}{1-z}\right) = 0 \tag{4.29}$$

so that unit circle stability will result if k_1 and k_2 are chosen with respect to T so that both solutions of

$$z = \frac{\sqrt{(1 + k_1) \pm (1+k_1)^2 - 4(k_1+k_2)}}{2} \tag{4.30}$$

are less than 1.0 in magnitude.

4.3.5 Linear Analysis; Stability. Although the control strategy depicted in this chapter is a nonlinear reference trajectory control scheme, it is important to study the properties of the linearized version. There are two basic reasons for which such a study is necessary:

(i) In the current control strategy a nonlinear decoupling law is implemented on line with some approximations. However, since the regulation is basically around either the offline ESOP or the real time reference trajectory, one may use a linear quadratic regulator around this trajectory. Such a regulator would feed back, linearly, all the observed states of the system and would achieve a certain level of optimization in following the reference trajectory. However, since the system is extremely nonlinear, the feedback gain matrix of the linearized system will change along the trajectory. But it is possible to use a limited number of feedback gain matrices (switching from

one to another along the trajectory) by sacrificing the reference trajectory tracking performance. A linearized stability analysis can, therefore, shed light on the stability of the control law, and on whether this approach is feasible.

(ii) A particular point at which the behavior of the system is of interest is the end point of the reference trajectory. At this end point the seat is sufficiently far from the aircraft and is decelerated so that a new control scheme can take over to prepare for the next phase, i.e., for the parachute deployment. The linearized version of the system at this end point specifies the level of controllability and stability of the seat. On the other hand, it should be kept in mind that stability analysis is asymptotic in nature and will only provide limited information for the short flight durations encountered in the ejection seat problem.

The study of the above properties of the linearized system has to rely on extensive numerical testing and analysis. In fact the complexity of the non-linear system and its precomputed reference solution preludes simple analytical deductions as to the feature of the linearized system. Fortunately for moderate size linear systems there exist a number of powerful and fast programs to test the stability of the open loop system and to compute the optimum gain matrix (in the LQ sense). The six degrees of freedom dynamic model for the seat corresponds to a 12 dimensional linear system. At SSI a program developed at the Stanford University (OPTSYS) has been adapted to a 12 dimensional system and has proved to be very robust and fast. In this section we will discuss the linearized system corresponding to these different points (T=0, T=0.1 and T=0.2) of the reference trajectory corresponding to a 12 state - 8 control model:

$\dot{x} = Ax + Bu$ (linearized version of $\dot{x} = f(x,u)$)

With A : 12x12 matrix

$$A = \frac{\partial f}{\partial x}$$

B : 12x8 matrix

$$B = \frac{\partial f}{\partial u}$$

$$x = (\Delta u, \Delta v, \Delta w, \Delta p, \Delta q, \Delta r, \Delta x, \Delta y, \Delta z, \Delta\theta, \Delta\phi, \Delta\psi)$$

$$u = (\Delta\theta_1+\Delta\theta_3, \Delta\phi_1+\Delta\phi_3, \Delta\theta_3-\Delta\theta_1, \Delta\phi_1-\Delta\phi_3, \Delta T_1, \Delta\theta_2, \Delta\phi_2, \Delta T_2)$$

where:

$\theta_1, \theta_3, \phi_1, \phi_3, T_1$, and T_2 stand for (see configuration in Section 3.2.2.3):

rocket nos. 1 and 3 nozzle pitch deflections (θ),
rocket nos. 1 and 3 nozzle roll deflections (ϕ),
thrust for rockets 1 and 3 (T_1), and
rocket 2 thrust (T_2), nozzle pitch (θ_2), and roll (ϕ_2).

The data used correspond to the low altitude high-Q escape condition. The matrices A corresponding to three points in time (T=0, T=0.1 and T=0.2) together with their eigenvalues are printed in Tables 4.1, 4.2 and 4.3. As it can be seen the matrix A and its eigenvalues vary significantly from one point to another. A remains singular and the corresponding linear systems are all unstable (eigenvalue having positive real parts). The input matrix B is the same for all these systems (Table 4.4) and the stabilizing gain matrix C is computed by the program OPTSYS to minimize a quadratic index of the form $\int_0^t [\|x\|^2 + \|V\|^2]dt$. These matrices, together with the corresponding closed loop eigenvalues are printed in Tables 4.5, 4.6 and 4.7. The gain matrices C corresponding to different points of the trajectory are different from each other, but the closed loop matrices (A-CB) have almost the same eigenvalues. This can be explained by the fact that in all the three cases the same index is minimized while keeping the control matrix B constant. The control data structure remains unchanged and C is each time adjusted so the matrices (A_i-B_iC_i) have approximately the same eigenvalues. Such a result would not be possible if the matrix B were to change from one point to another. However, if one relaxes the minimality of the index, or if one decides to minimize an index of the form

A

-1.434E+00	0.000E+00	6.679E-02	0.000E+00	4.500E+01
0.000E+00	-9.123E-03	0.000E+00	-4.500E+01	0.000E+00
5.137E-01	0.000E+00	-2.354E-02	0.000E+00	1.000E+03
-6.719E-03	1.395E-03	3.024E-04	-5.502E-01	-2.097E-02
-3.335E-01	2.262E-04	1.501E-02	-9.083E-03	-1.041E+00
1.268E-02	-1.172E-02	-5.436E-04	-2.632E-01	3.772E-02
0.000E+00	0.000E+00	0.000E+00	1.000E+00	0.000E+00
0.000E+00	0.000E+00	0.000E+00	0.000E+00	1.000E+00
1.000E+00	0.000E+00	0.000E+00	0.000E+00	0.000E+00
0.000E+00	1.000E+00	0.000E+00	0.000E+00	0.000E+00
0.000E+00	0.000E+00	1.000E+00	0.000E+00	0.000E+00
0.000E+00	0.000E+00	0.000E+00	0.000E+00	0.000E+00

0.000E+00	0.000E+00	-3.217E+01	0.000E+00	0.000E+00
-1.000E+00	3.217E+01	0.000E+00	0.000E+00	0.000E+00
0.000E+00	0.000E+00	0.000E+00	0.000E+00	0.000E+00
-3.637E-03	0.000E+00	0.000E+00	0.000E+00	0.000E+00
1.000E-04	0.000E+00	0.000E+00	0.000E+00	0.000E+00
-1.022E-02	0.000E+00	0.000E+00	0.000E+00	0.000E+00
0.000E+00	0.000E+00	0.000E+00	0.000E+00	0.000E+00
0.000E+00	0.000E+00	0.000E+00	0.000E+00	0.000E+00
0.000E+00	0.000E+00	-4.500E+01	0.000E+00	0.000E+00
0.000E+00	4.500E+01	0.000E+00	0.000E+00	0.000E+00
0.000E+00	0.000E+00	-1.000E+03	0.000E+00	0.000E+00
1.000E+00	0.000E+00	0.000E+00	0.000E+00	0.000E+00

0.000E+00	0.000E+00
0.000E+00	0.000E+00
0.000E+00	0.000E+00
0.000E+00	0.000E+00
0.000E+00	0.000E+00
0.000E+00	0.000E+00
0.000E+00	0.000E+00
0.000E+00	0.000E+00
0.000E+00	0.000E+00
0.000E+00	1.000E+00
0.000E+00	0.000E+00
0.000E+00	0.000E+00

T=0.

Eigenvalues (λi)

-2.00 $\pm$ j 1.838
-3.400
+3.419
+1.453
-.5945
-2.846 E-4
-2.081 E-5

$\lambda_9=\lambda_{10}=\lambda_{11}=\lambda_{12}=0$

Table 4.1

A

-1.432E+00	-6.532E-03	5.171E-01	0.000E+00	5.564E+01
6.935E-03	-8.313E-03	3.066E-03	-5.564E+01	0.000E+00
6.361E-02	-2.653E-03	-2.877E-02	-1.995E-01	9.676E+02
-6.438E-03	1.565E-03	3.702E-04	-5.754E-01	4.874E-03
-3.213E-01	6.355E-04	1.867E-02	-1.603E-02	-1.006E+00
1.137E-02	-1.100E-02	-6.560E-04	-1.500E-01	1.112E-01
0.000E+00	0.000E+00	0.000E+00	1.000E+00	-5.533E-06
0.000E+00	0.000E+00	0.000E+00	0.000E+00	1.000E+00
9.992E-01	3.076E-04	-4.001E-02	0.000E+00	0.000E+00
-3.131E-04	1.000E+00	-1.257E-04	0.000E+00	0.000E+00
4.001E-02	1.561E-04	9.992E-01	0.000E+00	0.000E+00
0.000E+00	0.000E+00	0.000E+00	0.000E+00	1.393E-04

1.995E-01	0.000E+00	-3.215E+01	0.000E+00	0.000E+00
-9.676E+02	3.215E+01	1.779E-04	0.000E+00	0.000E+00
0.000E+00	-4.443E-03	1.237E+00	0.000E+00	0.000E+00
-3.650E-01	0.000E+00	0.000E+00	0.000E+00	0.000E+00
-2.255E-02	0.000E+00	0.000E+00	0.000E+00	0.000E+00
4.934E-02	0.000E+00	0.000E+00	0.000E+00	0.000E+00
-4.004E-02	1.749E-02	-7.214E-03	0.000E+00	0.000E+00
-1.382E-04	7.202E-03	0.000E+00	0.000E+00	0.000E+00
0.000E+00	9.144E-03	-1.618E+01	0.000E+00	0.000E+00
0.000E+00	5.064E+01	5.270E-03	0.000E+00	0.000E+00
0.000E+00	1.071E-01	-9.670E+02	0.000E+00	0.000E+00
1.001E+00	-4.572E-01	2.836E-04	0.000E+00	0.000E+00

0.000E+00	0.000E+00
0.000E+00	0.000E+00
0.000E+00	0.000E+00
0.000E+00	0.000E+00
0.000E+00	0.000E+00
0.000E+00	0.000E+00
0.000E+00	0.000E+00
0.000E+00	0.000E+00
0.000E+00	9.545E-02
0.000E+00	9.591E-02
0.000E+00	0.000E+00
0.000E+00	0.000E+00

T=0.1

Eigenvalues (λi)

-5.870 $\pm$ j 1.702
4.306
-3.272
3.325
-.5900
1.159 E-4 $\pm$ j 7.610 E-3
1.049 E-8 $\pm$ j 3.049 E-8, $\lambda_{11} = \lambda_{12} = 0$

TABLE 4.2

A

-1.367E+00	-1.957E-02	-2.837E-01	0.000E+00	2.520E+01
1.670E-02	-8.419E-03	6.098E-03	-2.520E+01	0.000E+00
7.988E-01	-7.694E-03	-1.303E-02	-5.443E-01	9.241E-02
-6.081E-03	1.500E-03	1.658E-04	-4.579E-01	-5.330E-02
-3.075E-01	4.526E-04	8.337E-03	5.959E-03	-9.588E-01
1.628E-02	-1.069E-02	-2.805E-04	-3.087E-01	-1.873E-02
0.000E+00	0.000E+00	0.000E+00	1.000E+00	-3.618E-05
0.000E+00	0.000E+00	0.000E+00	0.000E+00	1.000E+00
9.987E-01	1.601E-03	-5.610E-02	0.000E+00	0.000E+00
-1.516E-03	1.000E+00	-6.463E-04	0.000E+00	0.000E+00
5.610E-02	7.269E-04	9.957E-01	0.000E+00	0.000E+00
0.000E+00	0.000E+00	0.000E+00	0.000E+00	7.223E-04
6.443E-01	0.000E+00	-3.213E-01	0.000E+00	0.000E+00
-9.241E+02	3.213E-01	1.153E-03	0.000E+00	0.000E+00
0.000E+00	-2.515E-02	1.612E+00	0.000E+00	0.000E+00
2.132E-01	0.000E+00	0.000E+00	0.000E+00	0.000E+00
5.154E-03	0.000E+00	0.000E+00	0.000E+00	0.000E+00
-6.332E-02	1.000E+00	0.000E+00	0.000E+00	0.000E+00
-5.616E-02	-1.510E-02	-1.919E-02	0.000E+00	0.000E+00
-7.214E-04	1.914E-02	0.000E+00	0.000E+00	0.000E+00
0.000E+00	5.072E-03	2.112E+01	0.000E+00	0.000E+00
0.000E+00	2.520E+01	-3.207E-02	0.000E+00	0.000E+00
0.000E+00	5.517E-01	-9.242E-02	0.000E+00	0.000E+00
1.001E+00	3.214E-01	9.612E-04	0.000E+00	0.000E+00
0.000E+00	0.000E+00			
0.000E+00	0.000E+00			
0.000E+00	0.000E+00			
0.000E+00	0.000E+00			
0.000E+00	0.000E+00			
0.000E+00	0.000E+00			
0.000E+00	0.000E+00			
0.000E+00	0.000E+00			
0.000E+00	7.471E-01			
0.000E+00	9.242E-02			
0.000E+00	0.000E+00			
0.000E+00	0.000E+00			

T=0.2

Eigenvalues (λi)

$-3.120 \pm j\ 4.021$
3.916
3.101
-3.122
$-.5346$
$-1.974\ E\text{-}3 \pm j\ 1.795\ E\text{-}2$
$\pm j\ 3.357\ E\text{-}6$

$$\lambda_{11} = \lambda_{12} = 0$$

TABLE 4.3

Input matrix B:

B

-1.653E+02	0.000E+00	0.000E+00	-5.895E+01	-1.204E+00
0.000E+00	1.000E+02	0.000E+00	0.000E+00	1.242E+00
-1.111E+02	0.000E+00	0.000E+00	1.033E+02	-1.204E+00
0.000E+00	-2.143E+02	-8.836E+01	0.000E+00	-1.043E+00
-2.020E+02	0.000E+00	0.000E+00	0.000E+00	0.000E+00
0.000E+00	-1.431E+02	1.331E+02	0.000E+00	-6.966E-01
0.000E+00	0.000E+01	0.000E+00	0.000E+00	0.000E+00
0.000E+00	0.000E+01	0.000E+00	0.000E+00	0.000E+00
0.000E+00	0.000E+00	0.000E+00	0.000E+00	0.000E+00
0.000E+00	0.000E+00	0.000E+00	0.000E+00	0.000E+00
0.000E+00	0.000E+00	1.000E+00	0.000E+00	0.000E+00
0.000E+00	0.000E+00	0.000E+00	0.000E+00	0.000E+00
-5.484E+02	0.000E+00	9.959E-01		
0.000E+00	7.000E+00	0.000E+00		
-6.978E+03	0.000E+00	-7.835E-02		
0.000E+00	-2.000E+02	0.000E+00		
-2.591E+03	0.000E+00	4.357E-19		
0.000E+00	-2.583E+00	0.000E+00		
0.000E+00	0.000E+00	0.000E+00		
0.000E+00	0.000E+00	0.000E+00		
0.000E+00	0.000E+00	0.000E+00		
0.000E+00	0.000E+00	0.000E+00		
0.000E+00	0.000E+00	0.000E+00		
0.000E+00	0.000E+00	0.000E+00		

TABLE 4.4

THE OPTIMAL CONTROL GAIN MATRIX :

-6.7246334592157510-01	-4.0116226103103362D-05	1.5057799718462127D-01
1.6310146434815323D-05	-4.6990736190311305D-02	-1.2192625755671633D-05
-2.2271362396854734D-05	1.1336041205551730D-01	-1.7417298528585962D-05
-7.3229351295026575D-01	-1.4844039511340311D-05	-4.8535135714637113D-02
-2.2330253983835752D-02	-1.1327337913399904D-05	-5.0544772559646383D-05
-5.6601814505418151D-02	-5.3573040203736219D-05	-9.9529026825407595D-01
6.4353225623710533D-07	9.9473431770293575D-01	-2.2215393369345367D-05
1.4272019325103705D-02	-1.3266945515925049D-03	2.4983970167711513D-03

-2.7455930775234884D-05	-3.2762575503125050D-04	-6.4733599135334334D+01
-1.3556716992634541D-01	-2.4236661173425105D+00	3.3363711352610840D-03
3.6004237129435227D-01	2.5744236423584459D+00	2.6959007785972750D-03
-4.6603775342428112D-05	2.0507965143534459D-04	1.0335440153882470D+02
-2.5470977305179936D-04	-3.0274657995523561D-03	5.7031932807269528D+00
-1.6932691257053771D-03	-1.0657340443933015D-05	-7.2722631027158968D-01
-3.6201871287573530D-01	-1.6590336825222215D-01	1.8170261141513265D-04
-5.3123495024582527811D-03	-6.9249657335773090D-05	-3.1533869258362959D+00

4.3053511117485889D-05	-3.3584594343194746D-01
-8.9683557213949225D-01	3.1429640152912349D-05
-4.4483428228569593D-01	4.8430299935438371D-05
1.1315160387362223D-05	3.2304370523930037D-01
-4.3719053593975398D-03	1.7795034276898495D-02
1.4174499551439706D-05	-3.1121471952635105D-01
-4.6569503735220846D-03	5.1574244766908823D-06
-3.9996698265675514D-03	-9.7467455163373282D-03

-6.4802248181259570D-01	-7.8854437505536964D-05
1.6855986377493199D-05	-4.5780301166044751D-01
-8.7902864007579683D-05	8.8770397592616192D-01
-7.5987228995273525D-01	-1.0284670837783706D-05
-2.3774566407198307D-02	-1.1083278463558061D-03
-4.3227037311261960D-02	-1.1957047082817050D-05
5.2944516044952102D-07	-4.8957324797353152D-02
1.5071570643010143D-02	-1.9057873637811355D-07

7.6602917767171307D-01	-5.5491539127917120D-03
-4.6215047246151421D-05	-3.3347997434534906D+01
-7.2701651552210314D-05	6.5923736574653159D+01
-6.4709956051467665D-01	-5.8241957561206212D-04
-5.7451694251124665D-02	-7.9469394915042755D-02
1.6554349731673562D-02	-6.6561302146333345D-04
-1.5705772381005331D-05	-4.0259617515695223D+00
2.6312338910138283D-02	-1.7204696733214873D-05

t=0.0

Closed loop eigenvalues:

-7.459 E3; -8.459 E3; -3.938 E2; -3.809 E2; -1.433 E2;
-2.240 E2; -7.380 ± j 7.149; -1.397 E1 ± j 1.398 E1; -1; -1

TABLE 4.5

THE OPTIMAL CONTROL GAIN MATRIX :

-6.732287340459024 5D-01	-1.046369539584501 9D-04	1.572388876651926 3D-01
1.231310030902981 0D-03	-4.531364149391094 5D-02	4.591467270803321 4D-04
9.577351159792821 5D-04	1.169218031709476 9D-01	2.034477191421552 1D-04
-7.246541213376484 0D-01	-5.036427457434251 0D-03	-4.401358266481266 0D-02
-2.193952896595939 5D-02	-1.796302398703275 3D-03	-4.948931130379845 2D-03
-1.036995195412410 0D-01	-1.667762347467323 0D-03	-9.955792832175746 4D-01
-2.086233070799539 3D-04	9.944467512903730 9D-01	-2.896344335673477 3D-05
1.405720072460392 5D-03	6.633953409975029 5D-07	2.425535402739170 3D-03
-2.857497330423550 1D-04	-1.502368145535527 1D-02	-8.245097287624383 9D+01
-1.310307840791093 9D-01	-2.567330113047374 0D+00	-4.965037631992293 0D-01
3.665541528147923 7D-01	2.087179816852496 3D+02	-2.737480523903395 1D-01
-1.032599432153212 0D-04	4.030552972604523 6D-03	1.070325112123149 7D+02
-2.292771939345750 3D-04	-7.158293603417332 4D-03	5.622195897541961 3D+00
-5.089234973306519 0D-03	6.023568532173822 3D-04	7.138471577357640 2D-01
-5.203392243395272 0D-01	-1.435105476613537 3D-01	3.442370556475545 3D-02
2.432469611430309 3D-03	-1.097438643023307 9D-03	-3.111544150652971 5D+00

-1.026345552524713 0D-04	-3.530540332617894 7D-01
-8.964403159372428 5D-01	-1.495330035410037 5D-03
-4.509509933331536 7D-01	-7.421553919052634 3D-04
2.468385852136500 1D-04	3.088587479652850 3D-01
-4.364328177824051 4D-03	1.742033173285789 3D-02
4.961233749230786 5D-05	-3.031367519273503 3D-01
-6.945290992930647 2D-03	1.332795439717726 5D-04
-6.698704353367398 5D-06	-9.498714921115276 2D-03

-6.745042550313660 7D-01	-1.421775392598593 7D-04
1.193169905953085 5D-03	-4.619170058977439 2D-01
9.655756899768893 0D-04	8.854729844021022 0D-01
-7.363247330802223 0D-01	5.817757456413934 7D-04
-2.242507503924181 9D-02	-1.102459321690027 2D-03
-4.646481119563646 2D-02	-1.102454913215825 1D-05
-7.311340471300147 7D-05	-5.068232002763136 0D-02
1.434104679374708 1D-02	-1.515923731325911 0D-05

7.374935176266543 7D-01	-3.939430324311 7 0D-02	
4.813413443515263 6D-03	-3.049213776535502 0D+01	
5.259044753014316 3D-04	6.501473912933476 3D+01	
-6.739459931443632 5D-01	8.398169470104042 6D-02	
-3.827168173243227 0D-02	-6.735443219524697 0D-02	
-9.007954057123219 3D-04	2.059237837187235 6D-04	
-2.291175830563241 3D-04	-4.078320525419153 0D+00	t=0.1
2.083313631155951 2D-02	-2.300128175243707 5D-03	

Closed loop eigenvalues:

-7.459 E3; -7.459 E3; -3.822 E+2; -3.710 E2;
-1.476 E2; -2.238 E2; -7.258 $\pm$ j 7.039;
-1.393 E1 $\pm$ j 1.396 E1; -1.; -1.43

TABLE 4.6

THE OPTIMAL CONTROL GAIN MATRIX :

-6.0205704719593470D-01	-2.8916015728617433D-04	1.4704703559840993D-01
3.1601512163839937D-03	-5.2106474639740112D-02	1.2154618442136311D-03
2.9167590536467502D-03	1.1695565719328853D-01	6.5713573685498575D-04
-7.4532030376976513D-01	-1.7741323347329371D-04	-5.4545579525271330D-02
-2.2984611293470668D-02	-3.4420863099833582D-03	-5.2563106391216123D-03
-7.4964237526526583D-02	-8.4041623657340333D-03	-9.9459142335794493D-01
-8.5530632517405584D-04	9.9413927294754044D-01	-5.9573600537670379D-03
1.4644956528803230D-02	2.7377266534761993D-03	2.6264164089355570D-03

-7.6681351734014377D-04	-3.2622519615131663D-02	-7.7387325769278462D+01
-1.4639959160335275D-01	-2.4599829550916731D+00	-1.1954177383060225D+00
3.0733337628132567D-01	1.5769607350273601D+00	-7.0777629052527792D-01
-5.5354[illegible]D-04	8.7384226463370150D-02	9.7213380537332247D+01
-3.1340035[illegible]D-04	-4.4454069440115543D-03	5.1322044301262292D+00
-3.5531661[illegible]D-03	-1.3334060143573397D-04	-2.0224381761651410D+00
-5.1983[illegible]D-01	-1.4513603315903734D-01	8.7544066156972289D-02
9.1[illegible]D-03	-2.3433234264231967D-03	-2.8383969080119633D+00

-3.0645643535109521D-04	-3.2715903487229831D-01	
-9.0040262923125333D-01	-3.9283571359916344D-03	
-4.4133945713514643D-01	-2.3791865701690970D-03	
6.7115934534087378D-04	3.4232271790101098D-01	
-4.3505792713293695D-03	1.8484432972153987D-02	
1.8424637570457316D-04	-3.0613303156493377D-01	
-1.2255971111505283D-03	3.3961897311935813D-04	
-1.8383416164472668D-05	-1.0175176365821123D-02	

-6.8757612582133326D-01	3.2957572147011164D-04	
2.4015039701376534D-03	-4.5137638324847691D-01	
3.3562089521168413D-03	8.9072434157491540D-01	
-7.2404536540627312D-01	2.6650245978123751D-03	
-2.1726536212070364D-02	-9.6474646913494443D-04	
-4.8089536509425823D-02	5.4916558229079521D-05	
-1.6830428319726271D-04	-5.3492684253576339D-02	
1.3964289567516063D-02	-6.5756663380751867D-05	

7.2442622224599577D-01	-1.0901203154552240D-01	
4.6018122595455564D-04	-3.2260100532844937D+01	
2.2053896[illegible]D-01	6.0322875592043389D+01	
-6.6765110[illegible]D-01	2.6403392[illegible]D-01	
-3.6[illegible]D-01	-6.7077191991763892D-02	t=0.2
1.9667954[illegible]D-02	-1.3873839436094330D-04	
-6.7515135745742185D-04	-4.0914705915952770D+00	
2.1087903745218263D-02	-7.2590789427753446D-03	

Closed loop eigenvalues:

-7.460 E3; -7.460 E3; -3.740 E2; -3.564 E+2; -2.240 E2;
-1.330 E2; -7.558 ± j 7.311; -1.387 E1 ± j 1.390 E1; -1; -1.318

TABLE 4.7

$\int(x^t P_i x + u^t Q\ u)dt$, then it becomes possible to select the gain matrix C_i in such a way that the closed loop matrices $(A_i - B_i C_i)$ have the same eigenvalues, that is, regulator maintains almost the same modes along the trajectory.

CHAPTER 5

TASK 3: HARDWARE IDENTIFICATION; TRADE STUDY

5.1 Introduction.

This section summarizes work to date on Task 3 of the project described in this report.

In Task 3, the control system was to be used to quantify energy requirements. Based on this and related analysis of escape trajectories, the control logic was made more efficient, and a parameter selection methodology was developed. Other Task 3 activities included a survey of microprocessor technology for suitable architectures to handle the control, sensing and sequencing activities of crew escape; and, an analysis of representative control system hardware components, to aid in selecting the appropriate ones for the control system.

The main results presented in this chapter are that the overall energy requirements are about twice the capacity of current technology seats, for control schemes which use only propulsive energy, although if a design develops which allows main thruster cutoff at dynamic pressures greater than 600 Q, the energy requirements would reduce. Also, although sensor technology seems capable of providing instruments which meet the needs of use on ejection seats, there remains a considerable "packaging" problem; if this forces elimination of key sensors, the microprocessor could be burdened with severe estimation duties. Ideally, the controller will receive angular and linear acceleration, angular rates, and local vertical, in addition to the atmospheric data now available on the ACES II prototype. Direct measurement of wind velocity direction would be a great aid in controller efficiency, but perhaps could be omitted. Finally, measurement of ambient temperature could be used by the controller to model more accurately the propulsive thrust profiles.

Our studies also indicate that near state-of-the-art propulsion technology will be adequate for the thrust levels and slew rates developed by the controller, provided the energy leads to units which can be fit on

the seat. The concurrent selectable thrust design project has provided useful data in quantifying propulsion requirements more completely.

5.2 Task 3 objectives

A major objective of Task 3 is to assess the degree to which the control requirements specified for this project, and the control system which is to implement these requirements, strain state-of-the-art hardware technology. There is no doubt that self-contained control of an ejection seat in the specified escape regime (cf., MIL-S-9479B) places several technologies near their current limits. The myriad requirements of size, weight, reliability, and performance in extreme dynamic conditions over very short time periods, necessarily represent an interesting and exciting challenge to designer and manufacturers of seat components.

The control system is at the heart of these issues. During the first part of this project, we have developed a design which offers promise of performing exceptionally the difficult control task. We now describe the phase of the project in which it is necessary to assess how well a concept developed on a computer will perform in the "real world". The answers are affirmative: that our control scheme is a viable one, and that the technology is at or near to the necessary levels to realize this major step in reducing the hazards of crew escape. We shall see this in upcoming chapters in this report.

The main goal of Task 3 is to study and identify hardware components so that a hardware breadboard design can be developed. The Task 3 SOW items are now summarized:

Quantify the energy requirements to accomplish the desired control task, while maintaining accelerations on the ejectee to within tolerable limits.

Investigate and identify state-of-the-art microprocessor technology with respect to its peformance of the digital computational requirements of the controller, and its duties in controlling and sequencing the major ejection events.

Conduct an evaluation and trade off analysis to select hardware for the control system design.

5.3 Microprocessor Hardware Component Survey.

This section documents the results of a preliminary microprocessor hardware component survey to determine microprocessor throughput requirements for the ejection seat controller, and then to compare these requirements with currently available and projected microprocessor technology.

In order to quantify throughput requirements while the actual control laws were under development, it was necessary to make some assumptions about the form the control laws would take. To this end the simple attitude controller shown in Figure 5.1 was examined. The inputs to the controller are noisy angular rate measurements. The state of the controller consists of estimated angular rate and estimated angular position (integrated angular rate). Notice that angular rate and angular position are scaled such that multiplication by the integration timestep is not necessary. It is assumed that the applied control has the same dimension as the angular rate measurement.

Therefore, Equations (1) through (5) in the figure represent a filter that estimates the full state based on a transition matrix to update angular rate (Equation (1)), first order integration of angular rate to obtain angular position (Equation (2)), and a set of filter gains to incorporate the new measurement (Equations (3),(4),(5)).

With the state estimate thus obtained the controller calculates a control linear in the state (Equation (6)).

To the right of each equation is an operation count. The count does not include the calculation of the transition matrix, filter gains or control gains. It is assumed for the moment that these quantities are constant or obtained by a table lookup. The gains for the filter could be precomputed Kalman filter gains, the control gains could be precomputed LQR gains, or they could be derived by some other technique.

EQUATION	# ADD | SUB	# MULT.
(1) $\hat{\omega}(t \mid t-1) = \Phi_\omega(t)\,\hat{\omega}(t-1 \mid t-1)$	$n(n-1)$	n^2
(2) $\hat{\theta}(t \mid t-1) = \hat{\theta}(t-1 \mid t-1) + \hat{\omega}(t-1 \mid t-1)$	n	0
(3) $z(t) = \omega_m(t) - \hat{\omega}(t \mid t-1)$	n	0
(4) $\hat{\omega}(t \mid t) = \hat{\omega}(t \mid t-1) + K_\omega(t)\,z(t)$	n^2	n^2
(5) $\hat{\theta}(t \mid t) = \hat{\theta}(t \mid t-1) + K_\theta(t)\,z(t)$	n^2	n^2
(6) $u(t) = C_\theta(t)\,\hat{\theta}(t \mid t) + C_\omega(t)\,\hat{\omega}(t \mid t)$	$2n^2-n$	$2n^2$
TOTAL:	$5n^2$	$5n^2$
TOTAL with $\Phi_\omega = I$:	$4n^2+n$	$4n^2$

IR 1

where:

$\hat{\omega}(\ell \mid m)$ - Angular velocity estimate at time ℓ, based on measurements up to and including time m. (dimension - n)

$\hat{\theta}$ - Integrated angular velocity estimate (n)

Φ_ω - Transition matrix for ω (n k n)

K_ω, K_θ - Filter gains (n k n)

u - Control vector (dimension - n)

C_θ, C_ω - Control gains (n k n)

Figure 5.1 Operation Counts for Attitude Controller

For the case of a full three degree of freedom controller (3DOF) the number of multiplication operations is 45, and the number of additions is also 45. A 1DOF controller requires 5 multiplies and 5 adds. Three uncoupled 1DOF controllers require a total of 15 adds and multiplies. Computational requirements for 2DOF controllers are calculated similarly. It should be noted that Kalman gain and covariance matrix calculations increase the computation requirements to about three times the total shown (15 n) if they are performed at runtime at the same rate. A similar increase would follow if LQR control gains were computed at runtime.

Currently, measurement rates and loop closure rates of 500 Hz are under consideration. This rate is consistant with the ejection seat dynamics observed in EASIEST simulation runs, although it may be possible to reduce the rate somewhat without affecting performance. At this measurement rate, throughput requirements are 22,500 multiplies and adds per second of operation for the 3DOF controller mentioned above.

The Intel 8086 was chosen as representative of current technology. Within the tolerance required for this discussion, it is comparable to, if not slower, than other parts such as the Motorola 68000. Sixteen bit integer arithmetic was assumed sufficient for the accuracy and stability requirments of the controller. An instruction mix of move to register, multiply from memory, and add to register repeated three times followed by a move memory to register instruction was taken as representive of the instruction mix that an assembly language programmer would generate for the algorithm given.

This instruction mix gave calulated execution times of 35 microseconds per multiply with a 5 MHz clock, and 22 microseconds for the 8 MHz clock. These times correspond to throughputs of 45,500 multiplies per second (8 MHz) and 28,400 multiplies per second (5 Mhz).

Thus, an assembly language programmer might be expected to implement the 3DOF attitude controller with constant coefficients, 16 bit integer arithmetic, and run it successfully at 500 Hz on an 8 Mhz 8086. The chances of success with 5 MHz 8086 would be marginal, due to simplifications made and overhead ignored in the argument above.

If the inner loop were implemented in a high order language the assumptions made above would hold only if the compiler's code generator were very efficient. This is generally not the case, but the situation may improve as compiler technology matures. It is very likely that compiler inefficiencies will be compensated for by increased hardware speed.

If 32 bit arithmetic, or floating point arithmetic were desired, or if any other of the assumptions made above are violated, it is likely that current microprocessor technology (as represented by the 8086) would not suffice. However, the addition of other hardware (i.e. floating point support chips, array multipliers) or a change in the algorithm would bring the system into the realm of feasibility with current technology.

Future microprocessor technology is difficult to predict. However, since the current technology appears marginally feasible, it is fair to predict that the situation can only improve. Commercial microprocessor technology is not necessarily moving toward greater throughput, but toward better high order language support (as in the Intel iAPX-432), or to greater miniaturization (higher memory density) or toward lower power consumption.

5.4 Microprocessor design

This section of the report will identify architecture and design issues relating to microprocessor implementation of the ejection seat control algorithm. The section will discuss system operational requirements, constraints and requirements on physical characteristics, computational requirements of the control algorithm and the implied architecture and software requirements, including event detection and sequencing, and, finally, will address requirements and capabilities for built in test and graceful degradation.

5.4.1 System Operational Requirements. Aside from the operational requirements of the escape system during an actual ejection, there remains to be discussed certain operational requirements on the escape system during times other than an escape event. It may be desirable to have some portion of the escape system operational when the aircraft is in flight,

either continuously or periodically, and when the aircraft is on the ground undergoing periodic maintenance.

Such operation could be justified for two reasons. First, built in test and system "fail safe" considerations provide an argument for continuous or intermittent operation of at least part of the system. The system's built in test equipment (BITE) can be more effective if it can isolate potential system failures prior to an ejection. The ability to do this in no way suspends the requirement to isolate faults occurring during an ejection, but it does simplify the task. In particular, microprocessor, memory, and power supply failures can be identified more easily on the ground or during normal flight than during an ejection for reasons of available time and reduced computation requirements. Should such failures be discovered during flight, the escape system could disable active control in favor of conventional control, and indicate to the pilot that the escape system will perform in a reduced performance mode if an ejection becomes necessary. It is doubtful that sufficient time would exist for the performance of a thorough system memory test during the few milliseconds available between the time the ejection is initiated, and the time that memory is required by the control algorithm.

A second argument for continuous operation is the potential requirement for the escape system to maintain an attitude reference independent of the aircraft's attitude reference. This attitude reference would be used for the vertical seeking function of the escape system, and could be periodically checked against the aircraft attitude reference, if available, as a means of verifying accelerometer and attitude sensor operation.

For example, if the escape system is equipped with strapdown angular rate sensors and accelerometers for the primary attitude rate and acceleration control function, the same sensors could provide a vertical reference as a secondary function by using a software mechanized, self erecting attitude reference. Using current strapdown rate sensors, the primary attitude rate information can be supplied in minimal startup time. Attitude information, if not available from other sensors such as radar

altimeters or ground/sky direction sensors, can only be obtained from long time averaged inertial acceleration information or similar estimates of the local gravitational acceleration vector. Thus, the requirement for a local level attitude reference, obtained independently of aircraft systems, can result in the requirement to operate the attitude rate sensors and accelerometers for some minutes prior the ejection. This requirement is independent of the physical startup time of the sensors, and can be eliminated if the attitude reference is obtained from the aircraft or an external reference.

The operational nature of the system, as discussed above, is mentioned for its effect upon the microprocessor energy requirements and cooling requirements. Continuous operation of at least some part of the system will require continuous power and continuous cooling requirements, implying an external power source as well as an on-board power source. If the system is operational only during an ejection, power requirements can be met solely by an on-board energy source.

The most desirable system configuration is one in which the escape system operates nominally without external power, and without information from the aircraft data bus, but which can take advantage of aircraft power or data if it is available, and can be used to good effect.

5.4.2 Computational Requirements. There are at least three distinct types of processing that must be performed by the microprocessor in its control of the escape system. First is what might be described as the synchronous processing performed by the closed loop controller and steering algorithm. This processing is synchronous with periodically sampled sensor inputs, it is cyclic, i.e., essentially the same processing is performed on each input sample set, and the processing is largely independent of the data being processed. This processing will largely determine the microprocessor throughput requirements, in terms of operations performed per second.

The second type of processing is that associated with event detection and sequencing. This category includes canopy jettison, restraint harness

retraction, drogue deployment, survival kit and parachute deployment, as well as critical subsystem self test. This processing is asynchronous, acyclic, and data driven. The throughput requirements that this processing imposes are not a primary concern, but the asynchronous nature of the processing and the precise timing requirements will determine the interrupt latency of the microprocessor, and possibly require additional hardware support if sub-millisecond timing requirements exist.

The last classification consists of off-line maintenance, self test or BITE processing, or similar low criticality "background" processing performed prior to an escape event. This type of software is, by definition, not critical to the primary function of the system, and does not impose limiting timing or throughput requirements. It may, however, impose non-volatile memory requirements if a significant amount of such software is required.

5.4.3 Microprocessor Event Timing Capabilities. With reference to system requirements outlined in the preceding section, it is necessary to review the capability of current microprocessors. In addition to the "raw" capability of the processor itself, some attention should be given to the capability of the processor in conjunction with the high order language compiler in use, as well as other software support that may be considered useful, such as a real time executive.

First, interrupt timing and latency will be examined. Taking the Motorola 68000 as representative of the class of processors under consideration, one finds that approximately 44 clock cycles are required to acknowledge the interrupt exception, that is, 44 cycles elapse from the time the microprocessor begins processing the interrupt to the time the first instruction of the interrupt handler can execute. Most interrupt routines require the use of several processor registers, an must therefore save and restore those registers to be used. A typical interrupt routine might save and restore eight registers; this requires 192 processor cycles if the move multiple instruction is used. Finally, the return from interrupt (or return from exception on the MC68000) requires an additional 20 cycles. The total, 256 cycles, represents the additional processor

overhead required to process a single interrupt, exclusive of the actual interrupt processing itself.

An event timing and sequencing implementation with a timing accuracy of one millisecond can be readily obtained with a software clock updated every millisecond by an interrupt handler. This level of accuracy is consistent with the escape system timing requirements. An eight MegaHertz MC68000 will therefore lose 256/8000 of its capacity, or about 3.2 percent, if it services interrupts every millisecond.

It should also be noted that the interrupt latency is insignificant in this context. An interrupt cannot be serviced until the currently executing instruction has completed. On the MC68000 the longer instructions range from 70 cycles for a multiply, to 158 for a divide, to 176 for a sixteen register move multiple register instruction. Again with an 8 MegaHertz clock, this only amounts to about .02 milliseconds in the worst case.

The timing and sequencing functions of escape systems are easily within the real of current 16 bit microprocessor implementation, so long as the implementation does not incur undue overhead in the event handling processing software (this possibility is discussed a following section).

5.4.4 Microprocessor Self-test Capability. The capability for self test in current microprocessor lies mainly in the realm of system design for fail safe hardware and software self test mechanisms. This type of system design is probably better understood in the hardware arena; a fail safe software design, along with graceful degradation properties desired in escape systems, can be difficult to achieve or demonstrate in actual practice, and the probability of success is directly realated to the complexity of the software. The use of currently accepted good design practice, high order languages such as Pascal or preferably Ada, and a sound testing and verification methodology provide a basis for software reliability.

Assuming that the system software is inherently reliable and free of design errors and coding errors, there remains the issue of incorporating the microprocessor controller into the overall system self-test mechanism.

The only microprocessor known to the author that directly provides inherent self-test capability is the Intel IAPX-432. This microprocessor (actually a micro-mainframe) can be configured as a dual processor system. In this system, each processor compares its data, address buss, and control lines with those of the other processor. Both processors are simultaneously executing the same program. Any discrepancy an indication of a failure. This approach will increase the overall system failure rate, but will reduce the probability of an undetected failure. Also, even though the system is redundant, microprocessor failures are only detected, not corrected.

Aside from using redundant system components as in the case above, a microprocessor can perform useful system self-test. During available system warmup time (quite likely limited in an escape system) various microprocessor self-tests can be performed, including verification of internal registers and the ALU, memory tests, power line condition, and certain types of I/O interface tests. For example, sensors can be designed to produce characteristic outputs during their warm-up time; a failure to observe the transient would indicate possible sensor or I/O interface failure.

Digital outputs can be verified when sensors exist to measure the desired effect of the output. Examples of this type of system self test are position sensors on motor gimbals to verify steering commands, or using the system's accelerometers to verify the correct operation the propulsion system.

Closed loop self tests of the type described above have the failing that a problem may not be easily isolated, and there remains the issue of how the system should be designed to respond to a fault condition detected by the microprocessor.

A simple but effective means of ensuring fail safe operation under certain types of failures is the use of a "keep alive" circuit. An example of this might be the inclusion of an additional output from the controller to the motor actuator hardware. This output would be strobed by the

controller software each time the control loop executed successfully as far as can be determined by the control software. Absence of that signal would be interpreted by the actuator as a system failure; the actuator would respond by slewing to a nominally centered position. This scheme is most reliable if the signal path of the keep alive is the same as that of the normal commands, and if each component in the path tends to fail in a way that blocks the signal.

Certain types of self test might well be avoided. It is tempting to run microprocessor register or memory test software in real time, as a low priority process executing in the background. This would, in principle, provide the earliest possible indication of memory or microprocessor failure, but the nature of such tests produces extremely unpredictable system failures when the self test software has, for some reason, failed. The more conservative approach of performing such tests prior to system operation is preferred.

A final type of self-test software remains, that of verification software that runs off-line, as when the system is down for maintenance. Off-line self-test can enhance system reliabilty by facilitating preventive maintenance. The operational caveat associated with this type of software is that it occasionally requires more memory and development time than the primary system software. In addition, it should be remembered that it is difficult to devise diagnostic software that stresses the system as thoroughly as actual operation does.

5.4.5 System Hardware and Software Architecture. The effect upon system architecture, both hardware and software, of the system requirements discussed is likely to be more due to reliability issues than throughput issues. As mentioned in the Task I interim report, the throughput capabilities of current microprocessors appear adequate to the task of ejection seat control, and as mentioned above, the event sequencing and detection requirements are also within the capacity of current microprocessors. Thus, multiprocessor configurations, or other architectural innovations, are not anticipated on the basis of throughput requirements alone. The overpowering need for system reliability may,

however, be addressed at the architectural level. Such architectural decisions such as whether to use redudant independent hardware, data and signal paths, or to take the alternate approach of a single, monolithic organization with conservative design, will generally be driven by considerations of reliability.

What hasn't been examined in detail in the area of microprocessor throughput is the effect of software tools and products, particularly the high order language compiler and the real time executive software used (if any). While the advantages of using a high order language can't be overstressed, one must consider the effect a compiler will have on the throughput of the microprocessor/compiler combination.

The efficiency of a compiler, compared to that obtained (presumably at greater expense) by assembler or hand coding techniques is determined partially by the nature of the instruction set of the machine or the language used, but is determined almost entirely by the effort put into the development of the compiler. Compilers that produce code that compares favorably with that produced by hand coding do exist, but unfortunately, are the exception. This is particularly true for microprocessors. It is hoped that Ada compiler developers will go to the effort required to achieve acceptable code optimization for that language, especially in view of the fact that the language was originally developed for imbedded, real time applications software. The Pascal compiler being used for the demonstration software development is typical in that it is not known for producing highly efficient code, and can therefore be used to identify potential problems in this area.

Another area of software architecture concerns the use of a real time executive. A real time executive provides software support, generally to the user of a high level language, in the area of synchronous and asynchronous event handling. An executive will allow several independent processes to execute, apparently simultaneously, on the same processor. Here is another area that one gains utility and ease of development at the possible expense of run-time efficiency.

The escape system software design could be facilitated by use of a real time executive, or by multitasking features as incorporated in the Ada language specification. It is likely, however, that the overhead incurred would be unacceptable. The time required to perform a task swap, that is, to save the status of a process executing on the machine, find a process that is eligible for execution, and initiate it, can consume several hundred to several thousand machine instructions or cycles. A task swap may therefore require a substantial portion of a millisecond. It would be best to perform event detection and sequencing directly from interrupt level software. The only remaining processing is the cyclic controller algorithm, which can be initiated by a single interrupt. Therefore the escape system can be characterized as one that requires a simple but efficient real time software design. For these reasons it is anticipated that only a minimal real time executive will be required, or that a very simple one will be developed specifically for the application.

5.4.6 Architecture Trade Study. Based on the observations in the preceding sections, Tables 5.1 and 5.2 give the results of a tradeoff between specific configurations, (Table 5.1) and general architectures (Table 5.2). The weighting factors are based on arguments presented above. The table entries are essentially quality factors between 0 and 1 that essentially rank order each system with 1 as "best." The values are otherwise somewhat subjective, particularly in Table 5.2, where a particular architecture class may have very dissimilar representative members.

Table 5.1 the specific example systems described in the preceding subsection. The reliability and performance quality factors are based directly on that discussion. As to the architectural classification of the five systems, the first four are essentially uniprocessor designs with differing types of failure detection and management, and the fifth is either a federated processing system or a distributed system depending on the implementation details. (Again, the terminology used here is taken from AFWAL-TR-81-3120.)

Table 5.2 compares the general processor classes. The federated processor and distributed processor classes are essentially equivalent in

Table 5.1

Microprocessor Architecture Analysis Tradeoff

System Architecture \ Criteria Weight	Reliability 0.4	Performance 0.4	Development Risk 0.2	Totals
Simple	0.8	0.6875	1	0.795
Simple + SW Self Test	0.9	0.625	0.9	0.79
Dual Redundant	0.9	0.5	0.8	0.72
Triple Redundant	1	0.43625	0.7	0.7145
Dual Distributed	0.75	0.8125	0.8	0.785

Performance Breakdown

System Architecture \ Criteria Weight	Throughput 0.625	Volume/Mass 0.25	Power 0.125	Performance
Simple	0.5	1	1	0.6875
Simple + SW Self Test	0.4	1	1	0.625
Dual Redundant	0.5	0.5	0.5	0.5
Triple Redundant	0.5	0.33	0.33	0.43625
Dual Distributed	1	0.5	0.5	0.8125

Table 5.2

Microprocessor Architecture Analysis Tradeoff

System Architecture \ Criteria Weight	Reliability 0.4	Performance 0.4	Development Risk 0.2	Totals
Uniprocessor	0.5	0.54375	1	0.6175
Federated Processor	0.25	0.76875	0.75	0.5575
Distributed Processor	0.25	0.76875	0.25	0.4575
Multiprocessor	1	0.2625	0.125	0.53

Performance Breakdown

System Architecture \ Criteria Weight	Throughput 0.675	Volume/Mass 0.25	Power 0.125	Performance
Uniprocessor	0.25	1	1	0.54375
Federated Processor	1	0.25	0.25	0.76875
Distributed Processor	1	0.25	0.25	0.76875
Multiprocessor	0.25	0.25	0.25	0.2625

every area save development risk. This is due to the fact that the major architectural difference between them is that while they both distribute processing among resources in a fixed way, the federated system need not have identical processors, but may use processors tailored to the task, or even use an already developed subsystem as a processing resource. An example of this might be the use of an existing attitude/heading reference subsystem with its own processor as an element of a control system.

The multiprocessor distinguishes itself from the rest by having the capability to dynamically assign processing tasks to resources, potentially improving reliability. This is achieved at the expense of operating system overhead reducing potential throughput, and increased development risk.

The uniprocessor architecture provides the baseline for best volume/mass/power and least development risk.

The reader is cautioned that when interpreting these results one must keep in mind that a good system design may well make use of more than one type of architectural feature to accomplish the task at hand.

Overall, it appears that the simpler systems fare well in comparison with the more complex systems, but at this level of investigation no single decisive architectural feature can be identified.

5.4.7 Vax-Tektronix 8550 IO Design. This subsection documents the design of the I/O interface and the general overall design of the MC68000 control software development. Further details are to be found in Volume II, Chapter 6. It was decided initially (prior to the amendment of Task 4, which then specified real time development) that fidelity of simulation was more important than real time simulation. This resulted in the following approach: Simulation software executing on the Vax was to supply simulated sensor data to the Tektronix 8550 emulating the 68000. The 68000 would execute the control software to calculate the control commands that would be transmitted to the escape system. The execution of this software would be timed for analysis of throughput requirements. The commands would be transmitted to the Vax, which would simulate the actuators, ejection seat dynamics, and sensors, and the process would repeat. The I/O interface to

be used was the RS-232 serial interface already available. The overall simulation would not run in real time, due to the simulation and I/O delays, but would still provide a facility for performing timing analysis and prototypic software development.

Development of several low level I/O routines was necessary to support the emulation, test and debug of Pascal code on the 8550. The low level I/O routines were required to support standard Pascal I/O and pointer management on the Tektronix 8550 MDL. The routines were written in C and added to the the Whitesmith's C and Pascal cross compiler support library. The routines are transparent to the Pascal user and support only standard Pascal IO. With this initial step completed the Vax-Tektronix 8550 IO interface development proceeded as documented below.

The following pseudo code (Tables 5.3 to 5.6) describes the IO protocol between the Vax, which simulates the escape system sensors, system, and actuators, and the Tektronix 8550 M68000 emulator running the control algorithm. The transfers are ASCII format over the the RS-232C remote IO interface between the Vax and the 8550.

The ASCII format was chosen because it is readable by a human, it is as standard and available an interface as currently exists, and is the only interface reasonably supported by standard Pascal. These qualities ensure portability and quick implementation. The single disadvantage is slow speed, as the same serial IO port could transfer the data in less than half the time if it were in binary format. Since only the controller execution will be timed for subsequent analysis, this disadvantage is inconsequential. The protocol defined by the pseudo code is not specific to this format as the same algorithm is suitable for binary transfers as well.

This interface simulates the digital or serial IO interface that will be required between the controller, sensors and effectors in an operational system.

A run is initiated by the operator at the Tektronix 8550. Using the 8550 'comm' command, the 8550 is established as a terminal communicating

with the Vax over the 8550's remote IO interface (serial RS-232C). Then, using the Vax 'RUN' command, the VaxIO procedure is brought into execution. VaxIO transmits an information message to the operator and performs a read on the remote IO interface.

The operator may abort VaxIO at this stage by typing an illegal message or an abort message, or he may simulate a normal run by typing start up and normal transfer messages to the Vax. (This is useful for test and debug purposes and would not be possible with a binary transfer format).

A normal simulation procedes when the operator exits the 'comm' command with the VaxIO read pending on the remote IO interface. The operator then uses the 8550 'X' (execute) command or its equivalent to run ControllerIO on the 8550. At this point, VaxIO is functioning as a slave and ControllerIO as the master. ControllerIO initiates the run by writing the startup message to the remote IO interface, and then waits for the first data transfer from the Vax by performing a read on the remote IO interface. Normal transfers between the Vax and 8550 then proceed until either processor transmits an abort message to the other, or until ControllerIO retransmits the startup message on operator request.

Each normal transfer contains a cycle count that is incremented by ControllerIO on each transfer to the Vax and is subsequently echoed by Vax in the transfer from the Vax to the 8550. The cycle count is allowed to "roll over" before it reaches a predefined magnitude (CycleModulus). The cycle count is used to ensure that the IO transfers procede in lock-step, without a missed transfer. The cycle count may also be interpreted as a timetag.

Note that VaxIO and ControllerIO (Tables 5.3 and 5.4) comprise the main routines for the Vax ejection system simulator and the M68000 controller emulator, respectively. The transfer scheme at this level is single rate. A multirate control system can be implemented in this framework by appropriate logic in the lower level routines called by VaxIO and ControllerIO.

Table 5.3. Vax I/O Procedure

```
procedure VaxIO;
    const
        CycleModulus = 1000;
    var
        Initialized : boolean;   Indicates receipt of start message
        Done : boolean;          Indicates completion of processing
        ExpectCycleCount : 0..CycleModulus-1;  Count expected next
    begin
        Initialized := false;
        ExpectCycleCount := 0;
        Transmit information message;
        repeat   Main Processing loop
            Read controller message;

            if ioError then begin
                Transmit abort message;
                Done := true
            end
            else if abort message received then begin
                Done := true
            end
            else if start message received then begin
                Initialize escape system state;
                Initialized := true;
                Compute initial sensor outputs;
                Transmit cycle count and sensor outputs to controller;
                ExpectCycleCount := received cycle count;
                Done := false
            end
            else if received cycle count <> ExpectCycleCount then begin
                Transmit abort message;
                Done := true
            end
            else if not Initialized then begin
```

```
            Transmit abort message;
            Done := true
        end
        else begin  normal cycle processsing
            Compute actuator response, escape system state,
              and sensor outputs from previous state and
              controller commands;
            Transmit cycle count and sensor outputs to controller;
            Done := false;
        end;
        Increment ExpectCycleCount mod CycleModulus
    until Done;
    Print termination conditions at operator console if abnormal
end; { VaxIO }
```

Table 5.4. MC68000 (controller) IO procedure

```
procedure ControllerIO;

    const
        CycleModulus = 1000;

    var
        CycleCount : 0..CycleModulus-1;
        Done : boolean;          Indicates completion of processing

    begin

        repeat

            Initialize;
            Done := false;
            CycleCount := 0;

            Transmit startup message and initial CycleCount;
            Read initial sensor outputs (from Vax);

            while not ( abort message received
                        or ioError
                        or received cycle count <> CycleCount
                        or Done ) do begin
                Increment CycleCount mod CycleModulus;

                Start digital timer;
                Compute controller outputs from sensor outputs received;
                Record computation time for analysis;
                Set Done as required;

                Transmit CycleCount and controller commands;

                Read sensor outputs (from Vax)

            end;
```

```
        print termination condition

    until operator requests termination of run

end;
```

Table 5.5. IO Transfer Formats

In what follows, read '::=' as 'is defined as'. Single quotes indicate a literal occurence of the enclosed symbol, and the vertical bars '|' separate optional forms of which one must occur. Curly braces '{ }' denote zero or more occurences of the enclosed object. Symbols and numbers are separated by one or more blanks, tabs, line feeds, or carriage returns.

```
message ::= start-up-message
          | abort-message
          | normal-transfer

start-up-message ::= 'S' cycle-count '.'

abort-message    ::= 'A' abort-code '.'

normal-transfer ::= 'N' cycle-count  data  '.'

cycle-count ::= unsigned integer mod CycleModulus

abort-code  ::= signed integer

data ::= signed integer
```

Table 5.6. Examples

Start up message (controller to Vax):

S 000 .

The 'S' indicates that this is a start-up message, and the initial cycle count is zero.

Abort message:

A -1 .

The 'A' indicates an abort initiated by the sender, the '-1' indicates the type of abort (a cycle count mismatch, for example).

Normal message:

```
N 056
100 120 35
-56 -34 500
67
98
.
```

In the above the 'N' indicates a normal data transfer with a cycle count of 56, followed by data. The definition and scale factors of the data depend apon the sender. Symbols and numbers may be separated by one or more blanks, tabs, line feeds, or carriage returns.

5.5 Control System Components Tradeoff Analysis.

In this section we analyze the relative strengths and weaknesses of the major control system hardware components, with respect to the ejection seat requirements. The hardware is divided into three categories: sensors, controller hardware (including microprocessors), and energy sources. These categories neglect other important components, such as restraint systems but these are felt at this time not to be critical elements for the actual control system design. The total control system is considered to consist of the sensors, the control logic and sequencing unit (microprocessor(s)), the thrust actuators, and the power supplies. The latter will not be discussed further here beyond pointing out that TLX signal actuating redundant thermal batteries are probably still the best type for ejection seat use.

The goal of this section is to compare and assess leading candidates in each category according to key criteria, and indicate preferences based on simulation requirements of the control system, and manufacturer's data sheets. All hardware is assumed capable of performance to the stated specs of the manufacturer. Performance as an integrated component cannot, of course, be evaluated at this time.

Another aspect is that manufacturers have to date not directed the application of their products to use on ejection seats. Thus, it will happen that several items each have many attractive features for seat control, but the ideal component will be a mix of state-of-the-art designs. Excessive "customizing" for seat use, however, could lead to unacceptable production costs.

The trade studies are presented primarily by means of "decision" matrices. These have been developed for each group of hardware components, e.g., angular accelerometer, and run to two or three levels. As best as possible, weights and figures of merit have been related to anticipated use of the design or component in the SSI-developed control system. Thus, for example, angular rate sensing is not as important for our system as angular acceleration sensing, so that performance for rate gyros is not weighted as

highly as performance for angular accelerometers. As another example, a three-axis sensing package whose volume exceeds that of an equivalent sensor will nonetheless score higher if the latter has fewer input axes, and if that results in a net greater volume for the number of such devices needed to provide data for the three axes needed by the controller.

It is expected that the sensing, control, propulsion, and ejection seat communities will provide further input into the selection of weighting factors and relative figures of merit.

Microprocessor architecture and related issues were discussed in Sections 5.3 and 5.4. Section 5.5.1 will discuss sensor hardware trade analysis, Section 5.5.2 will discuss energy source and actuation hardware trade analysis, and Section 5.5.3 will summarize and present our recommendations.

5.5.1 Sensor Hardware. In this analysis, we discuss several types of sensors which may be practical in providing necessary inputs for ejection seat control systems. The sensors are required to provide state variable information for the controller. The information most important for the SSI controller is: linear and angular acceleration, attitude, and altitude. Independent sensing of dynamic pressure, airspeed and wind direction would greatly help, and independent sensing of angular rate, inertial velocity and density or temperature would be useful for redundancy purposes. The number of such devices which can be accommodated is a packaging tradeoff with control system performance and capability.

The sensor categories selected for the trade analysis, then, are accelerometers, angular accelerometers, air data sensors, pressure sensors, attitude/altitude sensors, and angular rate sensors. The grouping has been dictated by the general trend in the product lines, although there is some overlap. Depending on the specific system, an air data sensor may provide altitude information, and a radar altimeter system could supply both attitude and altitude. The figures of merit and weights have been selected with such factors in mind.

There are two levels of decision matrix for the sensor hardware, in each of the above six sensor categories. The lowest level establishes

overall performance ratings, and the performance criteria producing this rating are: sensitivity range, start-up time, tolerable acceleration environment, operating temperature, frequency response, accuracy, hysteresis characteristics, resistance to impact, complexity (number of moving parts), and sensitivity to EMI/EMP effects.

The top level decision matrix for each sensor category includes the following design criteria: performance, reliability, weight, size (volume), power requirement, development risk, auxiliary hardware requirements (e.g., A/D converters or amplifiers), ease of maintenance, safety, interface compatibility, and development and production cost.

As is also the case with the propulsion system trade study (Subsection 5.5.2), the nature of this project leads to different weights than might be found in a more developmental project. Performance here is weighted much higher, for example, and production and development costs are weighted very low.

For the sensor trade analysis presented in this section, the top level weighting factors may vary from one sensor category to the next; however, at the lower level, the weights are the same, for each criterion (e.g., start-up time). The figures of merit for specific components are scaled between 0.1 and 0.9. If a product is seen to be adequate for any conceivable seat application, it will get a score of 0.9, even if another product is better in this criterion.

We now give an overview of the reasoning for the inclusion of certain of the performance and design criteria.

It was stated above that, for an exploratory development project, performance is most important. Also very important are weight and volume, which indirectly affect performance (it can be argued that weight is itself a performance criterion). Current operational seats have very small latitude for the inclusion of a new set of hardware, such as microprocessors and sensors. Although next generation seats will likely involve extensive redesign, all designs must have retrofit capability into existing aircraft. Thus, the size or "packaging" issue is a very real one, and it produces severe constraints.

Another packaging issue is that manufacturers have not yet integrated sensor electronics with microprocessor bit and bus structures. They are little to be blamed for this, since common digital standards do not exist yet. However, since the Air Force is developing one for its aircraft, it is a good opportunity to stress sensor integration for ejection seat and similar applications. For the present, interfacing is left to the customer.

Closely related to the size criterion in terms of retrofit capability is cost. This is always important, but even more so for seats; this should be kept in mind, although we are not weighing cost too heavily for the scope of our project. Today's operational seats cost $60 to $100K in current dollars, and do not have the sophisticated technology being planned for the next generation. A new design which more than doubles the unit cost of a seat will probably not be used extensively. In this regard, many of the state-of-the-art (SOA) components have a cost factor related to design and performance features which aren't critical for operation of the ejection seat. It is important to recognize and avoid, if possible, situations in which most of the cost is for unneeded features and/or performance.

Another factor is that the main seat structural mode usually falls within the bandwidth (sensitivity range) of many sensors, such as rate gyros. This type of problem can be eliminated, for example by using notch filters, but the designer must be aware of it.

Complexity and ruggedness are two criteria which can be considered reliability factors. In the crew escape application, extreme accuracy of measurements is usually less important than being guaranteed a measurement of some minimal accuracy. Due to the very short operational duration, such specifications as drift rates, null offsets, etc. are not critical. However, the unit must be capable of successful startup and operation, after long periods and conditions of storage, and during all of the anticipated operational conditions of vibration, shock, temperature variation, etc. Thus, while the system as a whole is to be much more sophisticated, the emphasis for most, if not all, of the key control system

components is on reliability. This implies in many cases foregoing complexity and sophistication for simplicity.

As a final introductory note, there is a tradeoff between control system performance and the type and number of sensors which will comprise the system. A minimal number of sensors will place a greater strain on microprocessor resources, as quantities not directly measured will have to be estimated by computer. On the other hand, seat geometry and weight limitations will force a conservative selection of sensors.

The rest of this section is devoted to an analysis of candidate sensor hardware. We have tried to examine as broad a spectrum of concepts and mechanizations as possible. Appendix E contains some specification sheets of components discussed here, which we were able to obtain. Attitude sensors include microwave radiometers, directional gyros, strapdown gyros and fluidic platforms. Attitude rate sensors include rate gyros, fluid rate sensors, angular accelerometers, strapdown gyros, and vibratory rate sensors. Accelerations will be sensed using linear accelerometers.

5.5.1.1 Attitude Sensors. Attitude can be measured by either electronic or fluidic systems. This section analyzes some likely candidates, from the standpoint of our particular control design, and of the system operational requirements.

Microwave Radiometer Attitude Sensing. A microwave radiometer can antenna is aimed toward the zenith (at its desired orientation) and the others are in the horizontal plane. Under the desired conditions the vertical-looking antenna will record cool temperatures, while the horizontal-looking antennas will see uniformly warmer temperatures. Because of symmetry, only pitch and roll information will be available.

This passive radiometer system could consist of hardware such as AEL H6100 horn antennas with 40 degree beam, Microwave Associates MA8430 solid state selector switch and a Honeywell R15-V receiver. Total weight would be less than three pounds total cost about $6000, and total power consumption of less than 60 watts. Although a similar system has been demonstrated by the Navy, the weight and size pose operational problems for

state-of-the-art systems. However, the basic state-of-the art exists for such systems, and a development effort geared to ejection seat applications does not represent a major advance in the technology. It is expected that both weight and power can be greatly reduced. The significant remaining concerns are temperature control of the receivers, and the fact that this system does not measure altitude.

Directional Gyro. Directional gyros are used typically to provide vertical or heading reference and represent a fairly mature technology. They are two-degree-of-freedom mechanical devices whose gimbal displacements about each output axis constitute a measure of angular deviation from the desired direction.

One example is the vertical gyro used to measure deviations from local vertical. Two accelerometers are orthogonally mounted on a platform whose desired orientation is horizontal. In steady-state (one g) conditions the accelerometers measure deviations from local vertical and "slave" the gimbal assembly to the local vertical. During dynamic conditions the accelerometers would give erroneous information; therefore, they are cut out. As a result, the local vertical during maneuvers will drift at the drift rate of the gyros (typically 10 to 15 deg/hr).

One problem with this system is the possibility of gimbal lock since this is restricted motion about the inner gimbal. This may be avoided by adding a third gimbal with a fast erection loop around the two inner gimbals.

Starting time is about 0.25 sec, so the system must be kept in an operating state continuously. This could be done concurrently with the erection of the aircraft's guidance sensors. If utilized on the seat, power may be turned off at ejection, since gyro wheels will not lose significant angular momentum for several minutes.

Timex manufacturers an interesting displacement gyro which has some attractive features. It is a 2-axis gyro which is gas-activated, eliminating the need for motors and associated electronics. Warm-up and uncaging takes place within 250 msec. This is a marginal startup time for

seat applications, but improvement may not present major obstacles. The device can operate for up to 20 seconds and has been used for anti tank missiles. Since the device is gimballed, gimbal lock can occur; one gimbal has full 360 degree freedom, while the other is limited to about 70 degrees. Weight is 11 ounces, volume is about 4 cubic inches (including gas supply), and cost is $500. Output is two angles, measured directly. These specifications are favorable for ejection seat use, although two units are needed for three axis coverage (one of the three axes will receive redundant measurements - a third unit could be added for full redundancy, but total size and weight become greater concerns). The device is rated up to 400 g shock and will handle angular rates up to 200 degrees/sec. The total error is about one degree in 15 seconds.

The rate sensing range is currently not adequate for ejection seat applications, where rates up to 1000 degrees/sec have been observed, even during initial phases of a controlled escape. Unless the design can be "customized" to meet this need, this particular unit will not be acceptable.

Strapdown Gyro. Strapdown systems generally come in two major categories; (1) inertial and (2) attitude and heading reference. The former uses a higher grade gyro than is required for our purposes. Thus, we will consider only the less sophisticated and cheaper attitude and heading reference systems.

This technology is more than twenty years old and is rather mature. As as result, even the simplest systems perform at a level which should meet all of our requirements. For example, attitude accuracy requirements are no more than about 10 degrees. Attitude systems are self-contained and require no outside intelligence. This is a very important consideration for ejection seats, which should be totally free of dependence on the aircraft avionics.

Types of gyros used in present day systems include laser-driven, dry-tuned, fluided-floated and even angular accelerometer with integration. An angular accelerometer can thus provide both acceleration and rate

information, greatly reducing system size and complexity. Laser-driven systems are still in the development stage and are quite expensive. Dry-tuned or floated gyros take several seconds to come up to speed, so must be turned on before ejection. Dry-tuned gyros appear more practical for ejection seat applications. This system would be aligned prior to flight and remain powered during the flight.

If the decision is made to "live with" the pre-ejection start up needs of inertial sensors, then the system can be periodically given an attitude reference from the main aircraft avionics system. The rate of update is related to the drift rate of the seat sensors; since these would be a lower grade, due to reduced performance needs in this area, the drift rate would perhaps require an update every 5 or 10 minutes. Between updates, the system is tracking the seat's attitude variations.

Strapdown systems consist of two major parts, a sensor package with associated electronics and a digital computer for performing the required strapdown calculations. One present system used for a torpedo uses no forced air cooling and the entire system, including sensors, power supplies and electronics are all in a box that weighs six pounds. All strapdown calculations are performed in the same unit.

Such systems require some modification prior to ejection seat use, particularly in the area of weight, size and power reduction. Data processing can be performed by the controller microprocessor; however, utilization of raw data from a strapdown system usually costs 300 to 500 KOPS in machine capacity.

The strapdown attitude reference system is attractive in several ways for application to ejection seat control. Because it contains rate integrating gyros, rates can be picked off and separate rate sensors for the control system are not required.

A three-axis strapdown rate assembly was tested for use in the B-1 ejectable crew model. The rate gyros were spring-restrained, employed a compensated damping mechanism and were operated both during pre-ejection and ejection phases. The GR-G5 gyro (Northrup Precision Products Division) was employed, which has the following characteristics shown in Table 5.[7]

TABLE 5.7 NORTHROP GR-G5 GYROSCOPE

input range	360 deg/sec
vibration	20 g; 20-2000 Hz
acceleration	40 g, any direction
shock	300 g/7 msec
temperature	-80 deg (F) to +203 deg (F)
rms bias error	0.9 deg/sec (resolution hysteresis + nonlinearity)
rms scale factor error	0.5%
rms linear acceleration-sensitive error	0.1 deg/sec/g
rms angular acceleration-sensitive error	0.0005 deg/sec/deg/sec**2

Model GR-G5 has been used in tactical missiles such as the Maverick, Sparrow and SRAM, as well as the F-16 autopilot. It weighs 4 ounces, occupies about 2 cubic inches and costs less than $900. Maximum angular rate is 600 deg/sec and the environmental limits are 10 g rms/20-2000 Hz for vibration and 100 g/11 msec for shock. The error characteristics are 0.05 /sec/g mass unbalance, and 0.10 /sec in null stability. This instrument could be used on the ejection seat without major problems, particularly if production per unit costs can be reduced.

Northrop Precision Products Division manufactures a rate integrating strapdown gyro, Model GI-G6, which weighs 4 ounces, occupies about 2 cubic inches and costs $2000. Other specifications are 10 g rms/20-2000 Hz vibration, and 100 g/11 msec shock. Total drift error would be less than 1 degree/minute for expected ejection seat maneuvers.

Radar Altimeter. These devices offer great potential for ejection seat use; however, there are some problems to be dealt with.

The technology is well established; there is only the need to apply it to ejection seats. These devices use LSIC or gate arrays. They are rugged, good at low altitude, and can be configured to provide attitude information as well. This would be a packaging benefit. If a sufficiently

large commitment for development were made, the devices could be reduced greatly in size and weight. There is also a need for comprehensive analysis to determine the optimum beam width and operating frequency for seat use. This is due in part to the fact that the aircraft interferes with the beam in its efforts to locate the ground. The problem is solvable, however. The tracker can acquire within a few msec, which is much faster than most comparable devices.

Fluidic Platform. At this time the principal developmental challenge is maintenance of accuracy over the required temperature range. This may require Reynolds number control.

Results. Tables 5.8 and 5.9 present the results of the trade analysis performed on attitude/altitude systems. With all factors considered, as we have weighted them, the radar altimeter offers the best option for ejection seat purposes. This is in part true here because we are not weighing development costs very high. This aspect also benefits the strapdown system relative to fluidic platforms. The former benefits from its proven technology, which tends to offset a performance disadvantage with respect to the fluidic platform. Final ranking properly awaits specific development for seat use.

5.5.1.2 Attitude Rate Sensors. Attitude rate sensors being considered are rate gyros, fluidic rate sensors, (integrating) angular accelerometers, strapdown gyros, and vibration rate sensors.

Rate Gyro. The conventional rate gyro is a device with a constant-speed wheel which establishes an angular momentum vector and resultant spin reference axis. The wheel is typically contained in a cylindrical chamber (float) which is, in turn, suspended in a viscous damping fluid. The float is constrained to rotate about an output axis which is orthogonal to the spin reference axis. Rotation angle of the float depends upon the spring rate of a torsion bar, and is measured by an electromagnetic pickoff.

Because of their small size and versatility, rate gyros are the most widely-used devices for rate sensing in the control field and are a mature

Table 5.8 ATTITUDE/ALTITUDE DECISION MATRIX

DESIGN CRITERIA / WEIGHTING FACTOR / DESIGN	PERFORMANCE CAPABILITY	RELIABILITY	WEIGHT	SIZE (VOLUME)	POWER REQUIREMENTS	DEVELOPMENT RISK	AUX. HARDWARE REQUIREMENTS	MAINTENANCE & SERVICEABILITY	SAFETY	INTERFACE COMPATIBILITY	DEVELOPMENT COST	PRODUCTION COST	TOTAL SCORE
	.35	.10	.10	.10	.08	.06	.04	.04	.05	.04	.02	.02	1.0
(Active) Radar altimeter	.71	.8	.8	.85	.9	.2	.8	.85	.9	.9	.6	.6	.75
Micrad	.65	.5	.8	.85	.9	.5	.2	.8	.9	.9	.7	.6	.69
Strapdown (Inertial)	.56	.8	.7	.7	.9	.9	.8	.4	.9	.9	.2	.3	.68
Fluidic Platform	.65	.8	.5	.5	.9	.7	.8	.8	.9	.9	.6	.6	.69

Table 5.9 ATTITUDE/ALTITUDE PERFORMANCE DECISION MATRIX

PERFORMANCE CRITERIA / WEIGHTING FACTOR / COMPONENT	SENSITIVITY RANGE	START-UP TIME	ACCELERATION ENVIRONMENT	OPERATING TEMPERATURE	FREQUENCY RESPONSE (BANDWIDTH, PHASE)	ACCURACY	HYSTERESIS, DEAD BAND	IMPACT RESISTANCE	MOVING PARTS	EMI/EMP SENSITIVITY			TOTAL SCORE
	.15	.15	.15	.12	.12	.08	.08	.05	.05	.05			1.0
(Active) Radar Altimeter	.7	.9	.5	.8	.8	.75	.5	.7	.8	.5			.71
Micrad	.7	.9	.5	.5	.8	.7	.5	.6	.8	.3			.65
Strapdown (Inertial)	.8	.1	.5	.8	.8	.8	.5	.4	.4	.3			.56
Fluidic Platform	.7	.5	.5	.9	.8	.5	.5	.5	.8	.9			.65

technology. MTBF's (Mean Time Between Failure) of 20,000 hours are realized with present systems. Due to warm-up times of 20 seconds or more, they would have to be turned on for the entire flight. This requirement makes them less appealing as a group than fluidic rate sensors. Other "problems" with respect to other devices such as fluidic rate sensors are that these systems usually cannot tolerate 20 g shocks (spin motor bearings). There are exceptions listed below, however. Also, some units require much power (4 watts or so), and linearity may not be as good (although likely adequate for seat control).

A typical representative of this group of rate sensors is the Northrop GR-G5 rate gyro. Its startup time is 30 sec, which requires that it be running continuously while the aircraft is in operation. It has an input range of +/- 360 deg/sec, which is also a liability, since rates up to 1000 deg/sec can happen. Its other features are fine for seat applications: very light (4.5 oz.), good temperature range, small, and can operate in a 40g acceleration field.

A better candidate in terms of performance is the Timex TAG030 series. This is a 2 axis, gas activated gyro which is being used on short range tactical missiles. A compressed inert gas spins the rotor, and the system can operate for 50 sec. Two such units would be needed for the seat control system. The unit tends to be large (1.8 x 1.9 x 3.45 in.), and weighs 8 oz. It is inexpensive (exact cost not available), and can be "customized". The TAG030 suffers from startup times also, although the time has been greatly reduced, to 300 msec. Reducing the rotor mass or increasing the gas pressure may make this unit a good choice. Any accuracy loss arising from such changes is a worthwhile tradeoff.

Honeywell offers a magnetohydrodynamic rate sensor which has several good features for seat use. The GG2500 is [illegible] axis sensor (thus, only 2 unit are needed), very small and light, with [illegible]e temperature range and good response time. It is rugged, low cost, mec[illegible]nically simple - offering excellent reliability, radiation insensitive, and [illegible]s been used successfully in related applications such as air and ground launched missiles, seekers and RPV's. Its major drawback at this time is the

startup time, which is 3.0 sec. Development is needed to improve this feature.

Fluidic Rate Sensor. Fluidic Laminar Rate Sensors (LARS) are based on a well-developed fluidic amplifier technology. A typical fluidic amplifier consists of a high pressure fluidic supply, amplifier nozzle and a jet splitter. With equal control pressures on at two oppositely-directed control pressure ports, the jet divides equally across the splitter. Differential pressure at the two ports leads to a higher differential pressure at the output ports.

In a LARS, the two control ports are not required. If the device rotates, the (inertial) effect is to divert the flow to one side of the splitter. However, the same amplification effect still operates, giving a sensitive indication of angular rate. In actual practice, control ports are sometimes employed for trimming of null offset.

LARS are relatively cheap, can come on-line quickly (less than ten msec), are very reliable and rugged and have a low power requirement. Linearity, null affect and threshold requirements are comparable to electro-mechanical rate sensors and the dynamic range is about 1000 deg/sec. Finally, this device has no moving parts.

A more expensive alternative to LARS is the super jet rate sensor, which uses the principle of Coriolis acceleration which deflects the jet stream in the presence of angular velocity. One such device, used in a cannon projective, weighs 12 ounces and has a 25,000 hr MTBF. Warm-up time is 1.5 sec, so that this system is not practical for ejection seat applications.

An interesting unit recently tested for the Air Force is the Singer/Kearfott Conductive Liquid Angular Rate (CLAR) sensor. A conductive liquid (mercury thallium) annulus in the gap of a permanent magnet moves in response to angular motion, and its conductivity in the magnetic field changes in a measurable way, according to Lenz' law. It is a single axis sensor, and requires no external power, an excellent feature. The liquid freezes at -75 deg (F), so this is acceptable as well. It offers high

reliability, low cost and long life. Each unit is somewhat large compared to many similar units (30 cubic inches), and it is new technology.

In our opinion the most attractive rate sensor for ejection seat applications will have performance similar to the Garrett Airgyro. This is a fluidic rate sensor with no moving mechanical parts, small size, low production cost (about $1 per laminate), minimal complexity, and very light. It has exceptional startup specs (2 msec), acceptable dynamic response (over 50 Hz bandwidth) and input range, and minimal hysteresis or deadband dynamics. It has been proven successful in high-g aerospace applications, long inaction times, and is insensitive to electromagnetic interference or pulses (EMI, EMP). The Garrett unit has electronic or fluidic interfacing.

Vibratory Rate Sensor. Vibratory rate sensors use an oscillating inertial body constrained to a base, against its natural tendency to preserve an inertially-fixed base, and the torque associated with such constraint is taken as a measure of the base rotational velocity. Two types of sensors will be discussed - vibrating wire and vibrating beam types.

The vibrating wire rate sensor uses a vibrating wire as its inertial reference. Equal lengths of wire are joined at the middle and each half passes through mutually orthogonal planes. Any turning rate applied to the sensor causes the wire to vibrate in an elliptical path due to Coriolis forces, crossing the perpendicular flux field in the other half of the wire containing the signal magnet. The resulting signal is picked off and amplified. One current system consumes less than one watt, has a warm-up time of 0.1 sec and a 75,000 hr MTBF.

The vibrating beam sensor consists of a rectangular cross section beam supported at its modal points and driven along one of the principal axes at its fundamental frequency. When an angular rate is applied along the beam's longitudinal axis, sinusoidally-varying Coriolis forces cause motion of the beam along an axis normal to the drive axis. This orthogonal sinusoidal motion provides the sensor output, which is proportional to the

input rate. System reliability is not high enough to warrant consideration for ejection seat control.

Results. Tables 5.10 and 5.11 present results of our trade analysis of rate sensors. It includes some devices not specifically mentioned above. Again, final rankings depend heavily on assigned weightings. The Honeywell GG2500 scores very well because of its very small size, and its multi-axis design. It is assumed that its startup problem can be overcome with development expense, not weighted heavily here. The CLARS sensor is less proven, although offering much promise, and it may lose performance if reduced to the size needed for seat use, due to physical limitations. We would also recommend consideration of the Delco hemispherical resonator gyro (HRG).

5.5.1.3 Angular Accelerometers. The angular accelerometer is comprised of two basic elements - a servoed angular accelerometer and a solid state integrator with automatic washout. It operates on the force-rebalance principle, with a seismic mass that tends to remain undisturbed when angularly disturbed. Relative angle between seismic mass and case is measured by a pickoff and integrated to give angular rate. Thus angular rate and acceleration information is available in principle. A washout circuit is used to offset long-term null and biases.

The typical unit weighs 10 ounces and has a 30,000 hr MTBF. This high reliability is due to the fact that there are no spin motors or wheel bearings to wear out. Power consumption is less than one watt, and it has been qualified to -40 deg to 200 deg F temperature and a 500 g/11 msec shock environment. Warm-up time is 0.05 sec so that it does not have to be started until the ejection procedure begins. It is a single-degree-of-freedom device and, with its self-test features, is an attractive candidate for rate sensing. Further, it can be multitasked to provide both angular acceleration and rate, as either main or redundant inputs.

One specific unit is the Systran Donner accelerometer. This is a fluidic device which requires less than 1 watt of power, and weighs less

Table 5.10 RATE SENSOR DECISION MATRIX

DESIGN CRITERIA / WEIGHTING FACTOR / DESIGN	PERFORMANCE CAPABILITY	RELIABILITY	WEIGHT	SIZE (VOLUME)	POWER REQUIREMENTS	DEVELOPMENT RISK	AUX. HARDWARE REQUIREMENTS	MAINTENANCE & SERVICEABILITY	SAFETY	INTERFACE COMPATIBILITY	DEVELOPMENT COST	PRODUCTION COST	TOTAL SCORE
	.15	.15	.15	.15	.10	.07	.05	.05	.05	.04	.02	.02	1.0
Honeywell CG2500 MHD 2-axis	.63	.8	.88	.88	.8	.9	.9	.8	.8	.9	.9	.5	.81
TIMEX TAG 031 2-axis	.62	.8	.3	.7	.8	.9	.9	.8	.8	.9	.9	.6	.70
Garrett Airgyro 2-axis	.85	.9	.7	.7	.8	.9	.9	.9	.9	.9	.9	.7	.82
CLAR, Singer/Kearfott single axis	.83	.9	.5	.5	.9	.2	.9	.9	.9	.9	.5	.7	.71
Northrop CR-G5 rate gyro	.55	.8	.5	.8	.8	.9	.9	.8	.8	.9	.5	.5	.72
Delco Hemispherical Resonator Gyro (HRG)			.5	.4								.7	(more data needed)

AD-A166 580 VECTORED THRUST DIGITAL FLIGHT CONTROL FOR CREW ESCAPE 3/3
VOLUME 1(U) SCIENTIFIC SYSTEMS INC CAMBRIDGE MA
J V CARROLL ET AL. DEC 85 AFWAL-TR-85-3116-VOL-1
UNCLASSIFIED F33615-C-82-3402 F/G 1/4 NL

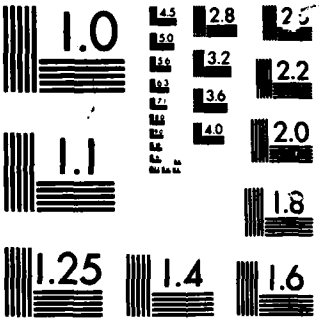

MICROCOPY CHART

Table 5.11 RATE SENSOR PERFORMANCE DECISION MATRIX

COMPONENT \ PERFORMANCE CRITERIA / WEIGHTING FACTOR	SENSITIVITY RANGE	START-UP TIME	ACCELERATION ENVIRONMENT	OPERATING TEMPERATURE	FREQUENCY RESPONSE (BANDWIDTH, PHASE)	ACCURACY	HYSTERESIS, DEAD BAND	IMPACT RESISTANCE	MOVING PARTS	EMI/EMP SENSITIVITY			TOTAL SCORE
	.15	.15	.15	.12	.12	.08	.08	.05	.05	.05			1.0
Honeywell GG2500 MHD 2-axis	.4	.1	.8	.9	.9	.9	.9	.2	.7	.5			.63
TIMEX TAC 031 2-axis	.8	.2	.2	.7	.9	.9	.9	.8	.7	.5			.62
Garrett Airgyro	.8	.9	.9	.8	.8	.8	.9	.9	.9	.9			.85
Clar, Singer/Kearfott	.8	.9	.9	.8	.8	.85	.9	.9	.9	.3			.83
Northrop GR-G5 single axis	.4	.1	.5	.9	.4	.8	.9	.8	.8	.5			.55
Delco HRG	.6					.9	.9	.8	.8	.9			(more data needed)

than 10 oz. It has been used on military and commercial aircraft as a rate sensor. Its size is rather large, but could be offset by a redesign to provide both acceleration and rate. Its output range is +/- 1150 deg/sec**2 for acceleration and +/- 20 deg/sec for rate. The rate limits are clearly unacceptable, but could presumably be improved. It can withstand 100 g shock, has no mechanical moving parts, is very linear in response, and easily interfaced with electronics. Two other appealing features are fast startup and low cost, and it also has self-test capability. The major drawback in addition to the rate range is the low temperature operating limit, now at -22 deg (F).

It seems that a better unit is the Schaevitz ASM. This device is a servo accelerometer, and it has very appealing size (1.8 cu. in.), weight (2 oz.) and operating temperature (-67 to 203 deg (F)) specs. Each unit is single axis, costs about $800, and requires 15 volts DC, and 10 ma.

Results. Tables 5.12 and 5.13 present the results of our angular accelerometer trade analysis. Again, the recommendation is to consider the top few scorers, since further development for specific seat use, not weighted heavily here, could produce a better device. In fact, all four devices here should be retained in consideration.

5.5.1.4 Acceleration Sensors. Conventional low cost acceleration sensing technology is accurate to within 2 percent or so, which is adequate for ejection seat control. There are several units in production today which appear to offer all of the key specs needed for ejection seat applications. Size, weight, performance, power requirements, and reliability of several candidates would be within seat requirements.

Sunstrand Corporation manufactures a flight control grade accelerometer, Model QA900, which has been used for Navy tactical missiles such as the SM1, SM2 and Harpoon. The instrument meets MIL-883B, weighs 65 grams (2.3 oz.), occupies less than one cubic inch of space and costs about $1000. Its operating temperature range is also acceptable. One unit is needed for each axis. The environmental specifications include:

vibration	;	30 g/20-1800 Hz
		12 g rms/random

Table 5.12 ANGULAR ACCELEROMETER DECISION MATRIX

DESIGN CRITERIA / WEIGHTING FACTOR / DESIGN	PERFORMANCE CAPABILITY	RELIABILITY	WEIGHT	SIZE (VOLUME)	POWER REQUIREMENTS	DEVELOPMENT RISK	AUX. HARDWARE REQUIREMENTS	MAINTENANCE & SERVICEABILITY	SAFETY	INTERFACE COMPATIBILITY	DEVELOPMENT COST	PRODUCTION COST	TOTAL SCORE
	.35	.10	.10	.10	.08	.06	.04	.04	.05	04	.02	.02	1.0
Honeywell GG2500 MHD 2 axis (Acceleration pickoff)	.67	.4	.8	.8	.4	.9	.9	.5	.8	.8	.9	.5	.68
Systran Donner 8160 Fluid Rotor Angular Acc. and Rate Sensor	.71	.8	.3	.2	.6	.9	.9	.9	.8	.8	.9	.6	.65
Schaevitz ASM Series Single axis	.79	.5	.6	.4	.8	.9	.9	.9	.8	.8	.9	.7	.72
Schaevitz ASB Series Single axis	.79	.5	.5	.3	.8	.9	.9	.9	.8	.8	.9	.7	.70

Table 5.13 ANGULAR ACCELEROMETER PERFORMANCE DECISION MATRIX

COMPONENT \ PERFORMANCE CRITERIA / WEIGHTING FACTOR	SENSITIVITY RANGE	START-UP TIME	ACCELERATION ENVIRONMENT	OPERATING TEMPERATURE	FREQUENCY RESPONSE (BANDWIDTH, PHASE)	ACCURACY	HYSTERESIS, DEAD BAND	IMPACT RESISTANCE	MOVING PARTS	EMI/EMP SENSITIVITY			TOTAL SCORE
	.15	.15	.15	.12	.12	.08	.08	.05	.05	.05			1.0
Honeywell GG2500 MHD 2 axis Rate Sensor (acceleration pickoff)	.85	.1	.8	.8	.9	.9	.8	.4	.5	.5			.67
Systram Donner 8160 Fluid Rotor Angular Acc. and Rate Sensor (1 axis); servo	.85	.5	.9	.6	.4	.9	.85	.8	.9	.5			.71
Schaevitz ASM Series Single axis	.9	.5	.85	.9	.8	.9	.85	.8	.8	.5			.79
Schaevitz ASB Series Single axis	.9	.5	.85	.9	.8	.9	.85	.8	.8	.5			.79

shock ; 250 g/5 msec

The instrument measures 50 g full scale and is quite accurate.

Another competitive instrument is a pendulous A/C excited accelerometer manufactured by Timex. Volume is less than one cubic inch, weight less than one pound and the price is about $500. Measurements up to 40 g can be made and shock up to 400 g can be tolerated. Error characteristics are:

temperature effect ; 0.04%/ C
total error ; 2% at full scale

Northrop Precision Products Division manufactures the APS-5 accelerometer, which weighs about 4 ounces, occupies about two cubic inches, and costs about $700. Measurements to +/-20 g's can be made, and the device meets the following specifications:

vibration ; 10 rms/20-2000 Hz
shock ; 100 g/11 msec, half sine
angular rate ; 600 /sec

The error characteristics are:

offset ; 1 ft/sec
scale factor ; 2%

Columbia Research Labs makes a servo accelerometer, the SA-120. In this unit the seismic mass is not mechanically constrained, so that there is minimal hysteresis and nonlinearity. The devices are very small in size and weight, and can sense over a range of 0 to 50 g's.

A final unit which is highly attractive is the Entran EGA3 series. A triaxial system can be placed in a 1 cubic inch volume, and the output signal(s) are high enough to not require amplification. It weighs 17 grams, requires 15 volts power, and has fine thermal properties (although its low temperature limit, -40 deg (F), could be a bit improved).

Results. Tables 5.14 and 5.15 present the results of our accelerometer trade analysis. A highly appealing device for seat use, not included here due to late arrival of data, is made by Insouth Microsystems. The unit is measured in milliinches, and is very rugged. It could well outscore the devices presented in Tables 5.14 and 5.15. Of the latter, the Entran performs best of several good designs.

5.5.1.5 Combined Angular Rate and Acceleration Sensors; Strapdown Systems. Strapdown systems differ from the more conventional gimballed systems in that the sensors are mounted directly on the ejection seat and the transformation from the sensor to inertial reference frame is computed rather than mechanized. The potential advantages of strapdown systems over stabilized platforms include lower cost, reduced weight and power consumption, increased reliability, ease of maintenance and manufacture, and redundant design. An on-seat microprocessor can perform computations.

Strapdown technology has been operational for over fifteen years and has achieved a mature status. Originally held back by computational requirements, there is now a widespread increase in their use, due both to major advances in computer technology and sensor designs with increased dynamic range and vibration accommodation. Lower costs are related to the fact that strapdown systems can perform well with lower cost production grade gyros. However, startup time is a major problem with most off-the-shelf strapdown units. This would offset any potential packaging/integration advantage.

Strapdown navigators generally include both gyros and accelerometers and associated special-purpose computer circuitry for performing the required sophisticated data processing. This self-contained, or modular, approach allows redundancy for increased reliability to be implemented at the sensor and component level, rather than the system level.

Strapdown gyros are usually of the rate integrating type and generate incremental angle pulses over fixed sampling intervals, which can be converted directly into angular rates. Spinning mass gyros are "caged" electronically to the gyro case by servo commands, called rebalance

Table 5.14 ACCELEROMETER DECISION MATRIX

DESIGN CRITERIA / WEIGHTING FACTOR / DESIGN	PERFORMANCE CAPABILITY	RELIABILITY	WEIGHT	SIZE (VOLUME)	POWER REQUIREMENTS	DEVELOPMENT RISK	AUX. HARDWARE REQUIREMENTS	MAINTENANCE & SERVICEABILITY	SAFETY	INTERFACE COMPATIBILITY	DEVELOPMENT COST	PRODUCTION COST	TOTAL SCORE
	.25	.10	.15	.15	.08	.06	.04	.04	.05	.04	.02	.02	1.0
ENTRAN EGA3 Series	.75	.8	.8	.8	.5	.9	.7	.9	.9	.7	.9	.8	.77
SUNDSTRAND 2180 MINI-PAL SERVO	.68	.6	.75	.3	.5	.9	.7	.5	.9	.8	.9	.7	.64
COLUMBIA RES. LAB piezoelectric	.72	.8	.75	.7	.5	.9	.7	.9	.9	.7	.9	.8	.74
COL. RES. LAB SA-1 servo	.69	.4	.6	.75	.5	.9	.7	.5	.9	.8	.9	.6	.66
Schaevitz SM Linear Series 1 axis	.63	.5	.4	.3	.5	.9	.7	.5	.9	.8	.9	.8	.57
TIMEX APS-000 Series 1 axis	.61	.5	.4	.5	.5	.9	.7	.5	.9	.8	.9	.6	.59

Table 5.15 ACCELEROMETER PERFORMANCE DECISION MATRIX

COMPONENT / PERFORMANCE CRITERIA / WEIGHTING FACTOR	SENSITIVITY RANGE	START-UP TIME	ACCELERATION ENVIRONMENT	OPERATING TEMPERATURE	FREQUENCY RESPONSE (BANDWIDTH, PHASE)	ACCURACY	HYSTERESIS, DEAD BAND	IMPACT RESISTANCE	MOVING PARTS	EMI/EMP SENSITIVITY			TOTAL SCORE
	.15	.15	.15	.12	.12	.08	.08	.05	.05	.05			1.0
ENTRAN EGA3 SERIES piezoresistive; no ampl. use Wheatstone bridge	.7	.9	.8	.7	.8	.4	.8	.8	.9	.5			.75
SUNDSTRAND 2180 MINI-PAL SERVO	.7	.9	.7	.8	.4	.8	.6	.5	.5	.5			.68
piezoelectruc crystal COLUMBIA RESEARCH LAB output 1.5 to 100 mV/g; higher lower freq. resp., larger mass.	.7	.9	.8	.5	.8	.4	.8	.8	.9	.5			.72
COL. RES. SA-120 SERVO	.7	.5	.8	.8	.8	.8	.6	.8	.5	.5			.69
Schaevitz SM Linear Series 1 axis	.7	.5	.8	.9	.3	.8	.6	.4	.5	.5			.63
TIMEx APS-000 Series 1 axis	.6	.5	.7	.9	.3	.8	.6	.6	.5	.5			.61

torques. Laser gyros are also available which do not require caging. However, current technology laser devices in general are not appealing for ejection seat application, due to power, cost, and reliability considerations.

The transformation from sensor to inertial frame is done using a set of attitude parameters such as Euler symmetric parameters, Hamilton's quaternions and Cayley-Klein parameters; a variety of other sets have been proposed, each capable of avoiding the "gimbal lock" singularity. The parameters are found by solving a set of kinematic equations. These equations must be solved at a very high rate to minimize computational error. An alternate approach, the electrostatic gyro, obviates this problem entirely by measuring the paramters directly.

Present-day systems are easily capable of accuracies exceeding 0.1 degrees in attitude and 0.02 ft/sec**2 in acceleration in a severe environment such as seat ejection, as long as the sensors are calibrated periodically (several times per hour).

Quite often, the capability of such systems is excessive, especially for the cost involved. Strapdown navigators made by Litton Systems and Honeywell, for example, cost $50,000 or more, totally unrealistic for ejection seat needs.

Conventional Systems. Conventional systems are often referred to as multisensors. An example of such a sensor package is the Rockwell (Collins Avionics Division) Multisensor which is a small, low cost device developed for tactical missile applications. Each sensor yields two rates and acceleration normal to spin axis. Two such sensors yield the required three axes of rate and acceleration while providing redundancy along a preselected, most sensitive, direction.

This system achieves somewhat higher accuracy than conventional systems. For example, rate measurements are accurate to about 0.03% of full scale, while the acceleration offset error is about 0.04% of full scale.

The unit is still under development, but prototype units and test data are available. Presently, a development effort is underway to design a sensor that is compatible with tactical missiles, for the U.S. Army Missile Command.

5.5.1.6 Pressure and Air Data Sensors. Direct measurement of pressure is a highly desirable ability for effective sequencing and control of the ejection seat. Some systems compute pressure altitude as well as static and dynamic pressure.

A pressure transducer which seems to satisfy most seat requirements is the Garrett quartz pressure sensor, P/N 2118132-1. This unit is light (5.4 oz.), small, does not require periodic maintenance, has an acceptable temperature operating range, dynamic range, and measurement range. The warmup time is 200 msec, which may be adequate, but could be improved. A larger problem which may be able to be designed out is the low acceleration tolerance, 10 g's along any axis.

Other manufacturers make pressure transducers of comparable performance to the Garrett, but the latter is at least as good in all specs important to seat use. Entran, Sensym, Rosemount and Foxboro/ICT are some of many suppliers of usable units.

In the area of wind direction sensing, Rosemount makes a flight test boom for direct measurement of angles of attack and sideslip, but this device is too bulky and limited in operation range to be considered. However, a technology effort aimed at the ejection seat application may pay off.

Another interesting device developed at the US Air Force Academy for NASA/Ames is the seven-hole probe. This conical device can measure angles of attack and sideslip, as well as airspeed. Only laboratory models have been built, however, and this type of technology may be lagging too much for ejection seat needs.

Finally, Garrett is committed to develop a sensor for seat use. It is a device about 0.5 inches in diameter, very light, and less than a foot long. It can measure airspeed magnitude and direction.

Results. Tables 5.16 and 5.17 present the results of our trade study for pressure sensors, and Tables 5.18 and 5.19 present results for the air data sensors.

There are several small, rugged and reliable pressure sensors to choose from. Three are clustered at the top, by our ranking scheme, but others should be considered should factors weighted less here, such as cost, become important later.

The air data sensors have not yet been adapted for seat use, but all offer new technology advances over current seat sensors, particularly in the ability to measure wind direction. Therefore, current seat air data sensors are not included.

5.5.2 Thrust Actuation Hardware. A somewhat different situation is encountered in performing a trade analysis of propulsion hardware for active control of ejection seats, than is the case in analyzing the sensor hardware for this control system. In the latter case, most of the components are nearly ready for use "off the shelf". Concerning propulsion systems, there is - as with the sensors - a wide range of devices and a technology level which offer promise of meeting the major goals of an active thrust control system. However, there is as yet no complete propulsion system ready to be attached to a seat and perform to the requirements of the controller being designed in this project.

Thus, we are doing much "projection analysis", assuming that sufficient development effort will be undertaken which will lead to a complete, integrated system. This means that the weighting factors for propulsion systems differ from their sensor counterparts. Also, we have kept the figure of merit scoring range closer, from 0.7 to 0.9, to reflect the notion that a concept which now scores relative poorly may outperform the others when full development for the seat application is initiated. Another aspect here is that the weighting is selected not only for the obvious system requirements, such as weight, cockpit size, etc., but for our specific control system design. This design, if fully implemented, will require, for example, at least three nozzle systems. More control

Table 5.16 PRESSURE SENSOR DECISION MATRIX

DESIGN CRITERIA / WEIGHTING FACTOR / DESIGN	PERFORMANCE CAPABILITY	RELIABILITY	WEIGHT	SIZE (VOLUME)	POWER REQUIREMENTS	DEVELOPMENT RISK	AUX. HARDWARE REQUIREMENTS	MAINTENANCE & SERVICEABILITY	SAFETY	INTERFACE COMPATIBILITY	DEVELOPMENT COST	PRODUCTION COST	TOTAL SCORE
	.20	.12	.12	.12	.10	.08	.06	.05	.05	.06	.02	.02	1.0
Garrett Airesearch Pressure Transducer P/N 2118132-1	.63	.9	.6	.2	.6	.9	.9	.9	.9	.9	.9	.9	.70
Microswitch, Series 230 PC	.65	.8	.9	.7	.6	.9	.9	.9	.9	.9	.9	.9	.78
Foxboro/ICT Model 1800	.71	.8	.7	.7	.8	.9	.9	.85	.9	.9	.9	.9	.79
Entran EP1-050	.68	.8	.7	.7	.6	.9	.9	.9	.9	.9	.9	.9	.77
Schaevitz P710	.75	.8	.6	.2	.6	.9	.9	.85	.9	.9	.9	.9	.71

Table 5.17 PRESSURE SENSOR PERFORMANCE DECISION MATRIX

COMPONENT / PERFORMANCE CRITERIA / WEIGHTING FACTOR	SENSITIVITY RANGE	START-UP TIME	ACCELERATION ENVIRONMENT	OPERATING TEMPERATURE	FREQUENCY RESPONSE (BANDWIDTH, PHASE)	ACCURACY	HYSTERESIS, DEAD BAND	IMPACT RESISTANCE	MOVING PARTS	EMI/EMP SENSITIVITY			TOTAL SCORE
	.15	.15	.15	.12	.12	.08	.08	.05	.05	.05			1.0
Garrett Airesearch Pressure Transducer P/N 2118132-1	.7	.4	.1	.9	.7	.8	.9	.9	.8	.8			.63
Microswitch (EDN rpt.)	.8	.9	.5	.3	.7	.5	.7	.4	.8	.8			.65
Foxboro/ICT Silicon-Diaphragm Chip, Model 1800	.8	.9	.5	.5	.7	.8	.85	.5	.8	.8			.71
Entran EPI-050	.8	.9	.5	.5	.7	.5	.7	.5	.8	.8			.68
Schaevitz P210	.9	.8	.5	.9	.8	.7	.7	.5	.8	.8			.75

Table 5.18 AIR DATA SENSOR DECISION MATRIX

DESIGN CRITERIA / WEIGHTING FACTOR / DESIGN	PERFORMANCE CAPABILITY	RELIABILITY	WEIGHT	SIZE (VOLUME)	POWER REQUIREMENTS	DEVELOPMENT RISK	AUX. HARDWARE REQUIREMENTS	MAINTENANCE & SERVICEABILITY	SAFETY	INTERFACE COMPATIBILITY	DEVELOPMENT COST	PRODUCTION COST	TOTAL SCORE
	.25	.08	.18	.18	.10	.10	.06	.05	.05	.06	.02	.02	1.0
Rosemount 92AX	.54	.7	.1	.2	.2	.8	.9	.9	.6	.9	.6	.8	.56
USAFA	.56	.3	.8	.7	.5	.4	.9	.9	.9	.9	.4	.8	.75
Garrett	.69	.5	.8	.8	.8	.6	.9	.9	.9	.9	.5	.8	.86

Table 5.19 AIR DATA SENSOR PERFORMANCE DECISION MATRIX

COMPONENT / PERFORMANCE CRITERIA / WEIGHTING FACTOR	SENSITIVITY RANGE	START-UP TIME	ACCELERATION ENVIRONMENT	OPERATING TEMPERATURE	FREQUENCY RESPONSE (BANDWIDTH, PHASE)	ACCURACY	HYSTERESIS, DEAD BAND	IMPACT RESISTANCE	MOVING PARTS	EMI/EMP SENSITIVITY			TOTAL SCORE
	.15	.15	.15	.12	.12	.08	.08	.05	.05	.05			1.0
Rosemount 92AX	.4	.5	.8	.2	.7	.7	.5	.4	.4	.8			.54
USAFA	.8	.5	.8	.3	.1	.7	.5	.6	.7	.8			.56
Garrett	.7	.8	.7	.6	.7	.7	.5	.6	.7	.8			.69

system requirements are discussed below and throughout this report. For now, we recommend that the two or three concepts which score well in this analysis receive detailed attention in future design and analysis work, but that the other concepts also receive consideration.

After much preliminary review, which included meetings and discussions with key manufacturers, we have selected seven generic concepts for analysis. The results are presented in Tables 5.20 - 5.21, which represent three levels, top to bottom respectively. The companies which supplied most of the data include: Garrett Corp., Stecel Aero Engineering, Atlantic Research Corp., Martin/Marietta, TRW, and Morton Thiokol Inc. Because much of their data is proprietary, we only reflect it indirectly in the decision matrices of Tables 5.20 - 5.21.

Blueline drawings for the MMOA and Stencel concepts are presented in Appendix B. We now discuss briefly these concepts, and later on, interpret the results.

The three major propulsion subsystems of interest to the control engineer are the energy source, and the means of vectoring and modulating the thrust. Key features of the propellant (energy source) include packaging, storage ability, reliability, high specific impulse density, and non-volatility. Almost certainly, solid fuels will be used because of their past performance in meeting the particular seat requirements. A very appealing fuel is a gel-like substance developed by TRW. It has very high volume efficiency, in addition to fine storage capability and the usual attributes of solids. However, the thrust modulation requirement and the fact that solids can be difficult to turn off may result in examination of liquid systems. (Fluidic systems are very prominent as actuation devices.)

Thrust vectoring is achieved by reaction jet control or thrust vector control, the two major generic classes. The concepts presented here are a mix of these classes. Actuation systems should be of the pyrotechnic warm gas or cold (stored) gas variety, as electrical or hydraulic systems are not practical for ejection seats. Many actuation concepts were reviewed during this project. Fluidic TVC, movable nozzle TVC (e.g., trapped ball),

and TVC via mechanical deflection were the key concepts considered. Mechanical deflection is achieved by inserting tabs into the exhaust stream. There is typically a large loss of axial thrust when the vanes are at maximum deflection. Also, the net angle of deflection generally is smaller. The fluidic systems offer high reliability, fewer moving parts, and generally lower weight. As such, they are quite attractive. Garrett is a leader in this technology.

Modulation of thrust is also critical for our control design, in order to achieve acceptable performance over the full escape envelope. Several concepts were examined, including pulse motors, overboard bleed, variable area nozzles, multiple motors, and manifolded systems.

The control system requirements dictate a minimum of three "independent" nozzle/actuation systems. By independent is meant that thrust magnitude and direction settings of any one nozzle are not dependent on those of any other nozzle or nozzles, but only on their own mechanical limitations. More strictly, two fully independent and one partially independent nozzle are sufficient to perform the combined attitude and trajectory control tasks. In Section 7 of this report we discuss the controllability aspects in more detail.

Our simulations to date indicate a requirement for about 4000 ft-lb torque capability, and about 9500 lb total force. The torque requirement is directly related to the aerodynamic moments which can be generated at the high Q (dynamic pressure) limits of the escape envelope. Similarly, the force requirement is derived from the need to offset the aerodynamic decelerations at high Q, so that the pilot's acceleration radical is tolerable, and by requirements relating to trajectory control - e.g., avoidance of parts of the aircraft during ejection, and achieving sufficient altitude rate for safe chute deployment.

The high Q escape condition and the various adverse attitude conditions force the propulsion system to react very rapidly to changes in the dynamic environment. Our studies done to date indicate that thrust vectoring rates of the order of 600 to 800 deg/sec are required, and that the sustainer rocket gimbal cone angles should be close to 40 degrees.

Table 5.20 THRUST VECTORING, MODULATION DECISION MATRIX

DESIGN \ DESIGN CRITERIA	PERFORMANCE	RELIABILITY, REDUNDANCY	WEIGHT	SIZE (VOLUME)	DEVELOPMENT RISK	MAINTENANCE & SERVICE-ABILITY (Standardization, Accessibility, etc.)	SAFETY	DEVELOPMENT COST	PRODUCTION COST				TOTAL SCORE
	.50	.10	.08	.08	.07	.04	.06	.04	.03				1.0
Manifolded (BIT) Motors with Trapped Ball or Jet Tabs	.81	.82	.75	.8	.8	.85	.8	.85	.8				.81
Variable Area Nozzle (VAN) Motors with Trapped Ball or Jet Tabs	.80	.82	.8	.8	.85	.85	.85	.85	.8				.81
Gated Fixed Pintle Poppet Valve	.84	.85	.9	.85	.8	.85	.85	.75	.8				.84
Pneumatic TVC Acutation	.83	.85	.88	.85	.8	.85	.85	.75	.85				.83
Fluidic Diverter Valve TVC	.84	.85	.88	.85	.8	.85	.85	.75	.85				.84
Trapped Ball Nozzle Motors	.79	.818	.75	.80	.88	.85	.8	.865	.8				.80
Twin Gimballed Motors	.79	.825	.75	.70	.88	.77	.8	.867	.8				.79

Table 5.21 THRUST VECTORING MODULATION PERFORMANCE DECISION MATRIX

DESIGN \ PERFORMANCE CRITERIA	CAPABILITY OVER ESCAPE ENVELOPE	START-UP TIME	ACCELERATION ENVIRONMENT	OPERATING TEMPERATURE	FREQUENCY RESPONSE (BANDWIDTH, PHASE)	IMPACT RESISTANCE	MOVING PARTS, COMPLEXITY						TOTAL SCORE
	.40	.15	.10	.10	.10	.05	.10						1.0
Manifolded (BIT) Motors with trapped ball or jet tabs	.81	.85	.8	.8	.8	.8	.8						.81
Variable Area Nozzle (VAN) Motors with trapped ball or jet tabs	.82	.75	.8	.8	.8	.8	.8						.80
Gated Fixed Pintle Poppet Value Actuation	.85	.85	.8	.8	.9	.8	.82						.84
Pneumatic TVC Actuation	.82	.85	.85	.75	.85	.82	.85						.83
Fluidic Diverter Value TVC	.82	.85	.85	.8	.85	.85	.9						.84
Trapped Ball Nozzle Motors	.82	.75	.80	.7	.8	.80	.8						.79
Twin Gimballed Motors	.80	.75	.80	.8	.8	.75	.8						.79

Table 5.22 THRUST VECTORING, MODULATION CAPABILITY DECISION MATRIX

DESIGN \ CAPABILITY ITEMS	FORCE LEVELS	CONTROL RATES	VECTOR ANGLES	RESPONSE TIME	STABILIZATION	ACCURACY	THRUST MAGNITUDE RATE OF CHANGE						TOTAL SCORE
	.16	.16	.16	.16	.16	.10	.10						1.0
Manifolded (BIT) Motors in Trapped Ball or Jet Tabs	.75	.8	.85	.85	.8	.78	.78						.81
Variable Area Nozzle (VAN) Motors in Trapped Ball or Jet Tabs	.85	.8	.85	.80	.8	.85	.8						.82
Gated Fixed Pintle Poppet Valve Actuation	.85	.88	.8	.9	.8	.85	.85						.85
Pneumatic TVC Actuation	.8	.75	.8	.88	.84	.88	.8						.82
Fluidic Diverter Valve TVC)	.8	.8	.8	.85	.8	.82	.85						.82
Trapped Ball Nozzle Motors	.85	.75	.85	.85	.8	.85	.8						.82
Twin Gimballed Motors	.85	.75	.85	.75	.8	.85	.8						.80

One model which has been analyzed extensively consists of three nozzles (motors). One is located in the x-z plane, and has more total impulse than the other two. This may be considered as the sustainer motor. The other two are "mirror images" with respect to the x-z plane, and have less total impulse than the sustainer. These "verniers" are like RCS rockets, while the sustainer will likely have a gimballed nozzle. See Section 3.2.2.3.

An extremely attractive candidate for the vernier actuation system is the Martin Marietta gated fixed pintle poppet valve. It has excellent response characteristics, and seems capable of achieving the high slew rates. This concept has been simulated and performs very well using the control law described in Chapter 4. See also Section 3.2.2.4.

Garrett Corp. also has attractive actuation systems, which could also be applied to the sustainer nozzle. Their systems have bandwidths to 100 Hz, and are offered as low cost, reliable, fluidic systems. The major question with regards to seat applications is can these systems move as quickly the thrust levels required by the seat. Garrett has developed fluidic reaction jet control systems for rocket nozzles, and these seem to be possible competitors to the Martin Marietta valve. They are lightweight, low cost, simple mechanically, very reliable, EMI insensitive, good dynamic response (not quite as good as Martin Marietta), and possess high packaging efficiency.

Summarizing the Tables 5.20 - 5.22 design concepts, the first two were studied by ARC in their selectable thrust project; the last two similarly were studied by MTI in their selectable thrust project. We state here that our weighting and performance scoring is different, because we are relating these concepts to our particular design. The Martin/Marietta High Force Gain Valve actuation system is listed, with the assumption that the extensive development work required, not weighted heavily here, will be done.

Finally, the fourth and fifth concepts in the tables are from Garrett. The pneumatic TVC actuation concept has proven performance in other applications.

Results. The rankings in the tables must be considered in light of the discussion above. There are built in assumptions and expectations relating to further development, which must occur if the concepts are to be realized. Nonetheless, our best available information to date leads to a clustering of concepts which coincides with what are felt now to be very attractive concepts. An integrated design effort for thrust modulation, actuation and propellant will likely include major subsystems from the Martin/Marietta actuation scheme or the Garrett fluidic or pneumatic concepts. It is recognized that other manufacturers may actually develop better systems than the ones presented here, but these are considered generic concepts at this time.

5.5.3 Summary and Recommendations. Many systems can comfortably meet the ejection seat control system requirements. An example of this is the accelerometer. Others, such as rocket actuators, must be carefully compared and evaluated, because the requirements are at the limits of the technology. All of the systems are subject to the real and severe constraints of size, storage ability, weight, reliability, low cost, and good performance in all extremes of the environment.

Based on manufacturer's specifications, the recommended control system hardware components are, in order:

1.) Attitude sensors: radar altimeters
micrad sensors
fluidic integrating rate sensors (Garrett)

2.) Attitude Rate Sensors: Garrett Airgyro
Honeywell GG2500
Northrop GR-G5 rate gyro
Singer/Kearfott CLAR

3.) Angular accelerometers: Schaevitz ASM
Systran Donner

4.) Linear accelerometers: Entran EGA3
Columbia Research Lab SA-120

5.) Pressure/atmospheric sensors: Microswitch 230 PC
Schaevitz P710

6.) Air Data Sensors: Garrett

7.) Thrust actuation systems: Martin Marietta
Garrett
(recommend using results of ARC and Thiokol selectable thrust design, analysis projects)

U.S. GPO: 646-066

END
FILMED

5-86

DTIC